Fundamental considerations and application of acoustics as a nondestructive evaluation technique of wood quality properties

by

Charles Essien

A dissertation submitted to the Graduate Faculty of
Auburn University
in partial fulfillment of the
requirements for the Degree of
Doctor of Philosophy

Auburn, Alabama
December 16, 2017

Key words: Hemicelluloses, lignin, cellulose, acoustic, time – of – flight, resonance.

Approved by

Brian K. Via, Chair, Professor of School of Forestry and Wildlife Sciences
Thomas Gallagher, Professor of School of Forestry and Wildlife Sciences
Timothy McDonald, Professor of Biosystems Engineering
Lori G. Eckhardt, Professor of School of Forestry and Wildlife Sciences

Abstract

The growing global demand for wood and wood products has resulted in a tremendous investment in tree improvement programs with the aim of improving growth, form, and disease tolerance. There has been significant success in achieving this overarching objective in *Pinus taeda* L (loblolly pine) over the past few decades in the southern United States, but at the expense of wood quality.

Currently, about 58% of the total United States timber is extracted from 13 million hectare of southern pine plantations in the southeastern US. Of all the seedling established plantations in the southeastern United States, loblolly pine (*Pinus taeda*) constitutes about 84% making loblolly pine the most dominant tree species in the southern United States. Fast growing trees produce wood with a considerable amount of juvenile wood which has reduced modulus of elasticity (stiffness), modulus of rupture (strength), high microfibril angle and therefore poses utilization challenges. Consequently, the design values for visually graded southern pine lumber (including loblolly pine) were generally reduced in 2013 to reflect the material quality on today's market. As a future direction for improvement of loblolly pine, stakeholders want to select and deploy elite families with superior wood quality properties to meet future demands. Acoustic techniques have been found to be one of the nondestructive tools for rapid characterization of seedlings and trees in tree breeding programs.

This study focused on understanding some fundamental concepts of acoustic techniques as a nondestructive evaluation tool for rapid characterization of trees in tree breeding and forest management operations with special reference to fifteen selected 14- year old elite loblolly pine families grown on two sites in the southern United States. The effect of distance between probes of the tree acoustic tool on velocity was investigated as well as the sensitivity to variation in equilibrium moisture content of the two main types of acoustic tools.

Fundamentally, cellulose, hemicellulose, and density are important drivers of strength, stiffness, and velocity. It was found that cellulose and lignin are the highest and lowest respectively contributor to acoustic stress wave propagation at the molecular level with cellulose being the most important conductor of the stress wave while lignin acts as a stress wave dispersant and hemicellulose acts as a special coupling agent between these components. These polymeric constituents are thus important drivers of sound wave propagation at the molecular level while density played a co-subsequent role at the macro scale.

With respect to the distance between probes, for distances below 60 cm, the waveform is dominated by the fundamental frequency of the transmitter probe hence the velocities determined within 10 to 60cm are not statistically different. Furthermore, velocity determined at distances below 60 cm is significantly higher than that determined at 120 cm suggesting velocity is dependent on the between probes distance. Using 120 cm as a standard distance, the dynamic stiffness of the tree is overestimated by 13, 50, 102, and 197 MPa respectively for 100, 80, 60, and 40 cm. Consequently, distances from 80 to 120 cm constitute the optimum range for velocity determination for this tree (time - of – flight) acoustic tool.

Finally, microfibril angle and the fiber wall thickness are the main anatomical properties driving the signal at the micro-level.

The two main types of acoustic tools used for stiffness characterization in the forest and wood industry are the resonance (harvested wood products) and time – of – flight (used for tree). The equilibrium moisture content of loblolly pine significantly affects the velocity measured below and above the hygroscopic region. The acoustic velocity decreased by 33.9 m/s and 28.8 m/s for time – of – flight (TOF) and the resonance tools respectively for a unit increase in EMC below fiber saturation point (FSP). The change was lower for EMC above FSP - 5.4 m/s for TOF and 6.1 m/s for resonance. This statistically nonsignificant slope in velocity above the FSP coupled with better accuracy in predicting green static MOE using velocity with oven-dry density supports the hypothesis that the cell wall material controls the acoustic velocity while the water in the cell lumen plays a nonsignificant role in stress wave propagation.

It was demonstrated that using the density at test (green density) to predict the dynamic MOE of trees and freshly harvested logs with the moisture content above the FSP, the dynamic MOE will be least 40% higher than similar prediction using oven-dry density.

Based on this observation, oven – dry or basic density is recommended for dynamic MOE computation for tree or products with moisture content above FSP.

The effects of site and genetic families on morphological, anatomical and wood quality properties of fifteen 14-year-old loblolly pines stock were studied. The dynamic MOEs of the trees were determined using the velocity with either basic density ($DMOE_B$) or green density ($DMOE_G$).

There were significant site and genetic family effects on diameter, microfibril angle, fiber length, and dynamic MOE. While there was a nonsignificant difference in $DMOE_B$ between sites; $velocity^2$ for site 1 was significantly higher than site 2, but $DMOE_G$ was higher for site 2 than site 1. This suggests that depending on the type of density used in computing the dynamic

MOE, a difference decision can be made. Therefore, practitioners should take care when extrapolation velocity reading of trees from different locations. Additionally, about half of the selected genetic families had statistically similar morphological and wood quality properties between sites suggesting that half of the planting stock exhibit stability and homogeneity in the southeastern USA. Therefore, foresters and landowners have the opportunity to select genetic families (T26 and T 18 – proprietary code) which are superior in both the morphological and wood quality traits for plantation development across sites. Also, the landowners have the opportunity to match some elite planting stocks to a specific site for greater productivity and quality outturn due to the significant effect of site or family or site by family interaction.

Acknowledgements

I am very grateful to God, for His mercies, protection, guidance, and favor throughout my study in Auburn University.

Dr. Brian K. Via has been a very wonderful advisor, tutor, and role model to me for all the period spent under his supervision. It has been a great privilege to develop my career under his mentorship. To Dr. Lori G. Eckhardt, Dr. Thomas Gallagher, and Dr. Timothy McDonald, I sincerely appreciate the vast opportunities you offered me. Their connections and network in the wood and forest industry helped in the completion of this study in diverse ways. I am very grateful to Dr. Ilari Filponnen for serving as my University reader.

I am very grateful to the Robert Lewis Adams Fellowship, Forest Health Cooperation, Rayonier, Plum Creek, Westervelt, and REX lumber for their financial and material contribution towards my study. My special thanks to School of Forestry and Wildlife Sciences, and Forest Products Development Center for given me this tremendous opportunity.

To the staff and colleagues at the Forest Products Development Center and Forest Health and Dynamics Laboratory, I say thank you for your wonderful contributions to improve the quality of this study.

I sincerely appreciate the spiritual, emotional, and physical support from my family and friends throughout my studying period here in Auburn. I sincerely appreciate the numerous sacrifices made on my behalf.

Table of Contents

Lists of Tables

Lists of Figures and Images

Chapter 1: Introduction and Literature Review

1.1 Introduction

The forested land in the United States has increased by about 1% to 310 million hectares in 2012 and accounts for93% of the total forest and woodland areas of the country. Out of the 310 million hectares of forestland, 211 million hectares are dedicated for timber production and an additional 0.3 million hectares are reserved for other purposes (Oswalt et al. 2014). The proportion of the total timberland area occupied by the saw-timber size tree increased consistently in the northern and southern parts of United States. In the southern U.S., the proportion of saw-timber increased from 30% in 1953 to 53% in 2012 (Oswalt et al. 2014). Conversely, the pole-timber size trees decreased from 40% to 26% within the same period. The 40.3% of the total timberland of the country is located the southern United States which is responsible for supplying 60% of the industrial round timber used within the country and over 16% of the global timber consumption. In 2012, it was estimated that southern yellow pine (SYP) constitutes about 84% of the 3 billion cubic meters (trees with dbh 12.5cm or greater) of the total growing stocks of softwood available in the timberland of the southern United States. Therefore, SYP constitutes the most important group of species in the southern United States (USDA, 2016), and accounting for 7.5% of the economic activities in the region (PINEMAP 2017).

Of all the seedling-established plantations in the southeastern United States, loblolly pine (*Pinus taeda* L) constitute about 84% making loblolly pine the most dominant tree species in the southern United States. Some of the reasons for the success of this species are fastest growing and adaptability to a wide range of edaphic conditions hence thriving in varying sites within the southern United States (McKeand et al. 2003). The enhanced productivity and popularity of loblolly pine plantation in this region is partially the result of intensive research and development programs in tree improvement and silviculture, which focused mainly on the girth growth, form, disease resistance and stand management.

However, the rapid volumetric growth and shorter rotation periods achieved over the years through intensive research and development have resulted in the production of wood with a high proportion of juvenile wood which consequently possesses wood quality issues for sawtimber (Zobel and Sprague 1998; Gapare et al. 2006). Juvenile wood has reduced stiffness, strength, specific gravity, but with high microfibril angle, shrinkage and swelling.

Eastin (2004) indicated that in the United States about 52% of the solid-sawn lumber consumed is used in the construction of new residential and nonresidential structures and another 30% is used for repair and remodel of existing structures. The authors continued that, much of the veneer production is also used in products where stiffness and strength are critical quality characteristics. These facts indicated that tree improvement and breeding programs without consideration for the wood quality of the produced trees is likely to be counter-productive. Therefore, wood quality trait improvement based research has been recently integrated into and become increasingly important in tree improvement programs (Yin et al. 2010; Jordan et al. 2011; Lenz et al. 2013)

According to Burdon (2000), the long term tree breeding goals are categorized into two themes; firstly, what qualities of wood are required by the silviculturist, product manufacturers and the consumers; and secondly, how can those qualities be inculcated into candidate materials as early as possible. Lenz et al. (2013) explained further that, there are two major constraints to the implementation of cost-effective tree breeding programs to enhance wood quality and they mentioned them as the high cost of traditional wood quality trait assessment methods and the long maturation period for the tree to be evaluated. Therefore, the search for nondestructive evaluation (NDE) tools that can effectively and accurately predict wood quality at the juvenile stage will be helpful in the selection of superior trees for onwards improvement (Lenz et al. 2013).

Over the years, wood quality properties especially stiffness and strength have been evaluated using traditional methods. These traditional methods are destructive, time-consuming, and labor intensive resulting in only a limited number of samples that can be tested for a given time span (Mora et al. 2009). These challenges associated with traditional testing methods generated interest in the search for alternative methods of evaluating wood quality properties including stiffness and strength with little or no damage to the products. This search has resulted in several nondestructive evaluations (NDE) and indirect methods of determining properties of wood including stiffness and strength (Carter et al. 2005; Mora et al. 2009; Yin et al. 2010; Schimleck et al. 2010; Wang 2013; Lenz et al. 2013). Some of these methods are spectroscopic analysis (Near Infrared Reflectance- NIR, FTIR), Thermogravimetric Analysis (TGA), Silviscan, ultrasonic and acoustic methods (Beall 2002; Mora et al. 2009; Wang 2013; Lenz et al. 2013). The application of these methods together with statistical tools had led to the successful prediction of several wood quality properties (Evans and Ilic, 2001; Schimleck et al. 2005; Via et

al. 2009). The successful application of these tools as nondestructive evaluation methods in the wood industry has led to their application in seedlings, saplings, and trees in the tree breeding and improvement programs (Yin et al. 2010 and 2011; Lenz et al. 2013).

Recently, acoustic and ultrasonic methods seem to offer the flexibility and rapidity of predicting wood quality in the juvenile wood as required in the tree breeding and improvement programs than the other methods (Evans 2003; Wang et al. 2007; Yin et al. 2010 and 2011; Lenz et al. 2013). The acoustic methods have been successfully used to predict the stiffness and strength of several different wood species such as Douglas fir (*Pseudotsuga menziesii* (Mirb). Franco), Eucalyptus (*Eucalyptus obliqua*), White spruce (*Picea glauca* (Moench).Voss) and radiata pine (*Pinus radiata* D. Don) (Wang et al. 2001 and 2004; Yin et al. 2010). The successful prediction of strength is likely due to the tight correlation between stiffness and strength (Via et al. 2009). It has been found that acoustic velocity is heritable with a heritability value ranging from low in Douglas fir (El-Kassaby et al. 2011), moderate in radiata pine (Wielinga et al. 2009) to high in White spruce (Lenz et al. 2013). Lenz et al. (2013) found a correlation between the genes controlling acoustic velocity and MFA.

1.2 Wood acoustics

Wood is a dispersive material indicating that wave propagated through it changes frequency with passage through the material (Beall, 2002). Generally, wood acoustics involves the transmission of high energy sound waves through the wood.

Acoustic waves have been broadly categorized into four groups based on the frequencies of the propagated waves. They are infrasonic, sonic, ultrasonic, and hypersonic. The infrasonic waves have frequency below 20Hz, sonic with the frequency range between 20Hz to 20 kHz,

ultrasonic with a frequency between 20 kHz to 1 GHz, and the hypersonic with frequency greater than 1GHz (Figure 1.1) (Smith 2001; www. Sengpielaudio.com). The authors further explained that frequencies within the sonic and the ultrasonic range are utilized in wood acoustic studies while hypersonic frequency waves are utilized in the acoustic microscopy. However, Beall (2002) noted that since material attenuation increases exponentially with frequency, 100 – 200 kHz upper limit of transducer frequencies are utilized in wood – based material characterization studies.

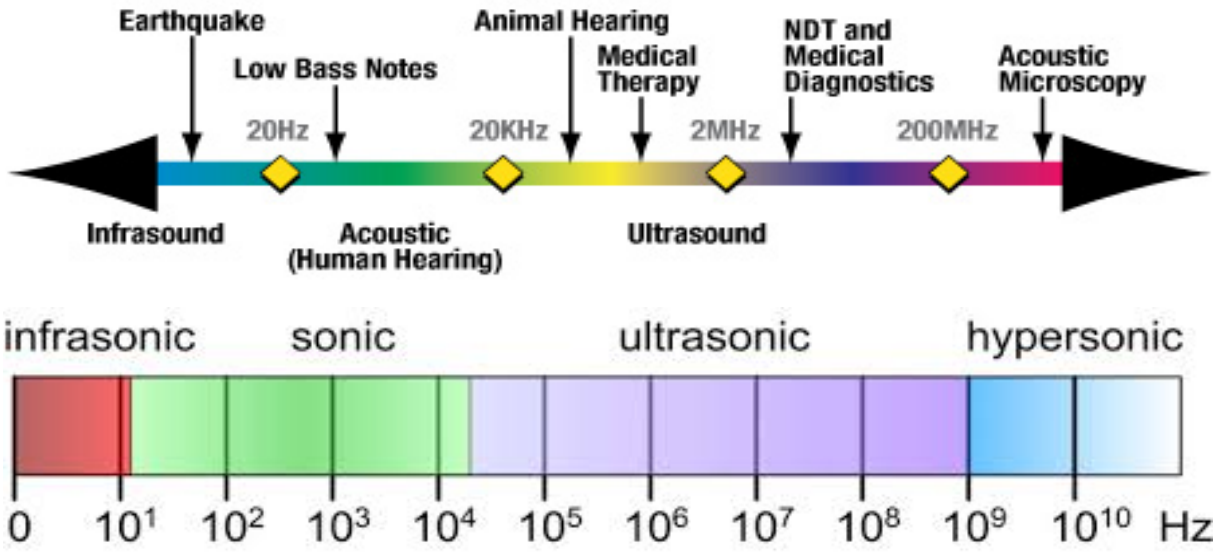

Figure 1.1 Categorization of the sound wave based on the frequency (adapted and modified from Google, accessed Jan. 2017)

Basically, there are two types of acoustic techniques based on the mode of generating the sound waves in the wood. They are the stress wave and the ultrasonic wave techniques (Yin et al. 2010). The stress wave involves striking the wood or the inserted probe to generate the sound wave and detecting the generated waves with either accelerometer or microphones while the ultrasonic wave(Portable Ultrasonic Nondestructive Digital Indicating Tester (PUNDIT)) entails detecting the sound pulse through electrical means using transducers (Yin et al. 2010).

Within the stress wave category, different approaches are used to determine the velocity of sound in wood or wood-based material, but the two main types are the resonance and time – of – flight (TOF) methods. The resonance approach depends on the length of the material and the fundamental frequency of the sound wave (Ilic 2001; Wang et al. 2007; Yin et al. 2010; Wang 2013) (Figures 1.2 – 1.4). The TOF method determines the velocity based on the distance between the accelerometer (probes) and the time required for the generated signal to cover that distance (Yin et al. 2010; Wang et al. 2004; Wang 2013; Essien et al. 2016a) (Figure 1.5 – 1.7).

However, the velocities estimated by these two approaches differ significantly with the velocity estimated by the TOF approach been higher than the resonance approach (Grabianowski et al. 2006; Mora et al. 2009; Wang 2013). Several reasons have been assigned to this observation by different authors. Chauhan and Walker (2006), Mora et al. (2009) attributed this difference to the fact that single-pass transit-time velocities of the time -of- flight method is sensitive to the localized stiffer outerwood zone which lies in the pathway of the propagated waves between the accelerometers. However, Wang et al. (2007) and Wang (2013) explained that these two approaches determine acoustic velocity differently. They explained that the fundamental wave equation in a long, slender and isotropic material (Figure 1.4), strain, and inertia in the transverse direction is neglected; hence, the velocity is dependent on density and modulus of elasticity of the material but independent of the Poisson's ratio (Equations 1 and 2). Hence, the resonance based acoustic tools (which require cut end of the wood to append the accelerometers) are used to determine the velocity of logs, timber, and lumber (Figures 1.2 – 1.3). The resonance velocity is determined based on the one-dimensional wave equation (Equation 1). Therefore the resonance based approach requires materials with exposed ends as in logs.

$$C_L = 2f_o L \qquad \text{Equation 1}$$

$$C_L = \sqrt{\frac{E}{\rho}} \qquad \text{Equation 2}$$

where C_L is the sound velocity of the log, f_o is the fundamental frequency, L is the length of the log, E is the dynamic modulus of elasticity and ρ is the density of the wood.

Figure 1.2 www.fibre-gen.com/ hitman PH330

Figure 1.3 www.fibre-gen.com/ hitman HM200

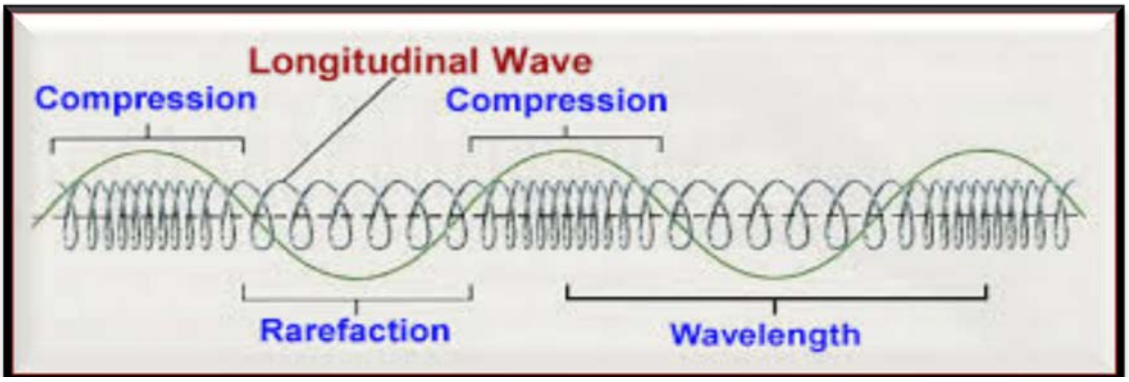

Figure 1.4 Model of wave propagation in long slender isotropic materials (adapted from Google, accessed Jan. 2017)

The TOF based approach, however, operates in an unbound elastic material such as a tree; the wave front is dominated by a dilatational wave (Figure 1.7). Mayer (1994) indicated that wave propagation is such an unbound material is governed by three-dimensional longitudinal

wave equation which is dependent on the density, modulus of elasticity and the Poisson's ratio of the material (Equations 3 - 4).

$$C_T = \frac{Distance}{Time}$$ Equation 3

$$C_T = \sqrt{\frac{1-v}{(1+v)(1-2v)}\frac{E}{\rho}}$$ Equation 4

where C_T is the sound velocity of standing tree, E is the dynamic modulus of elasticity and ρ is the density of the wood, , v is the Poisson's ratio of wood

According to Meyer (1994) and Wang (2013), three types of sound waves are generated when a piece of wood is suddenly stricken with a hammer (Figure 1.7). The generated waves are the Rayleigh wave, shear waves, and longitudinal wave. The Rayleigh wave is often confined to the area close to the surface and the particles are in to- and- fro as well as backward - forward motion forming an elliptical path. The longitudinal waves represent the vibrations of the particles in the direction of the propagated waves hence the particle velocity is parallel to the velocity of the waves. However, in the shear waves, the motion of the particles carrying the wave is perpendicular to the propagation direction of the wave. Even though shear and Rayleigh waves carry most of the energy from the disturbance, the longitudinal wave travels fastest and the easiest to detect hence it's frequently been used in material property characterization (Meyer, 1994).

Figure 1.5 www.fibre-gen.com/ hitman ST300

Figure 1.6 Fakopp microsecond treesonic

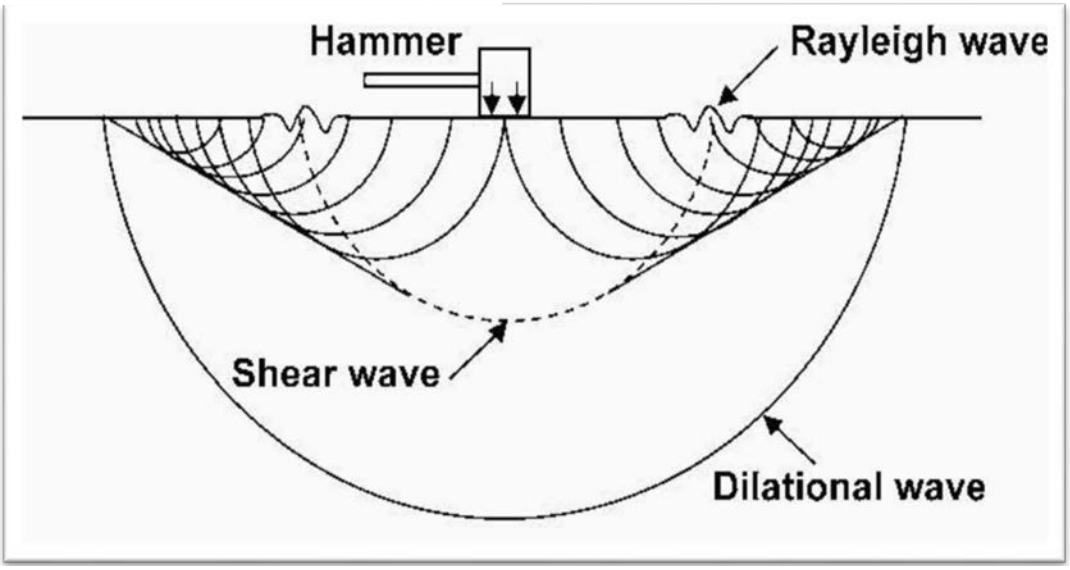

Figure 1.7 Model of wave propagation in an unbound isotropic material (adapted from Wang (2013))

The acoustic tools have been used to predict the stiffness and strength in several wood and wood-based products as indicated. Wood is an anisotropic and orthotropic material with the properties varying on the radial, tangential and the longitudinal directions. It also varied within and between species grown on same and / or different sites. These inherent variabilities make extrapolating results from one species to another inconsistent and inaccurate. More so, the

fundamental premise on which the acoustic tools are built is not valid for wood since wood is neither isotropic nor homogeneous.

The acoustic velocity differs with the orthotropic axes of the wood and it is about five times higher in the longitudinal direction as compared to the transverse direction. Also, it about 50% higher in the radial direction as it is in the tangential direction (Harris and Andrews 1999; Beall 2002; Chauhan et al. 2006; Hasegawa et al. 2011). The acoustic velocity has been found to decrease with increasing moisture content until the fiber saturation point is reached, above which changes in moisture does not significantly affect velocity (Olivito 1996; Chan et al. 2011; Gao et al. 2012). Biernacki and Beall (1993) found that sound velocity decreases with increasing grain angle. Different results have been reported on the relationship between density and acoustic velocity by different authors. Hasegawa et al. (2011) and Bucur (2006) found a negative correlation between longitudinal acoustic velocity and air-dry density. Mishiro (1995) reported that the acoustic velocity of seven softwoods and12 hardwoods were independent of their air-dry densities while Ilic (2001) and Lachenbruch et al. (2010) found a positive correlation between acoustic velocity and air-dry density. Acoustic velocity has a positive correlation with MOR and MOE (Ilic, 2001; Lachenbruch et al. 2010). Hasegawa et al. (2011) reported a positive correlation between the acoustic velocity and fiber length while a negative correlation MFA has been reported.

1.3 Problem statement

Previous studies on the use of acoustic techniques with loblolly pine focused on determining the passage pathway of the acoustic wave in 29 years old stand (Mahon et al. 2009), comparing the stiffness of 14 to 19 years old loblolly pine as predicted by acoustic techniques

and static bending test (Mora et al. 2009; Gonzalez et al. 2010). Mora et al. (2009) also found that using green density in estimating the stiffness of standing tree overestimate the stiffness hence recommended adjustment factors for the density. However, unlike other isotropic materials where only the weight changes with moisture, both the weight and volume of wood changes with alteration in moisture (FPL, 2010). Therefore, the moisture condition of the wood at which the density is determined must be stated to aid comparison. Green density is the mass per unit volume of wood with moisture content above the fiber saturation point. Green density is highly influenced by the weight of the moisture since beyond the fiber saturation point, the volume of wood is constant, and hence, any change in density is due to the moisture. Basic density is determined as the ratio of oven-dry weight to the unit green volume of the wood. It is very useful in designing wooden structural and products development where stiffness is a critical factor. Oven-dry density on the other is the ratio of oven-dry weight to the unit oven-dry volume of the wood and it useful in determining biomass yield in pulp and paper as well as bio-fuel related industries (FPL 2010). Also, it is useful in determining the design value of wood species (FPL 2010). However, the latter two densities which directly relate to the end products of the tree are invariant to moisture variation above the fiber saturation point.

Unfortunately, the basic and oven-dry densities have not been considered in determining the dynamic MOE of trees because above fiber saturation point, both velocity and these densities will not be affected by moisture (Olivito 1996; Chan et al. 2011; Gao et al. 2012). Understanding the combinative effects among these densities and the velocities determined by various acoustic tools in predicting dynamic stiffness in comparison with the MOE results obtained from static bending test will provide useful data for equipment calibration and direct product classification.

Via et al. (2009) reported that hemicellulose and cellulose associated wavelengths were very significant in predicting the strength and stiffness of 41 year old longleaf pine using principal component regression and near infrared reflectance (NIR) spectroscopy (Figure 1.8). Since acoustic tools are used to predict stiffness, it is expected that velocity will exhibit similar response to the polymeric constituents (cellulose, hemicellulose, and lignin). However, very little is known about the influence of the polymeric constituents on acoustic velocity. To date, only isolated examples exist where a study considered only one trait at a time, while the effect of all other traits that might influence velocity was assumed to be held constant. For example, Hori et al. (2002) found a positive correlation between acoustic velocity and cellulose crystallinity and a negative relationship between crystallinity and microfibril angle (MFA). The present study aimed at understanding the fundamental relationships between the elastic properties and polymeric constituents of wood (Figure 1.9).

Loblolly pine breeding program in the southern United States is one of the success stories in tree improvement in the world. The diameter gain of the improved stocks of loblolly pine is more between 15 to 30% more than the unimproved stocks in the southern United States (Roth et al. 2007). These fast growing trees produce wood with a considerable amount of juvenile wood which has reduced modulus of elasticity (stiffness), modulus of rupture (strength), high MFA and therefore poses utilization challenges. Consequently, the design values for the visually graded southern pine lumber (including loblolly pine) were generally adjusted in 2013 to reflect the material quality on today's market. As a future direction of improvements in loblolly pine, stakeholders want to select and deploy elite families with superior wood quality properties to meet the expected future demands. Acoustic techniques have been found to be one of the

nondestructive evaluation options for rapid characterization of seedlings and trees in tree breeding programs.

This study focused on understanding some fundamental concepts of acoustic techniques as a nondestructive evaluation tool for rapid characterization of trees in tree breeding and forest management operations with special reference to fifteen selected 14- year old elite loblolly pine families grew on two sites in the southern United States.

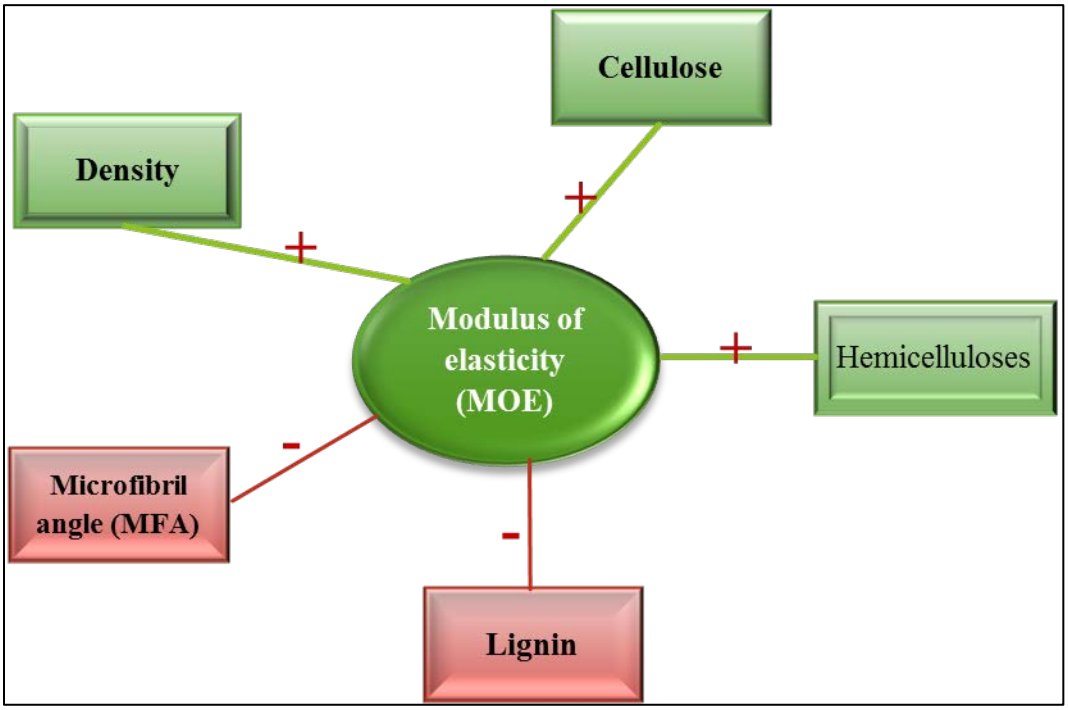

Figure 1.7 Model of relationship between MOE and other wood properties

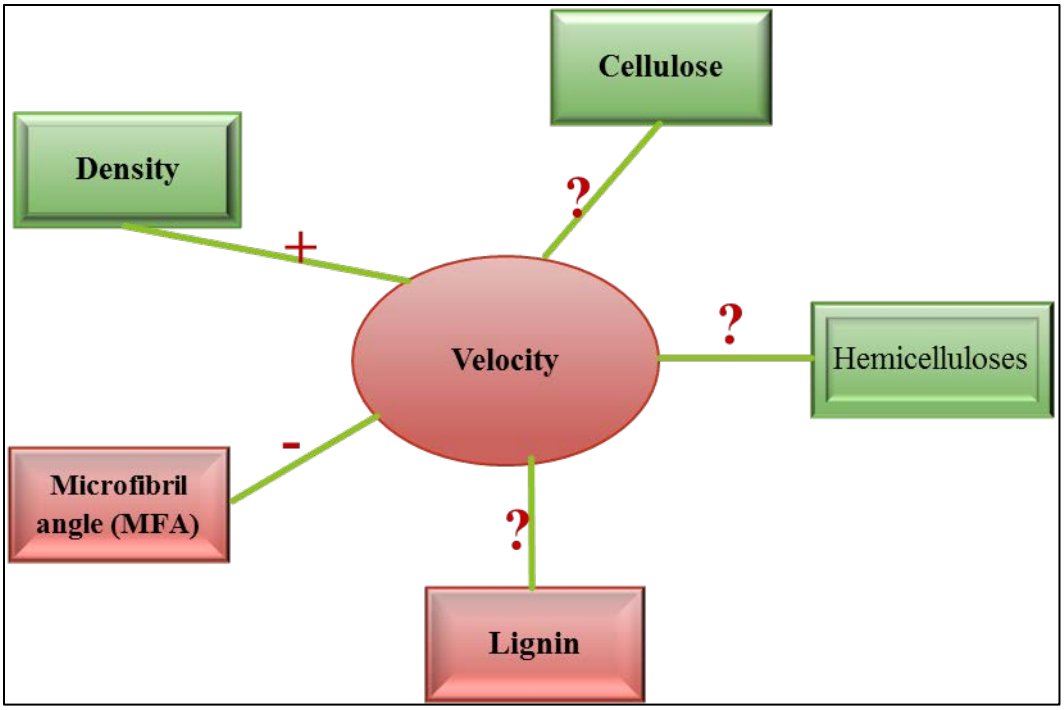

Figure 1.8 Conceptual model of relationship between velocity and other wood

1.4 References

Andrews, MK (2003) Which acoustic speed? *In* Proceedings of the 13th International Symposium on Nondestructive Testing of Wood. *Edited by* F.C. Beall. Forest Products Society, Madison, Wis. pp. 159–165.

Auty D., and Achim, A. (2008) The relationship between standing tree acoustic assessment and timber quality in Scots pine and the practical implications for assessing timber quality from naturally regenerated stands. Forestry, **81**(4): 475–487. doi:10.1093/forestry/cpn015.

Beall FC (2002) Overview of the use of ultrasonic technologies in research on wood properties. Wood Sci and Technol 36: 197-212

Biernacki JM and Beall FC. (1993) Development of an acoustic-ultrasonic scanning system for NDE of wood and wood laminates. Wood Fiber Sci 25:289–297

Bucur V (2006) *Acoustics of Wood*; Springer-Verlag: Berlin, Germany

Burdon RD, RD Kibblewhite, J. C.F. Walker, R. A. Megraw, R. Evans and Cown DJ (2004) Juvenile versus mature wood: a new concept, orthogonal to corewood versus outewood, with special reference to Pinus radiata and P. taeda. Forest Sci. 50: 399-415.

Carter PD, Briggs R, Ross J and Wang X (2005) Acoustic testing to enhance western forest values and meet customer wood quality needs. PNW-GTR-642. In: Harrington CA, Schoenholtz SH (eds) Productivity of western forests: A forest products focus. USDA Forest Service, Pacific Northwest Research Station, Portland, pp 121-129

Cave ID and Walker JCF. (1994). The stiffness of wood in fast-grown plantation softwoods: the influence of microfibril angle. Forest Prod J 44(5):43–48

Chan JM, Walker JC and Raymond CA. (2011). Effect of moisture content and temperature on acoustic velocity and dynamic MOE of radiata pine sapwood boards. Wood Sci Technol 45:609-626

Chauhan SS, and Walker JCF. (2006). Variations in acoustic velocity and density with age,and their interrelationships in radiate pine. For. Ecol. Manage. **229**(1–3): 388–394. doi:10.1016/j.foreco.2006.04.019.

Evans R and Ilic J. (2001) Rapid prediction of wood stiffness from microfibril angle and density. For. Prod. J. 51(3): 53–57.

Forest Products Laboratory (FPL).2010. Wood handbook—Wood as an engineering material. General Technical Report FPL-GTR-190. Madison, WI: U.S. Department of Agriculture, Forest Service, Forest Products Laboratory.

Ilic J (2001) Variation of the dynamic elastic modulus and wave velocity in the fiber direction With other properties during the drying of *Eucalyptus regnans* F. Muell. Wood Sci Technol 35:157-166

Eastin I. (2004). Does Wood Quality Really Matter to Builders? Productivity of Western Forests: A Forest Products Focus. Sept. 20-23, Kamiche, WA.

El-Kassaby YA, Mansfield S, Isik, F, and Stoehr M. (2011) *In situ* wood quality assessment in Douglas-fir. Tree Genet. Genome. *7*, 553–561.

Evans R. (2003) Wood stiffness by X-ray diffractometry. Proceedings of the workshop; characterization of the cellulosic cell wall, Grand Lake Colorado, 25-27 August 2003. The University of Iowa and the Society of Wood Science and Technology, Madison

Fox TR, Jokela EJ, and Allen HL. (2007). The development of pine plantation Silviculture in the southern United States. J. For. 105: 337-347.

Gao S, Wang X, Wang L, and Allison RB. (2012). Effect of temperature on an acoustic evaluation of standing trees and logs: part 1 – laboratory investigation. Wood and Fiber Science 44(3):286-297

Gapare WJ, Hathorn A, Kain D, Matheson AC, and Wu HX. (2007) Inheritance of spiral grain in the juvenile core of Pinus radiata D. Don. Can J For Res 37:116–127

Gapare WJ, Wu HX, and Abarquez A. (2006). Genetic control of the time of transition from juvenile to mature wood in *Pinus radiata* D. Don. Ann For Sci 63:871–878

Gonzalez-Benecke CA, Martin TA, Clark III A and Peter G.F. (2010).Water availability and genetic effects on wood properties of loblolly pine. Can. J. For. Res.40:2265-2277

Grabianowski M, Manley B, and Walker JCF (2006) Acoustic measurements on standing trees, logs and green lumber. Wood Sci. Technol., 40, 205–216.

Gindl W, and Teischinger A. (2002). Axial compression strength of Norway spruce related to structural variability and lignin content. Composite. A 33: 1623–1628.

Harris PD, and Andrews MK. (1999) Tools and acoustic techniques for measuring wood stiffness. In: Proceedings of the 3rd wood quality symposium: emerging technologies for evaluating wood quality for processing, Forest Industry Engineering Association, Rotorua, New Zealand

Hasegawa M, Takata M, Matsumura J and Oda K. (2011) Effect of wood properties on within-tree variation in ultrasonic wave velocity in softwood. Ultrasonics 52: 296-302

Ivkovic M, Gapare WJ, Abarquez A, Ilic J, Powell MB and Wu HX. (2009) Prediction of stiffness, strength, and shrinkage in the juvenile wood of radiate pine. Wood Sci Technol 43: 237-257

Jordan L, Schimleck LR, Clark III A, Hall DB and Daniels RF. (2007) Estimating optimum sampling size to determine weighted core specific gravity of planted loblolly pine. Can. J. For. Res. 37:2242-2249

Lachenbruch B, Johnson GR, Downes GM, and Evans R. (2010). Relationship of density, microfibril angle and sound velocity with stiffness and strength in matured of Douglas fir. Can. J. For. Res. 40:55-65

Lenz P, D. Anty, Achim A, Beaulieu J and Mackay J. (2013) Genetic improvement of White Spruce mechanical wood traits – Early screening by means of acoustic velocity. Forest 4: 575-594. Doi10.3390/f4030575

McKeand S, Mullin T, Byram T and White T. (2003) Deployment of genetically improved loblolly and slash pine in the South. J. For. 101: 32-37.

Meyers MA. (1994). Dynamic behavior of materials. Wiley, New York

Mishiro A. (1995). Ultrasonic velocity in wood and its moisture content I: effect of moisture gradients on ultrasonic velocity. Mokuzai Gakkaishi 41: 1086-1092

Mora CR, Schimleck LR, Isik F, Mahon Jr JM, Clark III A, and Daniels RF. (2009). The relationship between an acoustic variable and different measures of stiffness in standing *Pinus taeda* trees. Can. J. For. Res. 39:1421-1429

Olivito R S. (1996). Ultrasonic measurements in wood. Materials Eval 54:514–517

Pine Integrated Network: Education, Mitigation and Adaptation Project PINEMAP. (2017). Available online: http://www.pinemap.org/ (accessed on 1 January 2017).

Roth BE, Li X, Huber DA, Peter GF (2007) Effects of management intensity, genetics and planting density on wood stiffness in a plantation of juvenile loblolly pine in the southeastern USA. For. Ecol. Manage 246: 155 – 162 doi 10.1016/j.foreco.2007.03.028

Schimleck LR, Mora CR, Peters GF and Evans R. (2010). Alternative methods for nondestructively determining the modulus of elasticity in young trees. IAWA J 31(2): 161-167

Schimleck LR, Jones PD, Clark A III, Daniels RF, and Peter GF. (2005). Near infrared spectroscopy for the nondestructive estimation of clear wood properties of *Pinus taeda* L. from the southern United States. For. Prod. J. **55**: 21–28.

Smith WR. (2001). "Wood: Acoustic properties," In*:* Encyclopedia of Materials: Science and Technology, Elsevier Science Ltd., London, 9578-9583.

Via BK, So CL, Shupe TF, Groom LH and Wikaira J. (2009). Mechanical response of longleaf pine to variation in microfibril angle, chemistry associated wavelengths, density and radial position. Composites: Part A 40:60-66

Via BK, So C, Groom LH, Shupe TF, Stine M, and Wikaira J. (2007). Within tree Variation of lignin, extractives, and microfibril angle coupled with the theoretical and near infrared modeling of microfibril angle. IAWA J 28:189–209.

Wang X. (2013). Acoustic measurement on trees and logs: a review and analysis. Wood Sci Technol 47:965-975

Wang X, Ross RJ, Green DW, Brashaw B, Englund K and Wolcott M. (2004). Stress wave sorting of red maple logs for structural quality. Wood Sci. Technol. 37: 531-537.

Wang X, Ross RJ, McClellan M, Barbour RJ, Erickson JR, Forsman JW and McGinnis GD. (2001). Nondestructive evaluation of standing trees with a stress wave method. Wood and Fiber Sci. 33(4): 522-533.

Wang X, Ross RJ and Carter P. (2007). Acoustic evaluation of wood quality I standing tree. Part 1: acoustic behavior in standing tree. Wood Fiber Sci. 39(1): 28-38

Wielinga B, Raymond CA, James R and Matheson AC. (2009). Effect of green density values on *Pinus radiata* stiffness estimation using a stress-wave technique. NZ J. For. Sci. 39: 71–79.

Yin Y, Nagao H, Liu X, and Nakai T (2010). Mechanical properties assessment of *Cunninghamia lanceolata* plantation wood with three acoustic-based nondestructive methods. J. Wood Sci. 56:33-40

Yin Y, Jiang X, Wang L. and Bian M. (2011). Predicting wood quality of green logs by resonance vibration and stress wave in plantation grown *Populus X euramericana.* Forest Prod. J. 61(2):136-142

Zobel BJ, and Sprague JR (1998). Juvenile wood in forest trees. Springer, Berlin, p 300

Chapter 2: Multivariate Modeling of Acousto-mechanical Response of Fourteen Year Old Suppressed Loblolly Pine (*Pinus taeda*) to Variation in Wood Chemistry, Microfibril Angle and Density

2.1 Abstract

The polymeric angle and concentration within the S_2 layer of the softwood fiber cell wall are very critical for molecular and microscopic properties that influence strength, stiffness and acoustic velocity of wood at the macroscopic level. The main objective of this study was to elucidate the effect of cellulose, hemicellulose, lignin, microfibril angle and density on acoustic velocity and material mechanical properties of 14 year old suppressed loblolly pine.

Cellulose, hemicellulose and density are consistently the most important drivers of strength, stiffness and velocity. Cellulose and lignin are the highest and lowest contributor to velocity respectively with lignin acting as a sound wave dispersant, while cellulose is the most important conductor of sound wave at the molecular level and hemicellulose acts as a special coupling agent between the these components. The polymeric constituents are thus important drivers of sound wave propagation at the molecular level while density played a subsequent role at the macroscale.

2.2 Introduction

Wood is a fibrous material made up of tubular cells that account for 90% of all softwood cells in the tree. These cells provide resistance to load bearing forces caused by tree weight and wind loading (Marra 1979). At the macroscopic level, wood is an anisotropic material that can be used as solid lumber and in the reinforcement of advanced composite products (Bodig and Jayne 1982). At the molecular level, wood is composed of cellulose, hemicellulose and lignin. Cellulose is the stiffest polymer in wood due to its high degree of polymerization, crystallinity, and linear orientation. Hemicellulose is a non-crystalline branched molecule composed of a linear backbone of galactoglucomanan and glucomanan, which is attached with side chains of pentose and hexose (Winandy and Rowell 2005). Winandy and Rowell (2005) stated that hemicellulose functions to connect the non-crystalline part of hydrophilic cellulose to the amorphous and hydrophobic lignin. Thus hemicellulose acts to transfer stress between cellulose and lignin (Via et al. 2009). Lignin is a large hydrophobic tri-dimensional and highly branched phenolic molecule which binds and holds other polymers together. It is also a stiffening agent for cellulose and provides resistance to compression forces (Winandy and Lebow 2001).

Researchers have hypothesized that these polymeric constituents influence the mechanical and acoustic properties of wood and wood products. These natural polymers are carefully engineered by nature to bear and distribute loads imposed on a growing tree. Several polymeric cross sectional structural models exist to explain the morphology of this composite matrix, but most agree that the elementary fibrils of cellulose exhibit the least variation in dimension due to their high crystallinity, coupled with the interaction between the lignin and hemicellulose matrix. The hemicellulose matrix is sandwiched between lignin and the amorphous portion of the cellulose elementary fibrils and is thus defined as a coupling agent

Reprinted from Wood Science and Technology DOI 10.1007/s00226-017-

between cellulose and lignin (Winandy and Rowell 2005; Via et al. 2009). The highly hydrophobic lignin polymer acts as a sheath around the hydrophilic cellulose and hemicellulose matrix. The lignin polymer is entangled in the xylan portion of the hemicellulose, while the glucomannan of hemicellulose is attached to the non-crystalline portion of the cellulose elementary fibrils (or microfibrils). Cellulose has been shown to significantly influence the elastic phase, when the load is applied nearly parallel to the cellulose plane, and thus is anticipated to impact modulus of elasticity (MOE) at the macroscale. Lignin and hemicellulose become dominant as the axis of the load is at an increased angle to the axis of the microfibrils. Strength is reduced by a factor of 10 at the nanoscale level for loads applied at a transverse angle to the fiber axis (Via et al. 2009; Gridl and Schoberl 2004). At the macroscopic level, softwoods are composed of 90% longitudinal fiber elements specialized for fluid conduction and mechanical strength. These fibers have multilayered cell walls consisting of one primary cell wall layer and three secondary layers (S_1, S_2, and S_3). These layers are differentiated by the degree of orderliness and orientation of the crystalline portion of the cellulose. The S_2 layer is considered most important for the acoustic, or elastic, response of wood because it is located at the middle portion of the cell wall and accounts for 83% of the overall secondary cell wall (Gridl and Schoberl 2004).

The acoustic properties of live trees have been of significant interest in recent years because stems currently being harvested without any knowledge of the internal stiffness quality which affects the performance of the material. The velocity of acoustic waves propagating through the tissue of trees has been measured to estimate the stiffness of wood, but little is known about the influence of the polymeric constituents on acoustic velocity. It has been hypothesized that the acoustic response of wood varies as a function of wood chemistry, macro

density, and the angle of the aggregate polymers. To date, only isolated examples exist where a study considered only one trait at a time, while the effect of all other traits that might influence velocity were assumed to be held constant. For example, Hori et al. (2002) found a positive correlation between acoustic velocity and cellulose crystallinity and a negative relationship between crystallinity and MFA. This was probably the result of increased acoustic velocity along the cellulose crystalline structure with MFA providing the primary direction of the fastest wave propagation. On the other hand, a polymer such as lignin is lower in density, three dimensional in structure, and is thus more likely to absorb or diffuse acoustic energy in multiple directions resulting in some energy loss and a reduction in acoustic velocity. However, to our knowledge, no studies have tested such a hypothesis, nor has the relationship between multiple polymeric constituents and velocity been reported within a single study. Thus, the main objective of this study was to explore the effects of polymeric constituents, density, and MFA on the modulus of rupture (MOR), modulus of elasticity (MOE), and acoustic velocity of 14 year old suppressed loblolly pine. Suppressed loblolly pine has been reported to contain less cellulose, more lignin and hemicellulose than the normal wood. It also has higher MFA, wider growth rings with higher proportions of latewood as compared to normal wood (Donaldson et al. 2004). Thus we suspect these properties will significantly affect the relationship between the polymeric constituents versus velocity and mechanical properties.

2.3 Materials and Methods

2.3.1 Materials

The materials for this study were selected from a plantation of genetically improved families of loblolly pine (*P. taeda*), located at Brantley County near Nahunta, Georgia, USA

(latitude 31°12′16′′N and longitude 81°58′56′′W). The topography of site is relatively flat with slope less than 2% and 20 m altitude above sea level. The soil is very fine sandy loam, poorly drained and generally poor in nutrients which was formed from loamy and silty Coastal Plain sediments. The mean annual temperature ranged 17 to 19°C and the annual precipitation from 1981 to 2010 averaged 1315 mm (NOAA 2011). The total size of site was 6744 m^2 which was divided into fifteen blocks measuring 450 m^2. Eighty seedlings from eighty different genetically improved loblolly pine families were randomly planted on bed at 1.8 m x 3.6 m.

The stand had not received any commercial thinning since establishment. Eight trees were selected randomly from each family, with care taken to avoid trees with visible defects, such as leaning, forked stems, chlorotic needles, as well as other less significant growth defects. The diameters of the selected trees were measured at breast height and ranged from 8.8 to 12.6 cm with a mean of 10 cm.

2.3.2 Acoustic measurements

The selected trees were acoustically tested using the Director ST 300 acoustic tool (Fibre-gen, Christchurch, New Zealand), which relied on the Time-of-Flight (TOF) principle (Wang et al. 2001; Mora et al. 2009; Essien et al. 2016a). Basically, the accelerometers (i.e., the transmitter and the receiver probes) were positioned on the same side of the tree, 120 cm apart, with the center of the path positioned at breast height. Both probes were deployed at a 45° to the tree axis, and the stress wave was generated by striking the transmitter probe with a steel hammer using a steady force. The generated wave was detected by the receiver and the amount of time it took for the sound wave to travel the distance between the probes was recorded by the data logger, which displayed the velocity reading automatically (Mora et al. 2009; Essien et al.

2016a). Acoustic measurements were taken on the north and south aspects of the tree using a compass to determine location. Three readings were taken on the north and south aspect of each tree, respectively, resulting in a total of six readings per tree.

The selected trees were then harvested and bucked into 180 cm logs and 10 cm thick disks, alternately along the entire length, yielding 3 - 5 logs, depending on the length of the tree. All 34 logs obtained from the 8 trees were used to determine log acoustics. The log acoustic velocity was determined while they were still green using a Director ST300 tool, with the same operational procedure as described above. Six readings per log were taken from the north and south aspects of the logs. The 180 cm logs were crosscut into two equal parts and four pair of disks, measuring 2 cm thick, were taken from the freshly cut surfaces, with 2 pairs taken from each piece. Three pairs were used to determine the moisture content and basic disk density (referred to as "disk density" in this study). The dimensions of the disk were taken to the nearest 0.025 mm using a digital caliper and weight was measured to the nearest 0.001 g. The remaining pair was used for the chemistry and MFA analysis.

2.3.3 Static MOE and MOR determination

Static MOE and modulus of rupture (MOR) were determined using the small clear specimens measuring 2.5 x 2.5 x 41cm (radial x tangential x longitudinal) prepared from the remaining log samples after the specimens were conditioned (at 65%RH, 23^{o}C for three month) to approximately 12% equilibrium moisture content (EMC). Four outermost specimens (the first 2.5 cm sample obtained from each log without the bark material of the tree) from the north, south, east and west directions around the circumference of each log – totaling 136 specimens were used for the static bending tests following the protocols of ASTM D143 (ASTM D143

2007). The load was applied on the tangential-longitudinal face in a three-point conFigureuration using a Z010 Zwick Roell Testing System (Zwick Roell, Kennesaw, GA, USA) at a loading rate of 1.3mm/min. The linear portion of the load-deflection curve was used to determine MOE, while MOR was calculated using maximum bending moment at the maximum load borne by the specimen. The moisture content and outerwood density [referred to as outerwood density (ODW) in this study and it is the first 2.5 cm sample obtained without the bark material of the tree at test were determined following the protocols described in ASTM D143. The outerwood density was determined by measuring the dimensions of the samples with calipers to the nearest 0.025mm and the weight to the nearest 0.001g, all at 12% EMC.

2.3.4 MFA determination

Strips measuring 1 cm in width were extracted through the pith of the pair of disk samples meant for the MFA measurement. One sample was prepared in the "south- north" direction while the other was in the "east-west" direction. Two thin sections of wood samples measuring 0.2mm were sliced from along the entire length of both 1cm strips per log – one along the north-south and the other east – west directions. The thin samples were macerated using equal volumes of hydrogen peroxide (30%) and glacial acetic acid at 80^{o}C for 24 hours for thorough maceration (Peter et al. 2003). Temporary slides were prepared from the macerated fibers and an MFA measured following the procedure described by Peter et al. (2003). The MFA measurements were performed on forty fibers selected from both the earlywood and latewood using Differential Interference Contrast (DIC) Microscope (Olympus BX53).

2.3.5 Chemistry

The remaining portion of the disks that were used for the MFA measurements were also used for chemistry; although the MFA measurements were extracted from subsamples of a smaller scale. The wood was ground to pass the 40-mesh screen sieve using a 3383L10 Wiley Mini Mill (Thomas Scientific, Swedesboro, NJ). Five grams of the ground sample were extracted with 150ml of acetone for six hours using a Soxhlet apparatus. The extractive free samples were then used to determine the lignin, cellulose and hemicellulose content according to the NREL/TP 510-42618. One-half grams of the air-dried extractive free sample was digested with 72% sulfuric acid and incubated in a water bath set at 30^{o}C for two hours with intermittent stirring to ensure full and uniform hydrolysis. The solution was diluted with deionized water to a concentration of 4% and was then autoclaved at 121^{o}C for one hour. The residue after hydrolysis was filtered and oven-dry to calculate the acid insoluble lignin (AIL). In order to account for the total lignin content in the specimens, UV- spectrophotometer was used to determine the acid soluble portion of the lignin. Portions of the filtrate were used to determine the Acid soluble lignin (ASL) using UV- spectrophotometer (Genesys 10-S Thermo Fisher Scientific, Madison, WI) set at the absorbance wavelength of 240nm. The lignin content used in this study is the sum of the AIL and ASL. The remaining portion of the filtrate was used to determine the monosaccharide composition of the samples using High-Performance Liquid Chromatography (Shimadzu LC-20A) equipped with an Aminex 87 P column and differential refractive index detector, operated at 85^{o}C for 35 minutes. The holocellulose, cellulose and hemicellulose contents of the samples were calculated using equations 1, 2 and 3 respectively (Acquah et al. 2015; Jiang et al. 2014; Via et al. 2014)

$$Holocellulose = Glucan + Xylan + Arabinan + Mannan \qquad \text{Equation 1}$$

$$Cellulose = Glucan - (\frac{1}{3} * Mannan)$$ Equation 2

$$Hemicellulose = Holocellulose - cellulose$$ Equation 3

The actual moisture content of the air-dried extractive free samples used in this study were determined in order to calculate the dry weight of the samples used in the determination of the chemical composition of the samples and hence moisture was not included as weight during the computation of the cellulose, hemicelluloses and lignin. All experiments were performed in duplicate (Via et al. 2014)

2.3.6 Data analysis

The six acoustic measurements on each log were averaged to represent log velocity. The data gathered from the specimens of the same logs were collated and the average used to represent that particular log and those from the same logs were pooled together to represent the tree. The data analysis was performed using SAS program version 9.4 (SAS 2014). Pearson correlation method was used to determine the level of relationship among the predictors and response variables. The response variables were MOR, MOE and velocity while the predictors were cellulose, hemicellulose, lignin, MFA and density (outerwood and disk densities). The whole dataset was standardized by subtracting the mean and dividing by the standard deviation of each variable before the regression procedures were performed. Multiple linear regression and path analysis were performed to estimate the relative significance of the independent variables during the prediction of the response variables. The standard regression procedure in SAS was used to calculate the p-values for the independent variables and to build regression models. It is worth noting that the relationship between MFA and stiffness is not a linear response and thus

may be less sensitive to linear analysis than wood chemistry and density (Via et al. 2009; Via et al. 2012). To ensure the independent variables were not highly correlated, the variance inflation factor (VIF) was used and a VIF value less than 6 was set as the constraint to determine if the coefficient was stable while that greater than 6 meant that the coefficient was inflated and not reliable for interpretation purposes (Via et al. 2009; Via et al. 2012). The coefficient of determination (R^2) which demonstrates the proportion of variation within the response variable attributed to the predictor variables was reported (Via et al. 2009). The path analysis was then used to segregate the covariance coefficient into the direct and indirect components. Thus the effect of the predictor variable on the response variable will be the sum of both the direct and the indirect paths relationships (Lachenbruch et al. 2010). The fitted model:

$$Y_i = \beta_0 + \beta_1 density + \beta_2 cellulose + \beta_3 hemicellulose + \beta_4 lignin + \beta_5 mfa + \varepsilon_i$$

where Y_i is the response variable which can be MOR, MOE or velocity of the i-th sample, β_0 is the intercept of the model, β_1, β_2, β_3, β_4, and β_5 are the coefficients associated with density (either disk or outerwood density), cellulose, hemicellulose, lignin and MFA respectively. These parameters were test whether they are significantly different from zero.

2.4 Results and Discussion

2.4.1 Mechanical properties and velocity

The summary statistics of all the parameters studied are presented on Table 2.1. Generally there is a positive linear relationship between log velocity versus MOR and MOE with a coefficient of determination (R^2) of 52% and 69% respectively (Figure 2.1). A similar but statistically stronger relationship existed between tree velocity versus MOR and MOE with 66% and 84% R^2 respectively (Figure 2.2). There is a highly significant correlation between the log

velocity versus MOR (0.66) and MOE (0.79) with a $p<0.001$ (Table 2.2). There are significant linear relationship with coefficient of determination of 0.63 and 0.71 for tree velocity versus MOR and MOE respectively (Figure 2.2) at the tree level. There is a very tight positive relationship between MOR versus MOE (Figures 2.3 and 2.4, Table 2.2) indicating that trees can be segregated into strength and stiffness classes using acoustic TOF method (Wang et al. 2001; Mora et al.2009).

The results of this study is in conformity with Vikram et al. (2011) who reported a correlation coefficient of 0.40 and 0.90 for the relationship between static MOE versus log velocity and static MOE versus tree velocity respectively. In that study, 373 logs derived from 373 twenty-five year old Douglas fir trees (*Pseudotsuga menziesii*) were tested. Ilic (2001) reported a correlation coefficient of 0.63 and 0.76 for the relationship between MOR versus velocity and MOE versus velocity respectively when small clear samples obtained from 52 boards of mature *Eucalyptus delegatensis* were studied. The linear relationship of MOE versus tree velocity result presented in this work is in agreement with earlier studies (Ilic 2001; Vikram et al. 2011). The correlation coefficient for MOE versus log velocity reported in the present paper is probably higher than other studies due to the type of the acoustic tool used to measure log velocity. In this study Director ST 300 was used while Vikram et al. (2011) used the Director HM200. The Director HM200 is reported to measure the weighted velocity of the whole log instead of only the outer wood as measured by the Director ST 300 in large diameter trees (Raymond et al. 2008; Vikram et al. 2011). This approach has been argued to result in a 30% reduction in velocity for the HM200 versus the ST 300 (Mora et al. 2009).

For 20 year old Douglas fir, Lachenbruch et al. (2010) reported a correlation coefficient of 0.45 and 0.68 for the MOR versus tree velocity and MOE versus tree velocity respectively.

Ilic (2001) studied the relationship between MOR, MOE, and velocity of small clear samples and reported a 0.63 and 0.76 for MOR versus velocity and MOE versus velocity respectively. Although their correlation coefficients were lower than that reported in the present study, it follows a similar trend where there is a strong linear relationship between velocity and MOE than that with MOR. Fundamentally, report indicated that MOE had a stronger association with the cellulose (Via et al. 2009) while hemicellulose is strongly associated with MOR (Curling et al. 2000; Clausen and Kartal 2003). However none of these studies used acoustic technique and therefore could not elucidate the relationship between the polymeric constituents versus velocity and MOE. The tight relationship between velocity and MOE observed in this study is due to the close association of both properties to cellulose at the molecular level (Tables 2.2, 2.3 and 2.4). It is interesting to note that cellulose exerted stronger effect on velocity compared to density in both models (Tables 2.3 and 2.4). This explains the stronger linear relationship between velocity versus MOE than MOR observed in this study.

There is a very tight positive linear relationship between MOR and MOE (Figures 2.3 and 2.4). A similar relationship was reported by Via et al. (2009). This tight relationship between the MOR and MOE is due to the same set of polymeric constituents driving these properties at the macroscale as observed in this study. Primarily cellulose, hemicellulose and density are the major drivers of MOR and MOE.

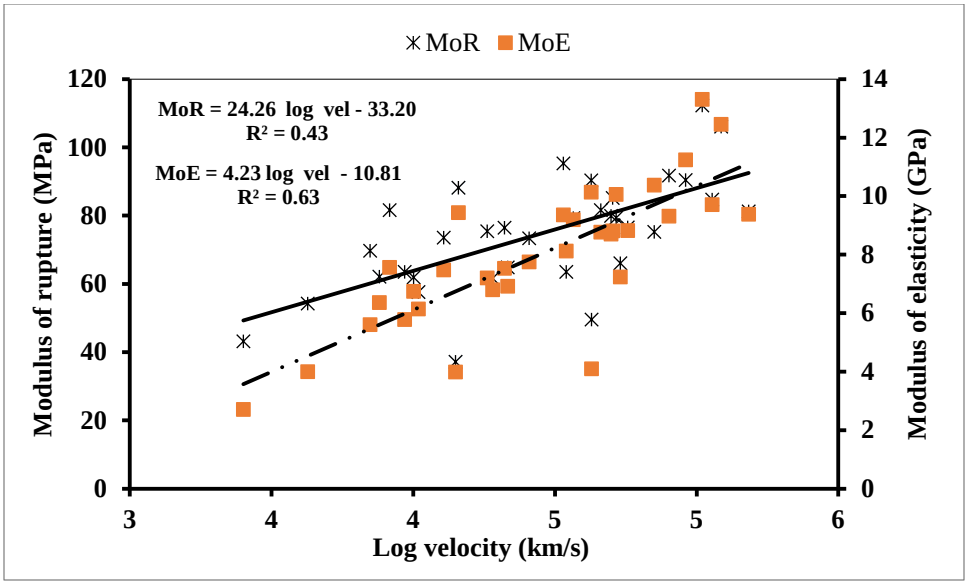

Figure 2.1 Fitted linear relations between log velocity versus MOR and MOE

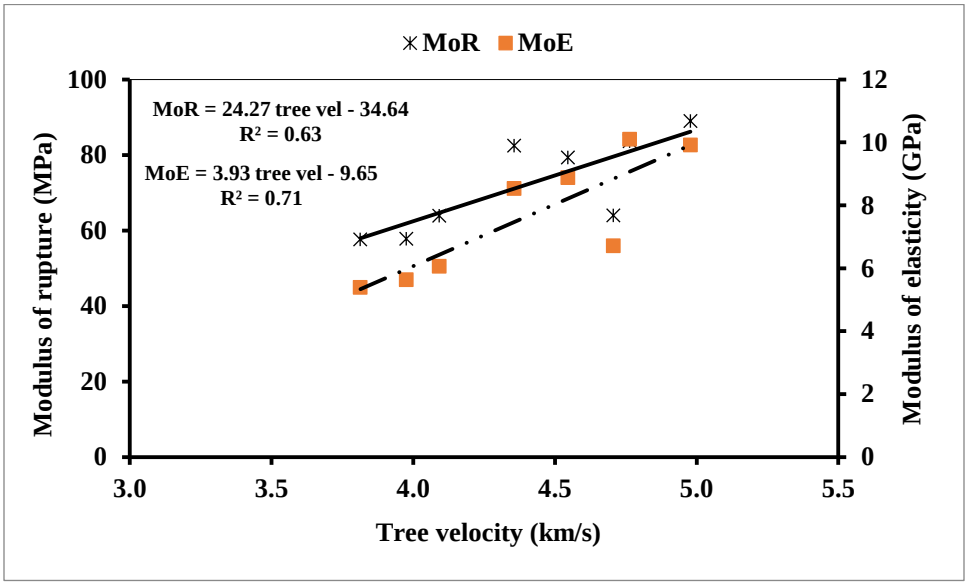

Figure 2.2 Fitted linear relations between tree velocity versus MOR and MOE

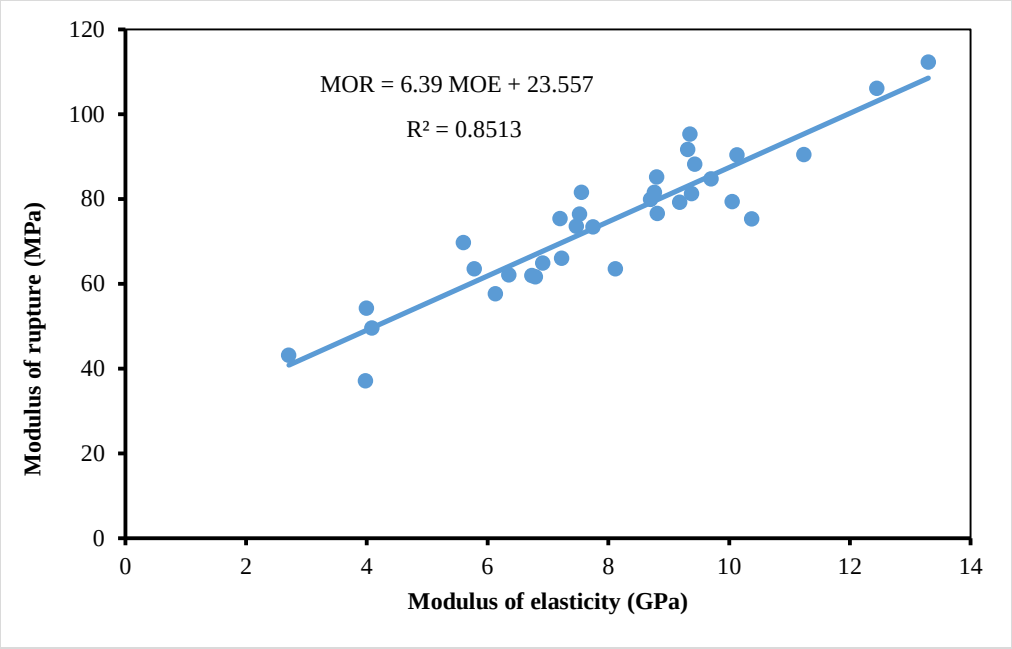

Figure 2.3 Relations between MOR and MOE for the 34 logs

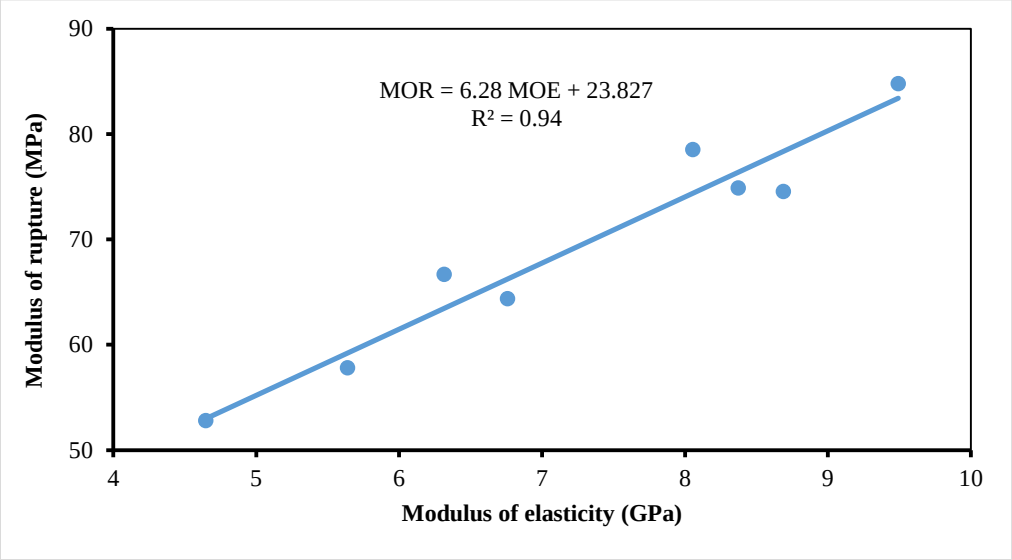

Figure 2.4 Relations between MOR and MOE for the 8 trees

Table 2.1 Summary descriptive statistics of log velocity, chemistry and wood properties

	Mean	Standard deviation	Minimum	Maximum
Disk density (DD) (g/cm^3)	0.57	0.06	0.47	0.73
Outerwood density (OWD) (g/cm^3)	0.56	0.08	0.42	0.76
Modulus of elasticity (MOE) (GPa)	7.97	2.37	2.71	13.30
Modulus of rupture (MOR) (MPa)	74.47	16.42	37.10	112.25
Cellulose (%)	42.01	2.30	38.46	48.15
Hemicelluloses (%)	23.84	3.55	16.86	29.91
Lignin (%)	27.39	0.99	25.20	29.39
log velocity (km/s)	4.44	0.44	3.40	5.18
MFA (^{o})	23.88	2.15	19.35	28.05

Table 2.2 Simple correlation coefficient among log velocity, chemistry and wood properties

	DD	OWD	MOE	MOR	Cellulose	Hemi-cellulose	Lignin	Log velocity	MFA
DD									
OWD	0.81***								
MOE	0.40*	0.72***							
MOR	0.54**	0.81***	0.92***						
Cellulose	-0.02 ^{ns}	0.27^{ns}	0.38*	0.22 ^{ns}					
Hemi-celluloses	-0.17 ^{ns}	-0.08 ^{ns}	0.25 ^{ns}	0.22 ^{ns}	-0.38*				
Lignin	-0.27 ^{ns}	-0.32 ^{ns}	-0.04 ^{ns}	-0.11 ^{ns}	0.05 ^{ns}	0.21 ^{ns}			
Log velocity	0.39*	0.59***	0.79***	0.66***	0.48**	0.10 ^{ns}	-0.14 ^{ns}		
MFA	-0.14 ^{ns}	-0.11 ^{ns}	-0.04 ^{ns}	-0.09 ^{ns}	-0.05 ^{ns}	0.16 ^{ns}	-0.06 ^{ns}	0.16 ^{ns}	

*p<0.05, **p<0.01, ***p<0.001, ns not significant at p >0.05 DD= disk density OWD = outerwood density, MOE= modulus of elasticity, MOR= modulus of rupture

2.4.2 Velocity and density

Generally, there is a linear positive relationship between velocity and density (Figures 2.5 and 2.6, Table 2.2). However, outerwood density explained a higher variation in velocity than disk density (Figure 2.7). The trend reported in the present study confirms the trends reported in previous studies (Wang et al. 2001; Ilic 2001; Lachenbruch et al. 2010; Vikram et al. 2011; Lenz et al. 2013). Vikram et al. (2011) studied the relationships among standing tree velocity, log velocity and basic density (calculated from whole disks), and reported significant correlations of 0.29 and 0.33 respectively for tree velocity versus basic density and log velocity versus basic density respectively. However, the same relations but with air-dry density (calculated from 5x10 cm stakes) yielded a correlation coefficient of 0.29 and 0.39 for tree velocity versus air-dry density and log velocity versus air-dry density respectively (Vikram et. al. 2011). Lachenbruch et al. (2010) reported a significant tree velocity versus air-dry density correlation of 0.42 (P=0.02).

The correlation between velocity versus air-dry density, for small clear samples was highly significant (p=0.0001) (Ilic 2001). These trends however contradicted results presented by Hasegawa et al. (2011). Hasegawa et al. (2011) studied 60-year old Japanese cedar (*Cryptomeria japonica*) and 28-year old Japanese cypress (*Chamaecyparis obtuse*). They reported a highly significant negative correlation between velocity and air-dry density of these two species (p=0.01). This negative correlation might be due to the decreasing density gradient from pith to the bark of their species. On the other hand, the density gradient increased from pith to the bark in most pine species including loblolly pine. These contrasting density gradients may be responsible for the positive relations between velocity and density reported in this study as compared to that reported by Hasegawa et al. (2011).

The observed high correlation between outerwood density and velocity (Figure 2.5) may seem to indicate the path of flight of the Time – of – Flight (TOF) acoustic tool is limited to the outerwood portion of the stem of trees and logs as supported by Raymond et al. (2008) and Chauhan et al. (2006). Those authors proposed that the one-dimensional wave equation is sufficient to estimate the stiffness of live tree when the TOF acoustic tool is used. However, other authors argue that the TOF stress wave is a tri-dimensional (dilatational) wave and hence it is probable that the propagated sound signal can collect some quality information of wood materials lying outside the path of flight. The one-dimensional equation is therefore not considered adequate to predict the stiffness of live trees (Mora et al. 2009; Wang 2013). It should be noted that most of these authors did not consider the complex relationships among the polymeric constituents and velocity that exists at the molecular level. In this study, cellulose and hemicellulose are found to be very important drivers of velocity at the molecular level (Tables 2.3 and 2.4). At the molecular level these polymeric components are tightly linked together to form a complex in wood, hence it is plausible that the high energy stress wave generated by the TOF tools probes resonate through adjacent materials beyond the path of flight of the stress wave. This molecular level evidence supports the dilatational wave theory.

Also one would expect that if the velocity follows the one-dimensional wave equation, then the outerwood density together with the polymeric constituents should explain higher variations within velocity than disk density as observed in Figure 2.5. However, the results from both the multiple linear regressions and the path analysis indicated that disk density and the chemistry explained equal or higher variations in velocity than outerwood density and chemistry (Tables 2.3 and 2.4). This trend confirms the heterogeneous nature of wood instead of isotropic material on which the one-dimensional wave equation is based.

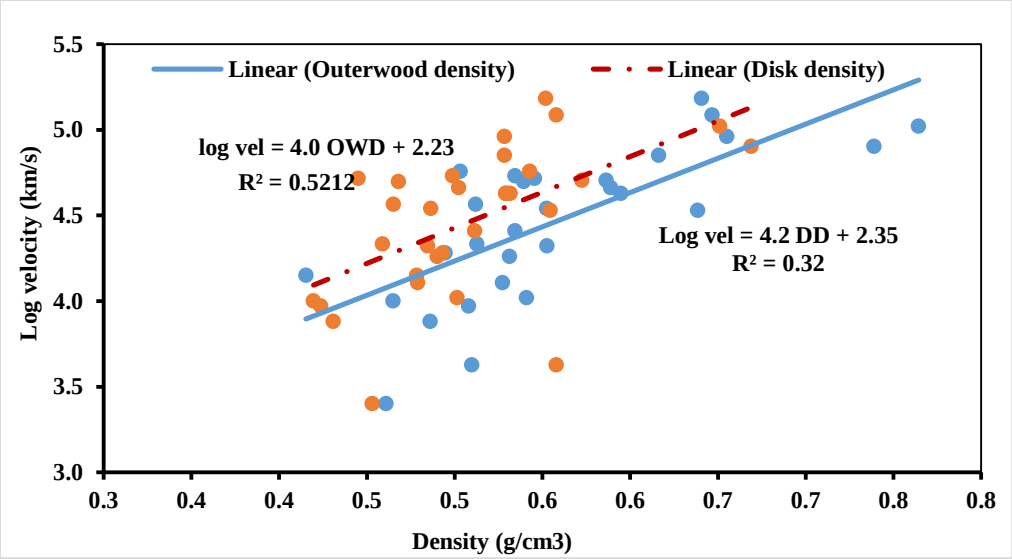

Figure 2.5 Relations between log velocity and outerwood density (OWD) and disk density (DD)

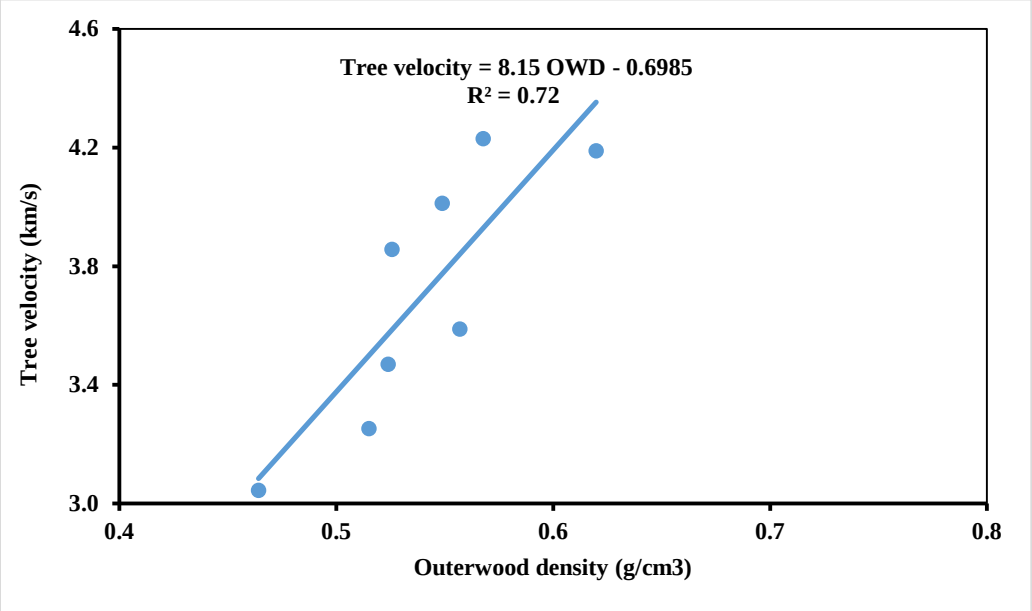

Figure 2.6 Relations between tree acoustic velocity and outerwood density at 12%MC for the 8 trees

2.4.3 Chemistry, MFA, density, velocity and mechanical properties

The influence of chemistry, MFA, and density on velocity, stiffness and strength are presented in Table 2.2. Cellulose had a positive relationship with MOE and velocity but a

negative correlation with hemicellulose and MFA (Table 2.2). MFA and lignin had a non-significant negative relationship with density (both outerwood and disk), MOR, MOE and velocity (Table 2.2). Multiple linear regression analysis and path analysis conducted reveal consistently significant positive relationship between the response variables and cellulose, hemicelluloses and density (Tables 2.3 and 2.4). On the other, MFA and lignin exhibit non-significant relationship with the entire response variables (Tables 2.3 and 2.4). From Tables 2.3 and 2.4, cellulose, hemicellulose and density are required to estimate MOR, MOE, and velocity. The results from the indirect path analysis indicate a significant positive and negative relationship between the outerwood density versus cellulose and lignin respectively (Figure 2.7). Also, there were significant negative and positive relationships between the hemicellulose versus cellulose and lignin respectively (Figure 2.7). However the relationship between the predictors when disk density was used in the indirect path analysis indicates a non-significant relationship among the predictor variables except a significant negative relationship between cellulose and hemicellulose (Figure 2.8).

Density is the most influential predictor of MOR and MOE while cellulose is slightly important predictor of velocity than density (Table 2.3). The importance of hemicellulose and cellulose in predicting stiffness and strength confirmed several reports (Winandy and Rowell 2005; Via et al. 2009; Curling et al. 2000; Clausen and Kartel 2003). Via et al. (2009) reported that hemicellulose and cellulose associated wavelengths were very significant in predicting the strength and stiffness of 41 year old longleaf pine using principal component regression and near infrared reflectance (NIR) spectroscopy. Furthermore, Clausen and Kartal (2003) attributed the initial rapid loss of MOR (strength) to degradation of side chain sugars especially arabinose and xylose associated with hemicellulose when the wood is subjected to bio – deterioration.

Density, cellulose and hemicellulose are required for predicting velocity and MOE support the theoretical fact that the acoustic tools are capable of estimating the stiffness of wood. The major variables driving the wave propagation in order of importance are cellulose, density and hemicellulose respectively. In softwoods, the S_2 layer which accounts for 80-86% of the cell wall and is composed of 32.7%, 18.4% and 9.1% for cellulose, hemicelluloses and lignin respectively (Reiterer et al. 1999). Mark (1967) estimated the densities of the cell wall to be 1.5 g/cm^3 for cellulose, 1.49g/cm^3 for hemicellulose and 1.4 g/cm^3 for lignin. The higher proportion and density of cellulose and hemicellulose may be responsible for their respective importance in driving the propagation of acoustic waves at the molecular level. Stamm (1964) asserted that more than 60% of the cellulose appeared as crystalline which is much stiffer and stronger than the amorphous portion. The high crystallinity of the cellulose in the S_2 layer may be responsible for the sound conductance at the molecular level (Hori et al. 2002). Hori et al. (2002) found a positive correlation between the acoustic velocity and crystallinity of cellulose. From Models 1 and 2 (Table 2.3), hemicellulose is less important as compared with cellulose and density in the transmission of sound waves. At the molecular level, the hemicellulose, which is linked to the non-crystalline portion of the cellulose and lignin, functions as a coupling agent for effective distribution of stresses (Winandy and Rowell 2005) just as couplants such as silicone grease function in improving the transmission of sound waves during acoustics studies of wood (Beall 2002; Hasegawa et al. 2011). It is therefore plausible that hemicellulose acts as a coupling agent for the lateral sound transmission between lignin and cellulose. The velocity had a negative correlation with lignin. This negative coefficient is important because it supports the hypothesis that increased lignin slows the sound velocity. It was hypothesized that lignin which has a highly branched tri-dimensional structure and hydrophobic in nature and hence may act as a sound

dispersant or sink at the molecular level. Via et al. (2009) indicated that hemicellulose and lignin becomes very important when wood is loaded in the transverse direction. Similarly, when sound wave is transmitted in the transverse direction of wood, the less sound conductive hemicellulose and sound dispersant lignin become very important sound driver hence they can influence the magnitude of the incoming wave at the receiver probe. This observation explains the 2 and 3 times respective reduction in sound wave velocity in the radial and tangential directions as compared with sound propagation in the longitudinal direction as reported by Hasegawa et al. 2011. Lignin appeared to be non-significant predictor in the present study perhaps because the absorption of sound energy by lignin is passive compared to cellulose which acts as a conductor of sound resulting in a more direct influence on TOF. When lignin was investigated independently through the path analysis (Figure 2.7), it has a significant positive relation with hemicellulose. Notwithstanding however, since these polymeric constituents accounts for over 95% of the weight of southern pines (Via et al. 2009), their roles may overlap and therefore different constituent may assume critical influence contingent to the experimental methods, instrumentation and/or the statistical analytical procedure used.

The relationship between MFA and velocity, MOE and MOR are consistently non-significant (Tables 2.2-2.4). This result is unexpected as it has been reported that a decrease in MFA will result in an increase in velocity because the sound wave travels through the axis of the cellulose along the MFA (Hasegawa et al. 2011). This unexpected result may be due to the sampling method used in the present study. Most studies investigating the effect of MFA on other wood properties optimize the range of MFA values through the use of matured wood (from 34 to 63 years) such that the MFA values cover wider range (Via et al. 2009; Hasegawa et al. 2011). In the present study, the random natural MFA range present in the 14 year old samples were used

hence there was no intention of selecting a wide range of MFA to optimize its variance. The MFA range of the suppressed wood used in the present study is from 19.3^{o} to 29.6^{o} (Table 2.1) which is narrower compared to the MFA range of 8 - 46^{o} used by Clark et al. (2006). The wood samples used for this study contained higher proportions of latewood which is not typical of 14 year old loblolly pine (Figures 2.11 a and b). The narrower range of MFA coupled with the higher density might have the potential to mask the importance of MFA on velocity, strength and stiffness as observed in this study.

Table 2.3 Full multiple linear regression models of chemistry, density and MFA for predicting MOR, MOE and velocity**.**

	MOR			MOE			Log velocity		
	Coefficient	SE	R^2	Coefficient	SE	R^2	Coefficient	SE	R^2
Model 1	74.47***	1.49	76.39	7.97***	0.23	72.9	4.44***	0.05	59.13
Cellulose	1.95^{ns}	1.74		0.84**	0.27		0.22***	0.06	
Hemicelluloses	5.18**	1.72		1.00***	0.26		0.14*	0.06	
Lignin	1.41^{ns}	1.67		0.17^{ns}	0.25		-0.04^{ns}	0.05	
OWD	13.6***	1.68		1.62***	0.26		0.21***	0.06	
MFA	-0.89^{ns}	1.54		-0.05^{ns}	0.23		0.08^{ns}	0.05	
Model 2	74.47***	2.06	54.4	7.97***	0.29	56.4	4.44***	0.05	60.04
Cellulose	6.94**	2.29		1.44***	0.32		0.30***	0.06	
Hemicelluloses	8.29**	2.38		1.37***	0.34		0.19**	0.06	
Lignin	-1.06^{ns}	2.23		-0.12^{ns}	0.31		-0.06^{ns}	0.06	
Disk density	9.99***	2.13		1.15***	0.31		0.20**	0.06	
MFA	-1.06^{ns}	2.21		-0.07^{ns}	0.30		0.07^{ns}	0.05	

*p<0.05, **p<0.01, ***p<0.001, ns not significant at p >0.05 DD= disk density OWD = outerwood density, MOE= modulus of elasticity, MOR= modulus of rupture

Table 2.4 Path analysis coefficients of models showing the relations among the predictors and the response variables

	MOR			MOE			log velocity		
	Coefficient	SE	R^2	Coefficient	SE	R^2	Coefficient	SE	R^2
Model 1			76.21			73.23			59.94
Cellulose	0.105^{ns}	0.099		0.343**	0.110		0.481***	0.119	
Hemicellulose	0.306**	0.104		0.411***	0.113		0.302*	0.126	
Lignin	0.091^{ns}	0.096		0.082^{ns}	0.101		-0.055^{ns}	0.128	
MFA	0.016^{ns}	0.087		0.051^{ns}	0.092		0.212^{ns}	0.123	
OWD	0.841***	0.078		0.695***	.096		0.475***	0.114	
Model 2			54.51			57.50			61.73
Cellulose	0.420***	0.130		0.604***	0.125		0.668***	0.119	
Hemicellulose	0.450***	0.136		0.566***	0.133		0.428***	0.128	
Lignin	-0.066^{ns}	0.126		-0.050^{ns}	0.122		-0.114^{ns}	0.116	
MFA	0.015^{ns}	0.120		0.048^{ns}	0.116		-0.222^{ns}	0.111	
Disk density	0.621***	0.113		0.504***	0.119		0.470***	0.116	

*p<0.05, **p<0.01, ***p<0.001, ns not significant at p >0.05 DD= disk density OWD = outerwood density, MOE= modulus of elasticity, MOR= modulus of rupture

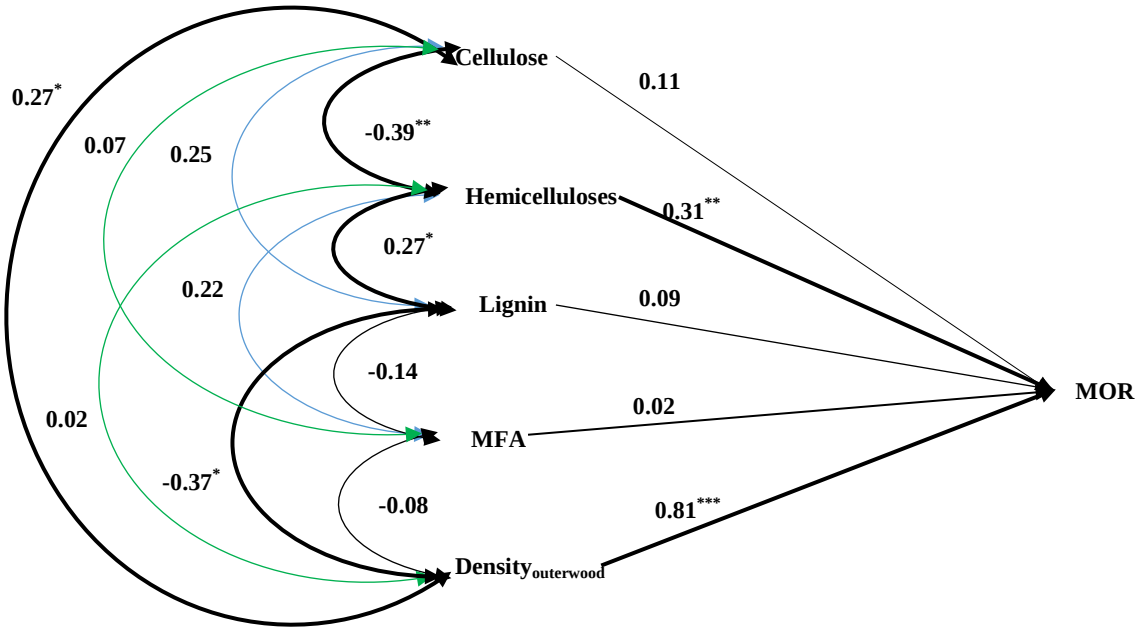

Figure 2.7 Path analysis of the chemistry, MFA, outerwood density and MOR to examine the effect of outerwood density on the variables in the model. *p<0.1, **p<0.01, ***p<0.001 ns= non-significant at p>0.1

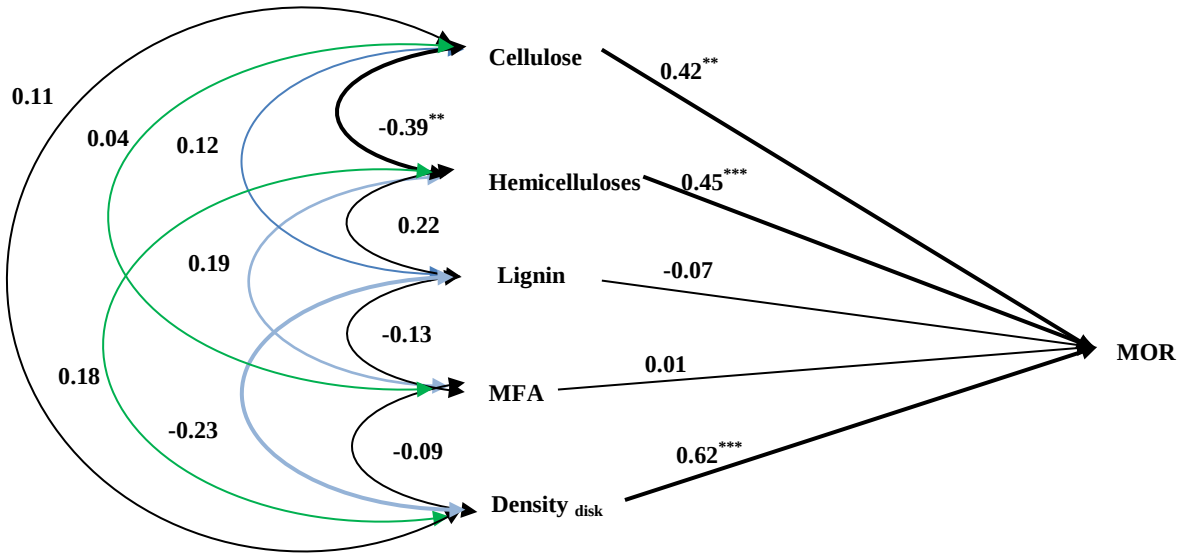

Figure 2.8 Path analysis of the chemistry, MFA, disk density and MOR to examine the effect of disk density in the model *p<0.1, **p<0.01, ***p<0.001 ns= non-significant at p>0.1

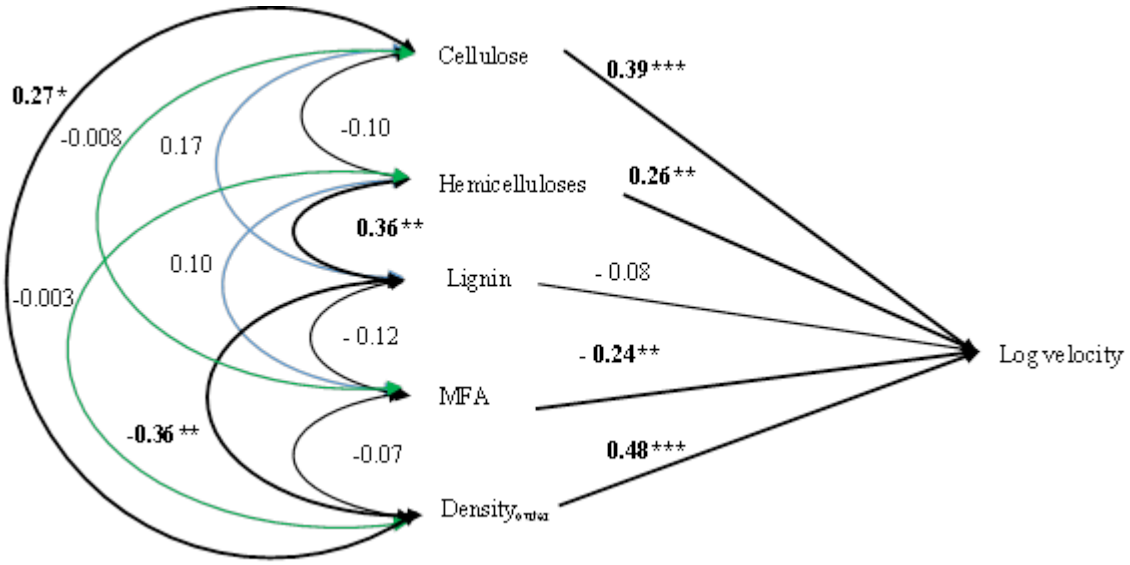

Figure 2.9 Path analysis of the chemistry, MFA, disk density and velocity to examine the effect of disk density in the model *p<0.1, **p<0.01, ***p<0.001 ns= non-significant at p>0.1

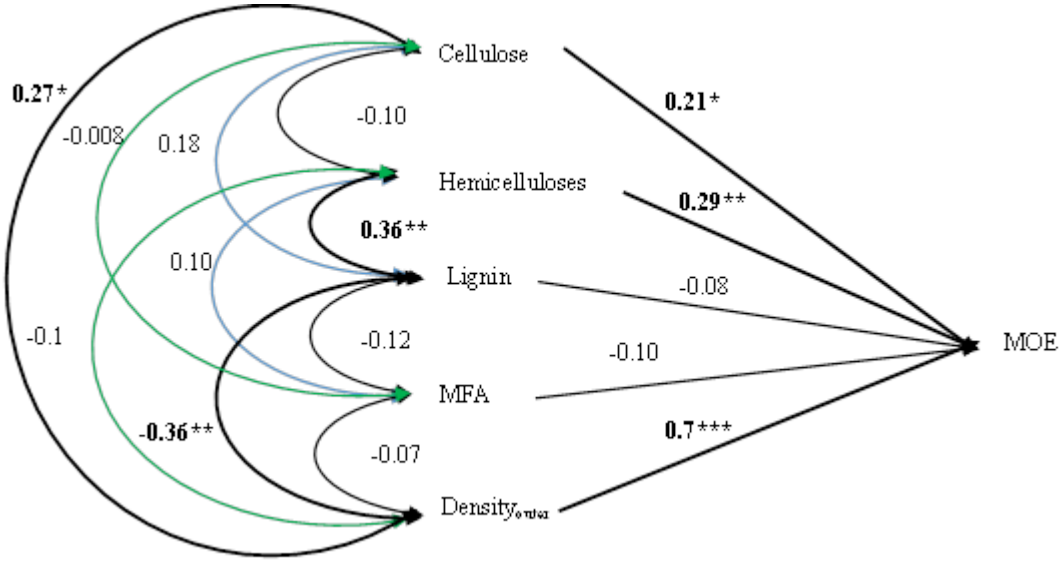

Figure 2.10 Path analysis of the chemistry, MFA, disk density and MOE to examine the effect of disk density in the model *p<0.1, **p<0.01, ***p<0.001 ns= non-significant at p>0.1

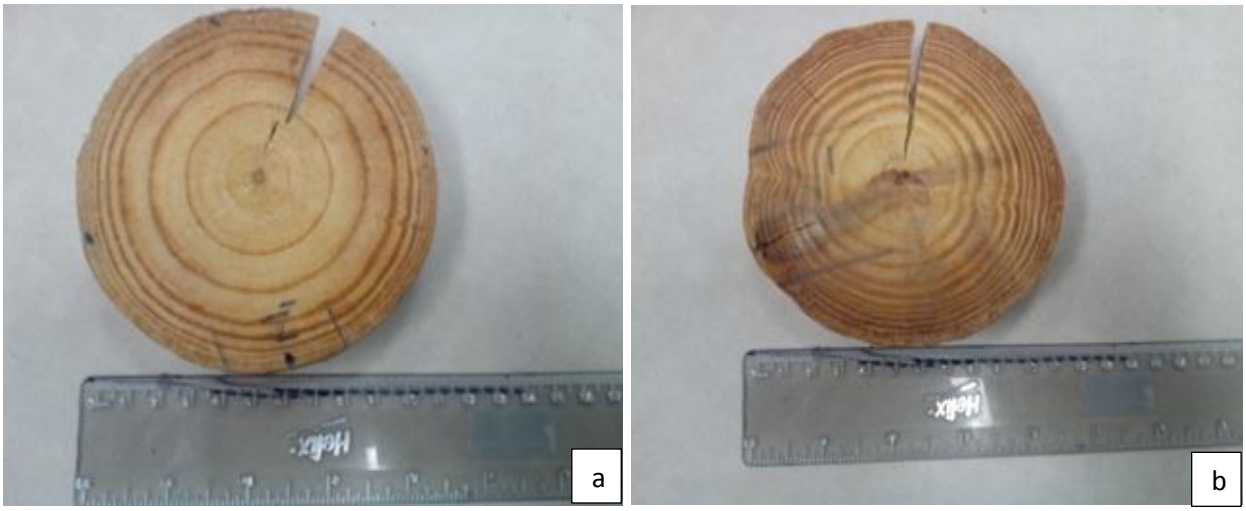

Figure 2.11 Typical growth pattern of (a) normal 14 year old loblolly pine and (b) suppressed 14 year old loblolly pine

2.5 Conclusions

Acoustic velocity and mechanical properties of the suppressed loblolly pine wood were predicted using the cellulose, hemicellulose, lignin, MFA and density. Both the multiple linear regression and path analysis indicate that the same set of variables is responsible for predicting the stiffness and velocity. This result provides a molecular level evidence to confirm the capability of TOF acoustic tools to estimate stiffness. The results revealed that at the molecular level, cellulose is the most important molecular constituent responsible for the acoustic wave propagation; followed by the hemicelluloses; while lignin acts as a dispersant or sink, thereby reducing sound transmittance.

Also the fact that the polymeric constituents and disk density explained higher proportion of variations in velocity than with outerwood density provides molecular level support that the TOF acoustic measurements on trees may rely on dilatational wave instead of the one-dimensional wave. It is possible that using matured trees may present a different picture which may further help us understand the theoretical operations of the acoustic tools.

2.6 Acknowledgements

The materials for the study were supplied by the Auburn University Forest Health Cooperation. We appreciated the technical and logistical support from students and staff of Forest Health Dynamics Laboratory and Forest Products Development Center of Auburn University. The financial support for this work is from Auburn University Intramural funds.

2.7 References

Acquah GE, Via BK, Fasina O, Eckhardt LG (2015) Non-destructive prediction of the properties of forest biomass for chemical and bioenergy application using near infrared spectroscopy. Journal of Near Infrared Spectroscopy 23(2): 93 – 102

ASTM Standard D 143-94. 2007. Standard test methods for small clear specimens of timber. ASTM International, West Conshohocken, Pa. Available at www.astm.org [accessed 5 Jan. 2014].

Beall FC (2002) Overview of the use of ultrasonic technologies in research on wood properties. Wood Science and Technology 36 (3): 197-212

Bodig J, Jayne BA (1982) Mechanics of wood and wood composites. Van Nostrand Reinhold Company Inc. p 584

Chauhan SS, Walker JCF (2006) Variations in acoustic velocity and density with age, and their interrelationships in radiate pine. Forest Ecology and Management 229(1–3): 388–394. doi:10.1016/j.foreco.2006.04.019.

Clausen CA, Kartal SN (2003) Accelerated detection of brown-rot decay: Comparison of soil block test, chemical analysis, mechanical properties, and immunodetection. Forest Products Journal 53(11/12): 90-94

Clark A, Daniels RF, Jordan L (2006) Juvenile/ mature wood transition in loblolly pine as defined by annual ring, specific gravity, proportion of latewood, and microfibril angle. Wood and Fiber Science 38(2): 292 - 299

Curling S, Winandy JE, Clausen CA (2000) An experimental method to stimulate incipient decay of wood by basidiomycete fungi. 31st Annual meeting of the international Research Group on Wood Preservation, Kona Hawaii, USA. 14 – 19 May.

Donaldson LA, Grace J, Downes GM (2004) Within-tree variation in anatomical properties of compression wood in radiate pine IAWA J., 25: 253–271

Essien C, Cheng Q, Via BK, Loewenstein EF, Wang X (2016a) An Acoustic operations study for loblolly

pine standing saw timber with different thinning history BioResources 11(3): 7512 – 7521 DOI: 1 0.15376/biores.11.3.7512-7521

Gindl W, Schoberl T (2004) The significance of elastic modulus of wood cell walls obtained from nanoindentation measurement. Composite Part A 35 (11):1345-1349

Hasegawa M, Takata M, Matsumura J, Oda K (2011) Effect of wood properties on within-tree variation in ultrasonic wave velocity in softwood. Ultrasonics 51 (3): 296-302

Hori R, Müller M, Watanabe U, Lichtenegger H, Frantzl P, Sugiyama J (2002) The importance of seasonal differences in the cellulose microfibril angel in softwoods in determining acoustic properties. Journal of Material Science 37 (20) :4279 – 4284

Ilic J (2001) Relationship among the dynamic and static elastic properties of air-dry Eucalyptus delegatensis R. Baker. Holz als Roh-und WerksTOFf 59: 169-175

Jiang W, Han G, Via BK, Tu M, Liu W, Fasina O (2014) Rapid assessment of coniferous biomass lignin-carbohydrates with near infrared spectroscopy. Wood Sci Technol 48(1): 109 – 122

Lachenbruch B, Johnson GR, Downes GM, Evans R (2010) Relationship of density, microfibril angle and sound velocity with stiffness and strength in matured of Douglas fir. Canadian Journal of Forest Research 40 (1):55-64

Lenz P, Anty D, Achim A, Beaulieu J, Mackay J (2013) Genetic improvement of White Spruce mechanical wood traits – Early screening by means of acoustic velocity. Forest 4 (3): 575-594. Doi10.3390/f4030575

Mark RE (1967) Cell wall mechanics of tracheids. Yale University Press, New Haven and London.

Marra G (1979) Overview of wood as material. Journal of Educational Modules for Materials Science and Engineering. 1(4): 699–710.

Mora CR, Schimleck LR, Isik F, Mahon Jr. JM, Clark III A, Daniels RF (2009) Relationship between acoustic variable and different measures of stiffness in standing *Pinus taeda* trees. Can. J. For. Res. 39 (8):1421 – 1429

Peter GF, Benton DM, Bennett K (2003) A simple direct method for measurement of microfibril angle in single fibres using differential interference contrast microscopy. J. Pulp and Paper Sci. 29: 274 - 280

Raymond CA, Joe B, Anderson DW, Watt DJ (2008) Effect of thinning on relationships between three measurements of stiffness in *Pinus radiata*: standing trees verse logs verse short clear specimens. Canadian Journal of Forest Research 38 (11):2870 - 2879

Reiterer A, Lichtenegger H. Tschegg S, Frantzl P (1999) Experimental evidence of a mechanical function of cellulose microfibril angle in wood cell walls. Philosophical Magazine A 79(9): 2173-2184

Stamm AJ (1964) Wood and cellulose science. The Ronald Press Co. New York.

Statistical Analysis Software (SAS) version 9.4 .2014. Cary, NC, USA

Via B, McDonald T, Fulton J (2012) Nonlinear multivariate modeling of strand density from near infrared spectra. Wood Sci Technol 46(6):1073–1084

Via BK, So CL, Shupe TF, Groom LH, Wikaira J (2009) Mechanical response of longleaf pine to variation in microfibril angle, chemistry associated wavelengths, density and radial position. Composites: Part A 40 (1):60-66

Via BK, Zhou C, Acquah G, Jiang W, Eckhardt L (2014) Near infrared calibration for wood chemistry: which chemometric technique is best for prediction and interpretation? Sensors 14 (8): 13532 - 13547

Vikram V, Cherry ML, Briggs D, Cress DW, Evans R, Howe GT (2011) Stiffness of Douglas-fir lumber: effect of wood properties and genetics. Canadian Journal of Forest Research 41(6):1160-1173

Wang X (2013) Acoustic measurement on trees and logs: a review and analysis. Wood Science and Technology 47(5):965-975

Wang X, Ross RJ, Carter P (2007) Acoustic evaluation of wood quality I standing tree. Part 1: Acoustic behavior in standing tree. Wood Fiber Science 39(1): 28 - 38

Wang X, Ross RJ, McClellan M, Barbour R J, Erickson JR, Forsman JW, McGinnis GD (2001) Nondestructive evaluation of standing trees with a stress wave method. Wood and Fiber Science 33(4): 522-533

Winandy JE Rowell RM (2005) Chemistry of wood strength In Handbook of chemistry and wood composite. CRC Press I.J.C. 305 - 343

Winandy JE, Lebow P K (2001) Modeling strength loss in wood by chemical composition Part1: An individual component model for southern pine. Wood and Fiber Science 33(2):239-254

Chapter 3: Distance error for determining the acoustic velocity of standing tree using tree morphological, physical and anatomical properties

3.1 Abstract

Time – of – Flight (TOF) acoustic tools is one of the most practical nondestructive methods for predicting tree stiffness. In the literature, 120cm between probes has been adopted as the standard for the assessment of tree acoustic velocity. However, there is no empirical study supporting this assertion, hence this study is aimed at determining the effect of distance on error for a common TOF acoustic tool. Twenty-five trees each were randomly selected from four loblolly pine plantations. Seven distances from 120 to 10 cm between probes were used to measure velocity. The morphological characteristics, physical and anatomical properties of the selected trees were also determined. The results indicated, at distances below 60 cm, the waveform is dominated by the fundamental frequency of the transmitter probe hence the velocities determined within 10 to 60cm are not statistically different. Consequently, distances from 80 to 120 cm constitute the optimum range for velocity determination for this time - of - flight acoustic tool.

Furthermore, velocity determined at 40 cm is significantly higher than that determined at 120 cm suggesting velocity is dependent on the between probes distance. Using 120 cm as a standard distance, the dynamic stiffness is overestimated by 0.013, 0.050, 0.102, and 0.197 GPa respectively for 100, 80, 60, and 40 cm. Finally, microfibril angle and the fiber wall thickness are the main anatomical properties driving the signal at the micro-level.

3.2 Introduction

Tree improvement programs in the United States have focused primarily on the selection of trees with superior tolerance to disease, growth, straightness and other morphological characteristics. This has led to the selection of tree species with better morphological and health characteristics but with no consideration for wood quality. Wood quality has often not been considered because of cost, time to maturity, lack of rapid assessment tools, the destructive nature of testing methods, and the cost of labor. These factors limit the number of trees that can be tested thereby hindering the inclusion of wood quality assessment (stiffness) from breeding and tree improvement programs.

Consequently, several research activities were designed to develop nondestructive and indirect evaluation methods, which have resulted in the development of different nondestructive and indirect assessment techniques. Some of these methods are spectroscopic analysis (Near Infrared Reflectance- NIR), Thermogravimetric Analysis, Resistograph, Silviscan, ultrasonic and acoustic tools (Beall 2002; Mora et al. 2009; Via et al. 2009; Wang 2013; Lenz et al. 2013). The application of these methods together with statistical tools has led to the successful prediction of several wood properties (Evans and Illic, 2001; Schimleck et al. 2005; Via et al. 2009). However, acoustic tools have received industrial approval due to their versatility, robustness, ease of use and integration into wood processing lines. Presently, acoustic tools are one of the best and most practical ways to estimate tree mechanical properties.

The most common tree acoustic tool is based on the time-of-flight (TOF) principle which measures the time it takes for a generated sound wave to travel a known distance. One principal limitation of the time-of-flight tools is that they may only measure outerwood stiffness of large diameter tree, rather than the stiffness across the entire stem (Lasserre et al. 2007; Mora et al.

2009; Wang 2013). However, Wang (2013) and Essien et al. (2017) reported that TOF tools are capable of assessing whole cross sectional stiffness for small diameter trees. This is due to potential signal dispersion across the entire cross section of the tree. Wang (2013) further explained that for small diameter trees, one-dimensional wave equation is adequate to determine velocity for both the resonance and the TOF acoustic tools. The one-dimensional equation (1) states that the modulus of elasticity (MOE) of a homogeneous and isotropic material is directly proportional to the product of square of the acoustic velocity (V) and density (ρ).

$$V = \sqrt{\frac{MOE}{\rho}} \qquad \text{Equation 1}$$

The major reason for the popularity of the TOF tools is the *in situ* nondestructive estimation of standing tree stiffness. This has led to a massive breakthrough in tree breeding programs where several thousands of trees are screened for stiffness heritability.

Acoustic velocity of wood has been found to change with several tree morphological, anatomical, physical, and mechanical properties. Some of these properties are age of tree, diameter, taper, density, fiber length, growth ring, cellulose, lignin, hemicellulose, microfibril angle (MFA), stiffness (modulus of elasticity), strength (modulus of rupture) and stand silvicultural history of the tree (Essien et al. 2017; Essien et al. 2016a; Wang 2013; Hasegawa et al. 2011; Briggs et al. 2007). In a study of 966 Douglas-fir (*Pseudotsuga menziesii* Mirb. Franco) trees of four age classes (32, 36, 45 and 51 years), Briggs et al. (2007) found acoustic velocity generally increased with increasing age. Essien et al. (2017) found that the acoustic velocity increased with increasing stiffness, strength, cellulose, and hemicellulose contents but decreased with increasing lignin content of trees. Essien et al. (2017) also looked at MFA but due to scale

differences the results were not conclusive; however, Hasegawa et al. (2011) reported that acoustic velocity had a negative correlation with density and MFA but positively correlated with fiber length. It has been reported that lignin content also had a positive correlation with MFA (Via et al. 2009) which may explain why both properties seem to affect acoustic velocity in similitude. The stiffness and strength of wood had a strong negative correlation with MFA. Cave (1966) and Via et al. (2009) reported that a reduction in MFA from 40^{o} to 5^{o} resulted in a four to five – fold increase in stiffness and about three – fold increase in strength. Essien et al. (2016) reported that acoustic velocity is affected by the silvicultural history of the trees.

Kang and Booker (2002) discovered that low-frequency waveform is the major component of the transmitted signal at 250cm or longer green board while the high-frequency waveform dominates for green board less than 50cm long. However, for green board between 50 and 250cm long, both the low and high-frequency waveform were present. This suggests that the green wood is highly attenuated and is capable of absorbing the high-frequency signal from the spectrum. Besides this observation, however, they concluded that velocity is independent of board length. However, the resonance and TOF acoustic tools use different algorithms in determining the velocity hence difference in trajectories are bound to exist. For the same length and diameter, TOF based velocity is generally higher than the resonance based ones (Wang 2013). There is no published study on the effect of between probes distance on tree velocity determined using TOF acoustic tool. This is important because alterations in velocity due to the distance error can significantly affect the predicted dynamic modulus of elasticity of the tree which subsequently affect the value of the trees. Additionally, it is hypothesized that shorter probe distances may help to differentiate tree stiffness when fiber morphology, such as MFA, is deemed important.

Over the past few years, several studies have presented theoretical models linking formation and wood quality to the crown indices of standing trees (Larson 1969; Sundberg et al. 2000; Amarasekara and Denne, 2002; Mansfield et al. 2007; Kuprevicius et al. 2014). Most of the available studies focused primarily on understanding the relationships between wood quality parameters such as density, stiffness, strength and standard forest inventory data such as stand density, basal area, tree diameter, height, tapering or slenderness, live crown ratio (Mansfield et al. 2007; Lasserre et al. 2008; Anthony et al. 2012; Kuprevicius et al. 2014). However, there is no reported study simultaneously connecting wood quality parameters to anatomical, physical and live crown characteristics of the trees. This is very important because these characteristics are nested within and between trees hence studying them in isolation might affect their true nature and level of complexities and hence the conclusion. It is also possible that these characteristics can affect the "error" differently or be detected better at different distances between probes due to scale differences.

We hypothesized that the distance between the transmitter and the receiver probes will significantly affect the velocity due to the frequency attenuation of green wood which increases with distance between probes. Also, anatomical properties will exhibit a significant effect as the distance decreased from 120 to 10 cm due to a progressive reduction in heterogeneity of the wood material. Therefore we expected the developed models to peak at a certain optimum distance. The study had two main objectives:

1. To examine the level of relationships among velocity, physical, anatomical and live crown properties of tree. This will help in variable selection for predictive model development which incorporates tree health indices and wood quality parameters.
2. To determine the range of distances that engenders accurate determination of velocity.

3.3 Materials and methods

3.3.1 Materials

In this study, four 17 – year – old loblolly pine plantations located in Georgia and Alabama were selected. Two of the plantations were located in Eufaula, AL and the remaining two were located at Cordele, GA. All of the selected plantations have received a row thinning at the time of sampling. Twenty-five trees each were randomly selected from each plantation. Care was taken to avoid trees with visible defects such as leaning or forked stems, chlorotic needles and/or other growth defects. The diameter at breast height of the trees averaged 18.72 cm and ranged between 15 and 23.8cm. This is a typical range for small diameter trees (Wolfe 2000)

3.3.2 Acoustic measurements of standing trees

All the selected trees on each site were acoustically tested using FAKOPP Microsecond Timer acoustic tool (Fakopp Enterprise, Agfalva, Hungary) which relied on the time-of-flight (TOF) principle (Wang et al. 2007; Mora et al. 2009; Essien et al. 2016a; Essien et al. 2017). Basically, the accelerometers (the transmitter and the receiver probes) were positioned on the same side of the tree at 120, 100, 80, 60, 40, 20 and 10cm apart with the center of the path occurring at breast height (Figure 3.1). Both probes were positioned 45^{o} to the tree axis and the stress wave was generated by striking the transmitter probe with a steel hammer at a steady force (Mora et al. 2009; Wang 2013). The generated wave was detected by the receiver and the time lapse for the sound wave to travel the distance between the probes was recorded by the data logger. Ten readings each were taken on each tree and tree velocity was estimated as the ratio of the distance to time (Equation 2).

$$Velocity = \frac{Distance}{time} \qquad \text{Equation 2}$$

Tree morphological characteristics such as diameter at breast height (DBH) and height were measured using diameter tape and clinometer respectively. The taper of each tree was determined according to Equation 3 (Lasserre et al. 2007). The live crown properties such as crown ratio (CR), crown light (CL), foliage transparency (FT) and crown density (CD) were determined of each selected tree following the crown condition classification (Schomaker et al. 2007).

$$Taper = \frac{Total\ tree\ height}{DBH} \qquad \text{Equation 3}$$

3.3.3 Physical properties measurement

The physical properties were determined using core samples taken from each of the selected trees at breast height. Moisture content, green and basic densities of all the 100 selected trees were determined following ASTM D2395 protocols. The volume of the core samples was determined using a digital caliper to the nearest 0.025mm and the weight measured to the nearest 0.001g using electronic balance while the core samples were green. The core samples were dried to a constant weight at 102^{o}C. The moisture content (MC), basic (ODD) and green density of the core samples were determined using Eqns. 4, 5 and 6

$$MC = 100 * \left(\frac{Mi-Mo}{Mo}\right) \qquad \text{Equation 4}$$

$$ODD = \frac{Mo}{V} \qquad \text{Equation 5}$$

$$GD = \frac{Mi}{V} \qquad \text{Equation 6}$$

where MC = moisture content, Mi = initial mass, Mo = oven-dry mass, v = volume, ODD= basic density, GD = green density.

3.3.4 Anatomical properties determination

Thin core samples measuring about 100µm in thickness were macerated using equal volumes of hydrogen peroxide (30%) and glacial acetic acid at 80^{o}C for 24 hours for thorough maceration (Peter et al. 2003). The macerated cells were then rinsed with water to remove the excess solution and stop the maceration reaction. Temporary slides were prepared from the macerated fibers. Fiber length, lumen diameter, wall thickness and MFA were measured following the procedure described by Peter et al. (2003). Measurements were performed on twenty full fibers selected from both the earlywood and latewood using Differential Interference Contrast (DIC) Microscope (Olympus BX53) (Essien et al. 2017)

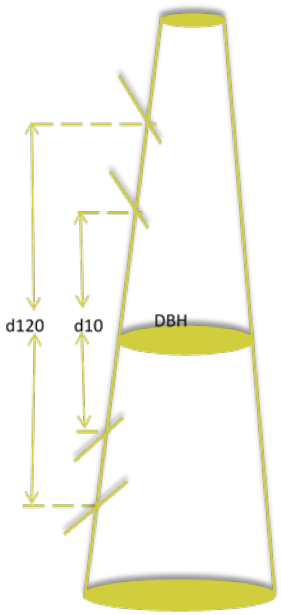

Figure 3.1. Representation of standing tree velocity measurement

3.3.5 Data analysis

For the velocity measurement at each distance, ten (10) replicated readings were taken while twenty (20) individual fibers were used to determine the anatomical properties of each tree. Simple descriptive statistics tables and charts were used to summarize the data. The velocity at each distance was treated as response variables while the crown ratio (CR), crown light (CL), foliage transparency (FT), crown density (CD), green density (GD), moisture content (MC), basic density (BD), fiber length (FL), fiber lumen diameter (FLD), fiber wall thickness (FWT) and microfibril angle (MFA) were used as predictors in the first part of the analysis. The data set was fitted using GLM and the results indicated very high variance inflation factors (VIF) for diameter, height, basic density and moisture content.

The GLM procedure produces root mean square error (RMSE) which indicated how the raw dataset deviates from the fitted line hence the smaller the RMSE value, the better the model fits the dataset. These high VIF values suggest high correlations between some of the predictors. Basic density with moisture content constitutes green density while taper was estimated as ratio of tree height to diameter. Hence tree diameter, height, moisture content and basic density were not used for further analysis. Pearson's correlation between the response and predictors were used to assess the level of relationships among the variables. Based upon the strong correlations among the response variables, principal component analysis (PCA) was used to explore the loadings of each of the response variables.

The results indicated the first principal component explained 82% of total variation with the response with the similar loadings for distances from 40 to 120 cm. This showed that the first principal component is basically the average velocities determined at distance from 40 to 120cm.

3.4 Results and Discussion

3.4.1 Relationships between response and predictor variables

There are significant linear correlations among velocity and the predictor variables (Table 3.1). Generally, velocity had a significant positive linear relationship with taper, crown light (CL), foliage transparency (FT), fiber length (FL) and fiber wall thickness (FWT).

The positive linear relation between velocity and taper has been reported by several authors (Roth et al. 2007; Lasserre et al. 2008; Anthony et al. 2012). This observed relationship is due to the fact that when tree plantations are established at a higher planting density, taller and thinner trees are produced as a result of high inter-tree competition for light at the juvenile stage. Therefore, the core wood attains stable and smaller MFAs leading to an increase in modulus of elasticity (stiffness) with tapering as reported in this study. The positive relationship between the velocity and taper confirm the theory that a more slender tree requires a higher stiffness to support itself from buckling under its own weight. Fundamentally, a taller tree is subjected to a higher wind loading, and the long distance to the bottom causes a higher moment. Therefore, the tree requires a stiffer material in order to withstand the wind loading. Since velocity is used as a surrogate for stiffness, it followed a similar pattern. Increasing crown foliage transparency indicated a reduction in the photosynthetic apparatus (leaves, branches, and twigs) of the tree thereby leading to caesura of growth, a phenomenon similar to the formation of latewood in trees. Latewood is formed when trees enter into dormancy due to limited water supply or in response to physiological, environmental, climatic, or edaphic factors.

Alternatively, trees can lose their photosynthetic apparatus through serious insect defoliation. This phenomenon can force the trees to enter into dormancy thereby leading to the formation of wood cells with similar characteristics as latewood. Therefore increasing crown

foliage transparency might lead to the formation of wood with thicker cell walls and hence increase sound wave velocity. Fiber length and wall thickness also increased with increasing velocity. Generally, the matured wood is formed near the bark of the tree with characteristics such as a lower microfibril angle, higher stiffness, strength, lower longitudinal shrinkage and longer fiber length as compared to the juvenile wood formed near the pith (Ivkovic´ et al. 2009; Hasegawa et al. 2011). The combined effect of reduced MFA, density, and higher stiffness might explain the positive relationship between the fiber length and velocity. Also, long fibers provide continuous avenue for sound wave propagation hence it is hypothesized that the longer the fiber, the faster sound will travel.

On the other hand, velocity had a significant negative linear relationship with crown ratio, MFA, and lumen diameter. Several studies have reported a negative relationship between live crown ratio versus stiffness and strength (Kuprevicius et al. 2014; Mansfield et al. 2007; Amarasekara and Denne 2002). Kuprevicius et al. (2014) reported a significant negative relationship between crown ratio (CR) versus strength and stiffness when they studied white spruce established to a different planting density. Mansfield et al. (2007) studied lodgepole pine and concluded that trees with deeper crowns produce less latewood than those grown under conditions that promote crown recession. It is interesting to note that there is no published study documenting the relationship between velocity and live crown ratio.

The observed negative relation between velocity and crown ratio (CR) might be due to the high concentration of growth promotion hormones such as auxin produced at the apical meristems of the tree. The hormones responsible for rapid cell division leading to the formation of thin-walled, large - diameter cell near the crown (Sundberg et al. 2000). As the distance from the auxin-producing live crown increased, earlywood production declines (Cato et al. 2006).

Therefore, as the live crown proportion of the tree increased, the height of the bole decrease hence tends to be in close proximity to the cell production zone. Therefore, wood with lower stiffness is produced. Since velocity is an indication of stiffness, lower stiffness wood translates into low velocity. Microfibril angle (MFA) is the angle at which cellulose microfibrils are aligned relative to the longitudinal axis of the fiber cells (Cave 1966). The larger the MFA, the longer the distances the signal has to travel at the micro-level and therefore increasing the propagation duration of the sound wave at the macroscale.

Table 3.1: Pearson's correlation coefficients and P-values for the relationship among the response and the predictors

	d120	d100	d80	d60	d40	d20	d10	Taper	CR	CL	FT	CD	GD	FL	FLD	FWT	MFA
d120	1.00																
d100	0.96**	1.00															
d80	0.97**	0.94**	1.00														
d60	0.93**	0.93**	0.94**	1.00													
d40	0.84**	0.83**	0.86**	0.90**	1.00												
d20	0.76**	0.76**	0.79**	0.82**	0.82**	1.00											
d10	0.55**	0.57**	0.60**	0.55**	0.54**	0.68**	1.00										
Taper	0.70**	0.69**	0.72**	0.67**	0.63**	0.56**	0.36**	1.00									
CR	-0.39**	-0.35**	-0.37**	-0.35**	-0.35**	-0.40**	-0.24*	-0.36**	1.00								
CL	0.40**	0.37**	0.39**	0.39**	0.38**	0.26**	**0.14ns**	0.21**	**0.066ns**	1.00							
CD	-0.42**	-0.40**	-0.41**	-0.33**	-0.24*	-0.36**	-0.37**	-0.32**	0.49**	**-0.033ns**	1.00						
FT	0.40**	0.39**	0.47**	0.42**	0.40**	0.46**	0.38**	0.33**	-0.21*	0.28**	-0.54**	1.00					
MFA	-0.48**	-0.43**	-0.43**	-0.42**	-0.39**	-0.32	-0.26**	-0.22*	0.42**	-0.26**	-0.38**	0.22*	1.00				
FL	0.27**	0.27**	0.30**	0.30**	0.36**	0.29**	0.24*	**0.16ns**	**-0.069ns**	0.26*	**-0.035ns**	**0.14ns**	-0.12ns	1.00			
FLD	**-0.17ns**	**-0.20ns**	**-0.18ns**	**-0.18ns**	-0.28**	-0.25*	-0.21*	**-0.07ns**	**0.08ns**	**-0.09ns**	**-0.03ns**	**0.019ns**	0.30**	-0.44**	1.00		
FWT	0.32**	0.34**	0.34**	0.31**	0.38**	0.29**	0.25*	0.24*	**-0.14ns**	0.31**	**-0.045ns**	**0.084ns**	-0.45**	0.71**	-0.71**	1.00	
GD	-0.49**	-0.44**	-0.47**	-0.44**	-0.42**	-0.45**	-0.54**	-0.32**	0.38**	-0.34**	0.42**	-0.37**	0.35**	**-0.12ns**	**-0.009ns**	**-0.07ns**	1.00

CR = crown ratio; CL = crown light; CD = crown density; FT = foliage transparency; MFA= microfibril angle; FL = fiber length; FLD = fiber lumen diameter; FWT = fiber wall thickness. ** indicated significant at 0.01; * = significant at 0.05; ns = not significant at 0.05

3.4.2 Effect of distance on determining tree velocity

The results of the velocity determined at distances 120, 100, 80, 60, 40, 20, and 10cm are presented in Table 3.2 and Figure 3.2. The results indicated a gradual increase in velocity as distance decreased from 120 to 40 cm and decreased afterward (Figure 3.2). This is similar to that reported by Kang and Booker (2002). Above 40 cm, velocity decreased with increasing distance (Figure 3.2). The velocity at 40cm is significantly higher than that at 120cm (Figure 3.2). Generally, the receiver probe is very sensitive to the fundamental frequency of the transmitter probe though it can detect several overtones frequencies generated as well. However, as the distance increases, most of the high frequency (fundamental frequency) signals within the spectrum are absorbed by the green wood hence reducing the proportion of the very sensitive frequencies (Kang and Booker 2002). This attenuation effect of green wood on the very sensitive fundamental frequencies is gradual as indicated by its effect on velocity in Figure 3.2.

Above 40 cm, the velocity is statistically different at each 40 cm increment. This indicates a significant reduction in the proportion of the sensitive fundamental frequency occur at each 40 cm increment away from the receiver probe. As explained by Kang and Booker (2002), within 50cm and 250cm, both the low and high-frequency signals are present but probably their proportions decrease with increasing distance. It is however possible that all the sensitive fundamental frequencies within the signal spectrum can be totally absorbed by the green wood as distance increases leaving the low-frequency signals. At a point where all the sensitive high frequency signals are removed, the velocity will remain virtually constant. Kang and Booker (2002) proposed 250 cm between probes distance as the point where all the sensitive high frequency is totally absorbed by the green wood. On the other hand, different trend is observed below 40 cm; velocity decreased marginally with decreasing distance (Figure 3.2). A similar

trend was reported by Kang and Booker (2002). The similitude in velocity below 60 cm indicated the waveform is dominated by the sensitive fundamental frequency of the transmitter probe.

In order to assess the optimum distance for velocity determination, all the predictor were used in a model to predict the velocity at a particular distance.

The model adequacies were determined using the root means square error of calibration (RMSE) and adjusted R^2 values. We set 50% adjusted R^2 as a limit for selecting the corresponding distance as a potential candidate for velocity determination. According to Hasegawa et al. (2011), MFA and density only accounted for more than 50% variations in the velocity of Japanese cedar and cypress. As a result, we assumed that the all the predictor variables including MFA and density should be able to explain at least half the variation within the response variable. However, this 50% does not apply to the models using only the anatomical properties since those properties were measured at the micro-scale while the velocity was determined at the macro level over at least 10 cm distance. From Figure 3.3, the RMSE increased from 120 cm to 100 cm and stabilized till 20 cm. However, there is a general decrease in adjusted R^2 with distance (Figure 3.3). Based upon these observations, 120 cm provides a better distance for velocity determination because it has the lowest RMSE and the highest adjusted R^2. Since the RMSE measures the precision of the fitted model to the dataset, distance from 20 to 100 cm provide similar precision but with different adjusted R^2 values. However, since the adjusted R^2 value for 20 cm is less than 50%, hence 20 cm is not considered to be a potential distance for determining tree velocity using this type of acoustic tool.

Using 120 cm as a standard distance since it provided the best model diagnostics, the velocity is overestimated by 3.3, 7.3, 10.4, and 13.9 respectively for 100, 80, 60, and 40 cm. This

translates into dynamic MOE values of 0.013, 0.05, 0.102, and 0.197 GPa for 100, 80, 60, and 40 cm respectively. Additionally, the mean velocity estimated between 10 and 60 cm is statistically not different hence based upon this studies, 80 to 120 cm constitutes the range for velocity determination. As stated earlier, below 60 cm, the sensitive fundamental frequency generated by the transmitter dominates the signal spectrum hence the receiver is able to recognize it faster.

Table 3.2: Summary Descriptive statistics of the velocity, morphological, physical and anatomical properties

Variable	Mean	Std Dev	Minimum	Maximum
d120	3.267	0.440	2.200	4.300
d100	3.375	0.494	2.300	4.600
d80	3.506	0.507	2.300	4.800
d60	3.608	0.471	2.400	4.600
d40	3.721	0.425	2.400	4.600
d20	3.663	0.414	2.600	4.500
d10	3.579	0.537	2.500	5.300
Taper	74.590	12.271	50.220	98.160
Crown ratio	45.050	6.875	30.000	60.000
Crown light	2.550	0.931	1.000	5.000
Foliage transparency	29.950	4.770	20.000	40.000
Crown density	46.790	6.250	35.000	65.000
Green density	0.881	0.110	0.610	1.180
Fiber length	2666	739.590	571.215	6126
Lumen diameter	21.417	10.968	1.981	68.040
Wall thickness	11.728	5.059	1.542	42.465
Microfibril angle	26.747	6.876	6.840	53.730

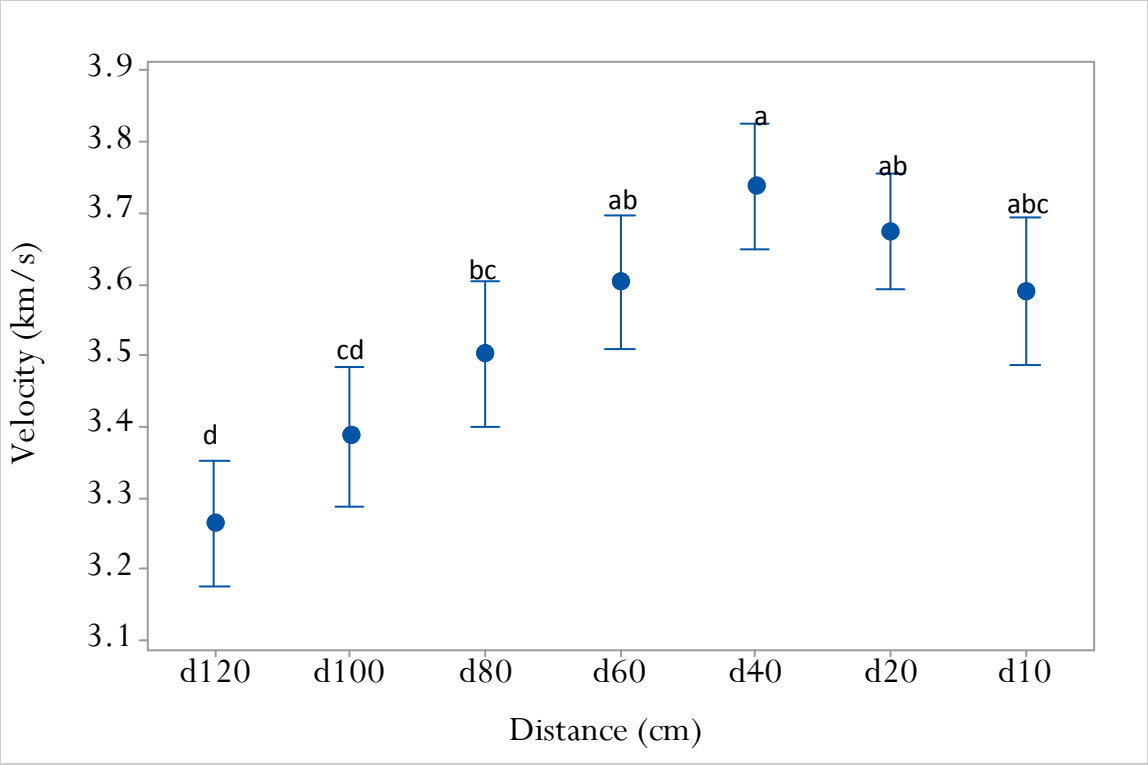

Figure 3.2. The mean and 95% confidence interval of the velocity at different distance. The different letter indicated significant difference at 5% confidence level.

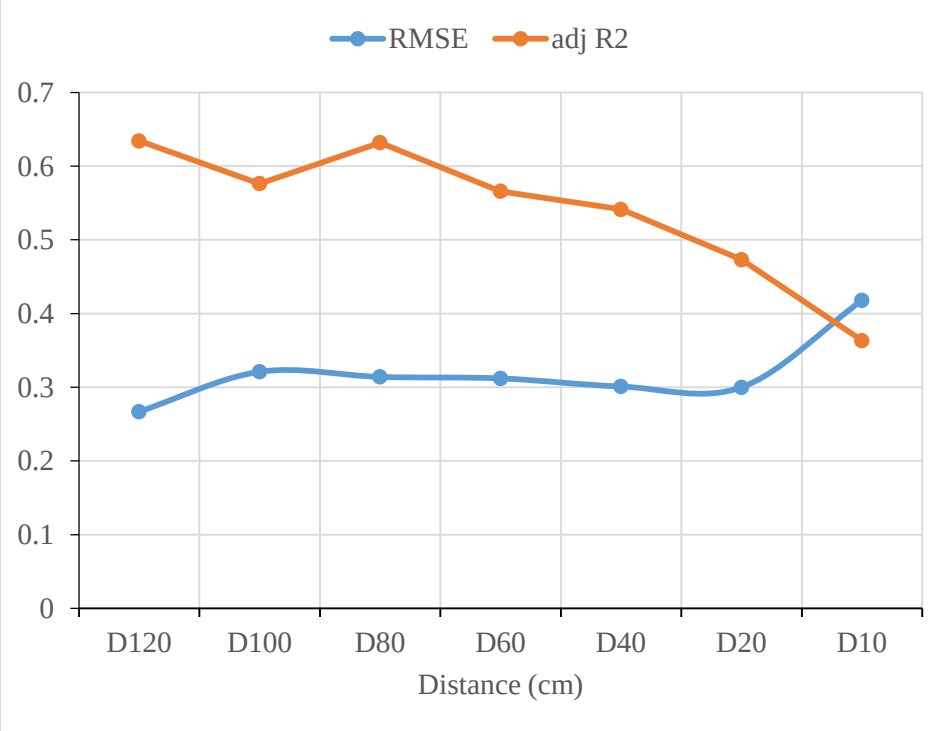

Figure 3.3 Root means square error of calibration (RMSE) and adjusted R2 for predicting velocity at various distance using all the predictors.

3.4.3 Effect of anatomical characteristics on velocity determined at different distance

We hypothesized that the anatomical properties namely the fiber length (FL), fiber lumen diameter (FLD), fiber wall thickness (FWT) and microfibril angle (MFA) will become the major driver of the signal at shorter distance, and to test this hypothesis, multiple linear regression with the velocity as the response (y) variable and the all the anatomical properties as predictors with stepwise selection method being used to determine the optimum model. The variable entry and staying in the model was set to an alpha value of 0.15, and the results are presented in Table 3.3.

The results indicated the MFA is the major anatomical property driving the velocity the micro level. As indicated earlier, higher MFA increases the distance the signal has to travel at the micro-level. Hasegawa et al. (2011) reported similar trend of increasing velocity with decreasing MFA. It is not surprising that the fiber wall thickness significantly influences the velocity because Essien et al. (2017) reported that cellulose and hemicelluloses which are the major constituents of the cell wall drive the signal at the nano-level. From the earlier discussions, it seems this acoustic tool is configured to function efficiently above 80 cm. Although the MFA and the FWT are measured at micro-levels, they provide impressive diagnostics (RMSE and adjusted R^2) for velocity at various distances. This suggests that with considerable configuration, acoustic techniques can be used to predict the MFA of trees.

Table 3.3: Coefficients, standard error, root mean square error of calibration, adjusted R^2 and the p-values models predicting velocity with the anatomical properties

Distance (y)	Variable	Coefficient (SE)	RMSE	Adj R2	P-value
D120	Intercept	4.68 (0.264)	0.389	22.45	0.000
	MFA	-0.053 (0.0097)			0.000
D100	Intercept	4.16 (0.448)	0.442	19.50	0.000
	MFA	-0.042 (0.012)			0.001
	FWT	0.030 (0.016)			0.063
D80	Intercept	4.33 (0.471)	0.465	19.28	0.000
	MFA	-0.044(0.013)			0.001
	FWT	0.031 (0.017)			0.069
D60	Intercept	4.45 (0.434)	0.428	17.98	0.000
	MFA	-0.042 (0.012)			0.001
	FWT	0.023 (0.015)			0.138
D40	Intercept	4.149 (0.406)	0.4005	18.80	0.000
	MFA	-0.031 (0.011)			0.007
	FWT	0.036 (0.014)			0.015
D20	Intercept	4.02 (0.395)	0.390	11.04	0.00
	MFA	-0.024 (0.011)			0.031
	FWT	0.025 (0.014)			0.078
D10	Intercept	3.92 (0.51)	0.505	7.20	0.00
	MFA	-0.025 (0.014)			0.084
	FWT	0.028 (0.018)			0.13

MFA = microfibril angle; FWT = fiber wall thickness

3.5 Conclusions

In this study, twenty-five trees each were randomly selected from four loblolly pine plantations. Seven between probes distances from 120, 100, 80, 60, 40, 20, and 10cm were used to estimate velocity. Morphological characteristics, physical and anatomical properties of the selected trees were studied.

The results indicated significant positive relationships between velocity and foliage transparency, taper, fiber wall thickness and fiber length. However, velocity had significant negative relations with the crown ratio, microfibril angle, and lumen diameter.

Additionally, at distance below 60 cm, the waveform is dominated by the fundamental frequency of the transmitter probe hence the velocities determined within this distances are not statistically different. Consequently, distances from 80 to 120 cm constitute the optimum range for velocity determination for this time - of - flight acoustic tool. This implies that this type of acoustic tool is conFigured to operate effectively at distances from 80 cm and above.

Furthermore, velocity is dependent on the distance used for its determination. The velocity determined at 40 cm is significantly different from that determined at 120 cm. Using 120 cm as a standard distance since it provided the best model diagnostics, the velocity is overestimated by 3.3, 7.3, 10.4, and 13.9% respectively for 100, 80, 60, and 40 cm. This translates into dynamic MOE values of 0.013, 0.05, 0.102, and 0.197 GPa for 100, 80, 60, and 40 cm respectively.

Finally, microfibril angle and the fiber wall thickness are the main anatomical properties driving the signal at the micro-level. Although the MFA and the FWT are measured at micro-levels, they provide impressive diagnostics (RMSE and adjusted R^2) for velocity at various distances. This suggests that with considerable conFigureuration, acoustic techniques can be used to predict the MFA of trees.

3.6 References

ASTM D2395-07 (2007) Standard methods for specific gravity of wood and wood-based materials. ASTM International, West Conshohocken, Pa. Available at www.astm.org [accessed 11 March 2017].

Antony F, Schimleck LR, Jordan L, Daniels RF, Clark A. (2012) Modeling the effect of initial planting density on within tree variation of stiffness in loblolly pine. Ann. of For Sci 69:614 – 650 DOI 10.1007/s13595-011-0180-1

Amarasekara H, and Denne MP. (2002) Effects of crown size on wood characteristics of Corsican pine in relation to definitions of juvenile wood, crown formed wood and core wood. Forestry 75, 51–61.

Beall FC. (2002) Overview of the use of ultrasonic technologies in research on wood properties. Wood Science and Technology 36 (3): 197-212

Briggs DG, Thienel G, Turnblom EC, Lowell E, Dykstra D, Ross RJ, Wang X, and Carter P. (2007) Influence of thinning on acoustic velocity of Douglas fir trees in Western Washington and Western Oregon. In: Proceedings of the 15th International Symposium on Nondestructive Testing of Wood, September 10-12, 2007, Duluth, Minnesota-USA. Pp113-123

Cave ID. (1966) Theory of X-ray measurement of microfibril angle in wood. For. Prod. J. 16:37–42

Cato S, McMillan L, Donaldson L, Richardson T, Echt C. and Gardner R (2006) Wood formation from the base to the crown in Pinus radiata: Gradients of tracheid wall thickness, wood density, radial growth rate and gene expression. Plant Molec. Biol. 60, 565–581.

Evans R. and Ilic J. (2001) Rapid prediction of wood stiffness from microfibril angle and density. For. Prod. J. 51(3): 53–57.

Essien C, Via KB, Cheng Q, Gallagher T, McDonald T, Wang X and Eckhardt LG. (2017) Multivariate modeling of acousto mechanical response of 14-year old suppressed loblolly pine to variation in wood chemistry, microfibril angle, and density. Wood Sci and Technol 51:475 -492. DOI 10.1007/s00226-017-0894-9

Essien C, Cheng Q, Via BK, Loewenstein EF, Wang X. (2016a) An Acoustic operations study for loblolly pine standing saw timber with different thinning history BioResources 11(3): 7512 – 7521 DOI: 1 0.15376/biores.11.3.7512-7521

Kang H and Booker RE. (2002) Variation in stress wave velocity with MC and temperature. Wood Sci Technol 36: 41 – 54

Hasegawa M, Takata M, Matsumura J, Oda K. (2011) Effect of wood properties on within-tree variation in ultrasonic wave velocity in softwood. Ultrasonics 51 (3): 296-302

Ivkovic M, Gapare WJ, Abarquez A, Ilic J, Powell MB and Wu HX. (2009) Prediction of stiffness, strength, and shrinkage in juvenile wood of radiate pine. Wood Sci Technol 43: 237-257

Kuprevicius A. Anty D, Achim A, and Caspersen JP (2014) Quantifying the influence of live crown ratio on the mechanical properties of clear wood. Forestry 86, 361-369

Lasserre JP, Mason EG, and Watt MS (2007) Assessing corewood acoustic velocity and modulus of elasticity with two impact based instruments in 11-year-old trees from a clonal-spacing experiment of *Pinus radiata* D. Don. For. Ecol. Manage. 239:217–221.

Lenz P, Anty D, Achim A, Beaulieu J, Mackay J (2013) Genetic improvement of White Spruce mechanical wood traits – Early screening by means of acoustic velocity. Forest 4 (3): 575-594. Doi10.3390/f4030575

Mansfield SD, Parish R, Goudie JW, Kang KY, and Ott P. (2007) The effects of crown ratio on the transition from juvenile to mature wood production in lodgepole pine in western Canada. Can. J. For. Res. 37, 1450–1459.

Mora CR, Schimleck LR, Isik F, Mahon Jr. JM, Clark III A, Daniels RF (2009) The relationship between the acoustic variable and different measures of stiffness in standing *Pinus taeda* trees. Can. J. For. Res. 39 (8):1421 – 1429

Peter GF, Benton DM, Bennett K (2003) A simple direct method for measurement of microfibril angle in single fibers using differential interference contrast microscopy. J. Pulp and Paper Sci. 29: 274 – 280

Roth BE, Li X, Huber DA and Peter GF (2007) Effects of management intensity, genetics and planting density on wood stiffness in a plantation of juvenile loblolly pine in the southeastern USA. For. Ecol. Manage 246: 155 – 162 doi 10.1016/j.foreco.2007.03.028

Sundberg B, Uggla C and Tuominen H. (2000) Cambial growth and auxin gradients. In Cell and Molecular Biology of Wood Formation. Savidge, R., Barnett, J.R., and Napier, R. (eds). Bios Scientific Publishers Ltd, Oxford, pp. 169–188.

Schimleck LR, Jones PD, Clark A, Daniels RF, and Peter GF. (2005) Near infrared spectroscopy for the nondestructive estimation of clear wood properties of *Pinus taeda* L. from the southern United States. For. Prod. J. **55**: 21–28

Schomaker ME, Zarnoch SJ, Bechtold WA, Latelle DJ, Burkman WG and Cox SM (2007) Crown-condition classification: A guide to data collection and analysis. USDA Southern Research Station General Technical report SRS-102. 75pp.

Via BK, So CL, Shupe TF, Groom LH, Wikaira J (2009) Mechanical response of longleaf pine to variation in microfibril angle, chemistry associated wavelengths, density and radial position. Composites: Part A 40 (1):60-66

Wang X (2013) Acoustic measurement on trees and logs: a review and analysis. Wood Science and Technology 47(5):965-975

Wang X, Ross RJ, Carter P (2007) Acoustic evaluation of wood quality I standing tree. Part 1: Acoustic behavior in standing tree. Wood Fiber Science 39(1): 28 – 38

Wang X, Ross RJ, McClellan M, Barbour R J, Erickson JR, Forsman JW, McGinnis GD (2001) Nondestructive evaluation of standing trees with a stress wave method. Wood and Fiber Science 33(4): 522-533

Wolfe R .(2000) Research challenges for structural use of small –diameter round timbers. Forest Prod J. 50(2): 21.-29

Chapter 4: Sensitivity of Acoustic Tools to Variation in Equilibrium Moisture Content of Small Clear Samples of Loblolly Pine (*Pinus taeda*)

4.1 Abstract

There are several types of acoustic tools commercially available for wood characterization, but they are generally classified into resonance and time – of – flight (TOF) tools. This classification is based upon the mode of velocity estimation for wood. In this study, we explored how the equilibrium moisture content of small clear wood samples (2.5cm x 2.5cm x 41cm) affect the predictive capabilities of two types of acoustic tools namely a microsecond timer (TOF) and a resonance log grader (resonance).

The results indicated the acoustic velocity is sensitive to equilibrium moisture content of loblolly pine, and sensitivity to EMC is similar for both type of tools. The acoustic velocity decreased by 32.9 m/s and 28.8m/s for TOF and the resonance acoustic tools respectively for a unit increase in EMC below fiber saturation point (FSP); 5.4m/s and 6.1m/s respectively for a unit increase in EMC above FSP although the slope was statistically equivalent to zero. Also, the static MOE of the green samples was overestimated by 16% by both resonance and TOF tools with oven-dry density, while it was 72% when estimated with density at test. The insignificant slope coupled with better accuracy in MOE supports the hypothesis that the cell wall controls the acoustic velocity while the water in the lumen of the cell wall is insignificant.

These results bring into question the standard use of green density to estimate acoustic MOE of live trees and oven dry density is instead recommended.

4.2 Introduction

Mechanical properties including modulus of elasticity (MOE) and modulus of rupture (MOR) of wood from different tree species have been extensively studied over the years (Bodig and Jayne 1982; FPL 1989, 2010). They reported that, generally, MOE and MOR decrease with increasing moisture till the fiber saturation point (FSP) is attained, above which insignificant difference occur. For most timber species, the FSP occurs between 20 – 35% moisture content, hence one does not expect MOE to vary significantly above this moisture range. Similarly, the volume of wood changes (shrink or swell) in response to alterations in moisture content (MC) below the FSP but it remains constant above the FSP. This is because above the FSP, the free water which occupies the cell lumen does not affect the structural matrix of the wood constituents hence the load bearing properties (MOE and MOR) are unaffected. Therefore, MOE and MOR above the FSP are generally reported as the green condition or state (FPL 2010). On the other hand, wood density increases with increasing moisture both above and below FSP, hence the density attains the maximum value when the cell lumen is fully filled with free water. This is because the free water adds to the weight of the wood but the volume remains constant. Similarly, the basic density (which is the ratio of oven-dry weight to fully saturated volume of the wood) is the possible minimum density value a wood can attains. Consequently, one has to state the condition of the wood under which the density was determined (FPL, 2010). Generally, wood is utilized in the dry condition below the FSP hence most of the mechanical and technological properties are reported in either dry usually 12% MC or green or both. The use of acoustic techniques as a nondestructive MOE characterization tool for live trees, freshly cut logs, and other wood products requires density - (velocity^2 *density). The type of density to use

continues to be one of the major challenges confronting the practitioners and researchers due the complex and confounding effect of MC on both density and velocity.

Wood is a dispersive material indicating that wave propagated through it changes frequency with passage (Beall 2002). Generally, wood acoustic quantification involved the transmission of high energy sound waves through the tissue to ascertain internal stiffness. The acoustic velocity of wood is different with respect to the direction of propagation. It is about five times higher in longitudinal direction as compared to that in the transverse direction. Similarly, it is estimated to be about 50% higher in the radial when compared to the tangential direction (Harris and Andrews 1999; Beall 2002; Chauhan et al. 2006; Hasegawa et al. 2011). The acoustic velocity has been found to decrease with increasing equilibrium moisture content until the fiber saturation point, above which changes in moisture insignificantly affect velocity (Olivito 1996; Chan et al. 2011; Gao et al. 2012).

Above the fiber saturation point, for example, moisture content positively and significantly affects the density of wood, but it does not significantly influence velocity. However, both moisture content and density disproportionally influence velocity. This relationship is further compounded by the effect of temperature and relative humidity. There are several studies undertaken to understand the effect of moisture content and temperature on acoustic velocity in order to determine correction factors to adjust the velocity to the desired moisture and/or temperature (Sandoz 1991; Kang and Booker 2002; Chan et al. 2011). But less is understood about how different acoustic based techniques differ in their response to moisture variation for the same test materials. This is important because various types of acoustic tools are designed for different wood products. For example, time – of – flight (TOF) acoustic tools are designed primarily to estimate the velocity of live trees whose moisture content rarely drop

below FSP. However, resonance tools are designed for logs and wood products whose moisture can be above or below FSP. Thus a head to head comparison between tools across the entire moisture range is needed.

The longitudinal velocity decreased dramatically with increasing equilibrium moisture content (EMC) up to the FSP for both the resonance based tool (Kang and Booker 2002; Gonçalves 2008; Chan et al. 2011; Yang et al. 2015) and time – of – flight based tool (Wang et al. 2008). However, the rate of change in velocity is much lower when EMC was above FSP (Chan et al. 2010; Yang et al. 2015). Chan et al. (2011) found that acoustic velocity decreased by 32m/s for a unit increase in moisture content below the fiber saturation point while the change ranged between 6-10m/s for moisture above fiber saturation point for the resonance based tools. Since the different type of acoustic tools estimates velocity with different algorithms, it would be useful to understand the behavior of the velocity – EMC relationship for both the resonance and TOF acoustic tools.

We hypothesized that for the same specimen and moisture content, the resonance tools will be more sensitive to variations in moisture content below FSP as compared to the TOF tools because resonance tools are designed for products with higher potential of having moisture below the FSP. Therefore the main objective of this study was to explore the sensitivity of acoustic tools to variation in EMC below and above the fiber saturation point of loblolly pine.

4.3 Materials and methods

4.3.1 Materials

The materials for this study were obtained from a plantation of genetically improved loblolly pine (*Pinus. Taeda* L) families established in the year 2000. The trees were sampled by

the Forest Health Cooperative at Auburn University when they were 14 years old. The plantation was located in Nassau County Florida near Yulee (latitude 30°63′N and longitude 81°57′W). The soil was poorly drained and formed from a thick bed of alkaline loamy and clayey marine sediments terraces with a slope less than 1%. The mean long-term temperature and precipitation from 1981 to 2010 are 21°C and 1350mm respectively (NOAA 2016). It should be noted that this study was not aimed at quantifying the variations within the genetic families but instead materials from different families were selected to ensure that the results were reflective of a wood mix that is common in today's market.

The trees were bucked into small billets and were further converted into small clear samples with dimensions of 25mm x 25mm x 410 mm in the radial, tangential and longitudinal directions respectively. The mean equilibrium moisture content (EMC) of all the samples was 62%. Forty-five (45) samples were used for the conditioning study and additional fifteen samples were used for static modulus of elasticity (MOE) and modulus of rupture (MOR) determination following ASTM D143. Wang et al. (2008) indicated that for small specimen of wood, one-dimensional wave is sufficient to quantify the velocity for both the TOF and resonance tools.

4.3.2 Acoustic measurement

Two acoustic tools namely FAKOPP Microsecond Timer (TOF) and FAKOPP Resonance Log Grader (R) (Fakopp Enterprise, Agfalva, Hungary) were used to determine the acoustic velocity of each sample. The FAKOPP Microsecond Timer relies on measuring the time it takes for the generated stress waves to travel a known distance between two probes. The tool is equipped with a pair of piezo sensors (SD 20/60) by the manufacturer. Basically, the sensors (the transmitter and the receiver probes) were positioned on the same side of the samples. Both

probes were positioned 45^{o} to the sample plane and the stress wave was generated by striking the transmitter probe with a steel hammer at a steady force (Mora et al. 2009). The generated wave was detected by the receiver and the time lapse for the sound wave to travel the distance between the probes was recorded by the data logger (Figure 4.1). The data logger displays the time and velocity determined using equation 1.

$V_{TOF} = D / t$ Equation 1

where V_{TOF} is the velocity estimated by the TOF (FAKOPP Microsecond Timer) tool, D is the distance between the probes, t is the time for the sound wave to travel the distance between the probes.

The FAKOPP Resonance Log Grader (R) tool determined the velocity using the resonance principle. The sample length is entered and the tool held firmly at the end of the sample. The wave is generated by striking the end of the sample with a hammer, the microphone picks up the acoustic wave signal as it resonates back and forth along the entire length of the sample at a rapid rate of hundreds of passes per second (Figure 4.2), and display the velocity according to equation 4 (Wang et al. 2007).

$V_R = 2f_1L$ Equation 2

where V_R is the velocity estimated by the resonance tool, f_1 is the natural fundamental frequency mode (Hz), L is the length (m) of the sample.

All the forty-five small clear samples were weighed to the nearest 0.001g and dimensions measured using digital calipers to the nearest 0.025mm. The samples were subjected to a drying process in an airtight conditioning chamber set at a temperature of 22.7^{o}C and 55% relative humidity. The samples were acoustically tested after twelve hours exposure period using both

FAKOPP Resonance Log Grader and FAKOPP Microsecond Timer acoustic tools. Six readings per sample were taken for each tool at any testing schedule in the conditioning chamber.

Acoustic readings, dimensions and weight of the samples were then taken twice daily for the first week, after which readings were taken once a week. It should be note that, the same set of samples was repeatedly used at each measurement cycle (Figure 3). This repetitive process continued until the samples attained constant weight in the chamber. The samples were then transferred to an electronic thermostatic oven set to 105^{o}C. The 105^{o}C was meant to oven dry the samples to zero percent moisture content. The EMC and density (GD) of the samples at each stage of the conditioning process were determined using equations 3 and 4 respectively (FPL, 2010). The oven-dry density (OD) was determined as the ratio of the oven-dry weight to the oven-dry volume measured using digital calipers.

$$EMC = (M_i - M_o/M_o)*100 \qquad \text{Equation 3}$$

where M_i is the initial weight and M_o is the oven-dry weight

$$GD = \text{weight} / \text{volume} \qquad \text{Equation 4}$$

where GD is the density at test, weight and volume are the measurement taken at each measurement period in an airtight conditioning chamber.

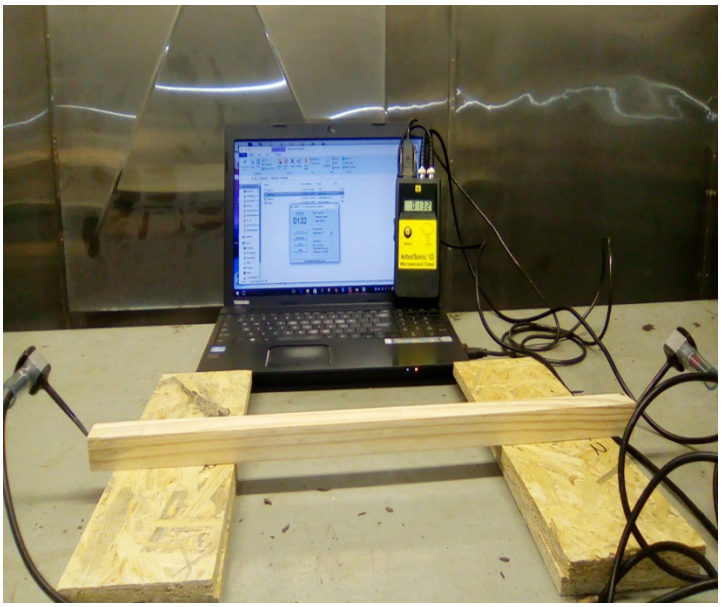

Figure 4.1 Setup for the estimation of the acoustic velocity using Microsecond Time

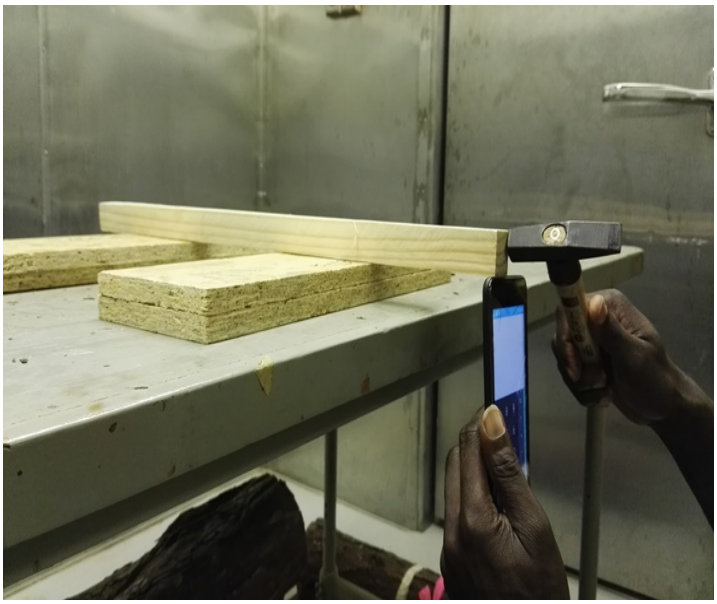

Figure 4.2 Setup for the estimation of acoustic velocity using resonance log grader

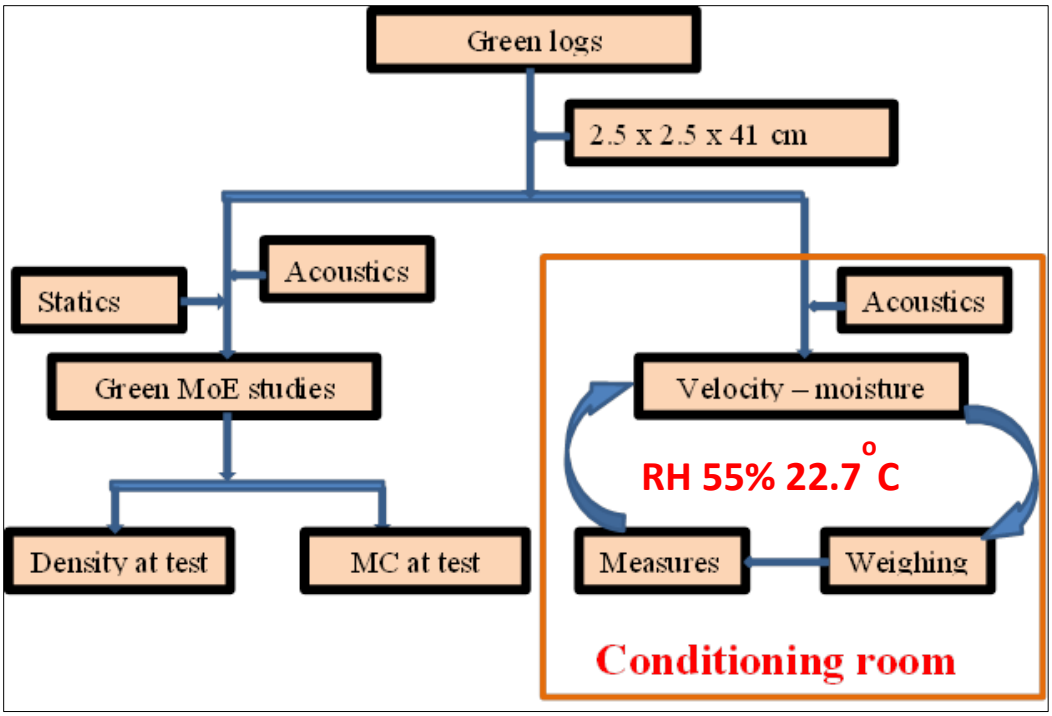

Figure 4.3 Flow chart of the experimental set-up

4.3.3 Static MOE and MOR determination

Static MOE and modulus of rupture (MOR) were determined using the fifteen green small clear specimens measuring 2.5 x 2.5 x 41cm (radial x tangential x longitudinal). The static bending tests were performed following the protocols of ASTM D143 (ASTM D143 2007). The load was applied on the tangential-longitudinal face in a three-point conFigureuration using a Z010 Zwick Roell Testing System (Zwick Roell, Kennesaw, GA, USA) at a loading rate of 1.3mm/min. The linear portion of the load-deflection curve was used to determine MOE, while MOR was calculated using maximum bending moment at the maximum load borne by the specimen. The moisture content and density at test were determined following the protocols described in ASTM D143. The density was determined by measuring the dimensions of the samples with calipers to the nearest 0.025mm and the weight to the nearest 0.001g.

The dynamic MOE of the samples were also determined using equations 5 and 6 for the resonance and the time – of – flight tools respectively.

$$DMOE_R = (V_R)^2\rho \quad \text{Equation 5}$$

$$DMOE_{TOF} = (V_{TOF})^2\rho \quad \text{Equation 6}$$

where $DMOE_R$ is the dynamic MOE estimated by the Resonance Log Grader tool, V_R is the velocity determined by Resonance Log Grade, ρ is the density (kg/m^3), $DMOE_{TOF}$ is the dynamic MOE estimated by the FAKOPP Microsecond Timer, V_{TOF} is the velocity estimated by the FAKOPP Microsecond Timer tool. The addition of GD and OD to the dynamic MOE - ($DMOE_{ROD}$, $DMOE_{RGD}$, $DMOE_{TOFOD}$, and $DMOE_{TOFGD}$) indicated the type of density used in the computation. GD and OD indicated density at test and oven-dry density respectively was used for the computation of their associated dynamic MOE.

4.3.4 Data analysis

The data was analyzed using proc mixed in SAS 9.4 (SAS 2014). The model was fitted for the tool, EMC below and above fiber saturation points (emc1 and emc2 respectively) and the two-way interaction terms (equation 7)

$$Y_{ijk} = \beta_0 + \beta_1 tool + \beta_2 emc1 + \beta_3 emc2 + \beta_4 tool * emc1 + \beta_5 tool * emc2 + \varepsilon_{ijk} \quad \text{Equation 7}$$

where Y_{ijk} is the velocity of i^{th} sample, j^{th} EMC, and k^{th} tool, β_0, β_1, β_2, β_3, β_4, β_5 are the intercept, mean change in velocity due to tool, mean change in velocity due to EMC1 below fiber saturation, mean change in velocity due to EMC2 above fiber saturation, interaction term for the tool and EMC below and above fiber saturation points (FSP) respectively. These parameters were tested whether they are significantly different from zero.

The analysis of variance of the fitted model in equation 7, indicated that EMC1 and tools have significant effect on velocity while there are no significant interaction term and EMC2. Hence simple linear regression models were fitted for each tool at EMC below and above FSP (emc1 and emc2) equation 8.

$Yi = a + b*EMC + \varepsilon_i$ Equation 8

where ***Y*** is the mean velocity, ***a*** is the intercept and ***b*** is the mean rate of change in EMC below and above FSPs for each tool.

4.4 Results and Discussions

4.4.1 Density

The density result is presented in Figure 4.4. There is a general decrease in mean density as equilibrium moisture content in the samples decreased (Figure 4.4). This result is in agreement with several previous reports (FPL 2010; Chen et al. 2011). Chan et al. (2011) reported linear increase in density with moisture content when they studied radiata pine boards. The fiber saturation point for loblolly pine has been reported to occur within 20 – 30% moisture content (FPL 2010). Based on our density and acoustic measurements, the FSP appeared to be around 29%, especially given the sharp drop in density at 29% (Figure 4.4). The density of wood is a function of the wood material and the amount of water contained therein. When wood interacts with water, both the weight and dimensions of the wood change until the fiber saturation point is attained after which additional water absorption increase the weight of the wood with no alteration to the dimension. Hence, above the fiber saturation point, the density of wood is highly influenced by the weight of the moisture hence reduction in moisture leads to a significant decrease in density (Figure 4.4). Below the fiber saturation point, however, reduction in moisture

caused both shrinkage in the volume and a reduction in weight resulting in a slight decrease in density (Figure 4.4) (FPL, 2010). Since the volume of the wood decrease but the weight of the wood material remains relatively constant at certain point below the fiber saturation point (oven-dry weight), the density tends to increase as desorption progresses well below the saturation point.

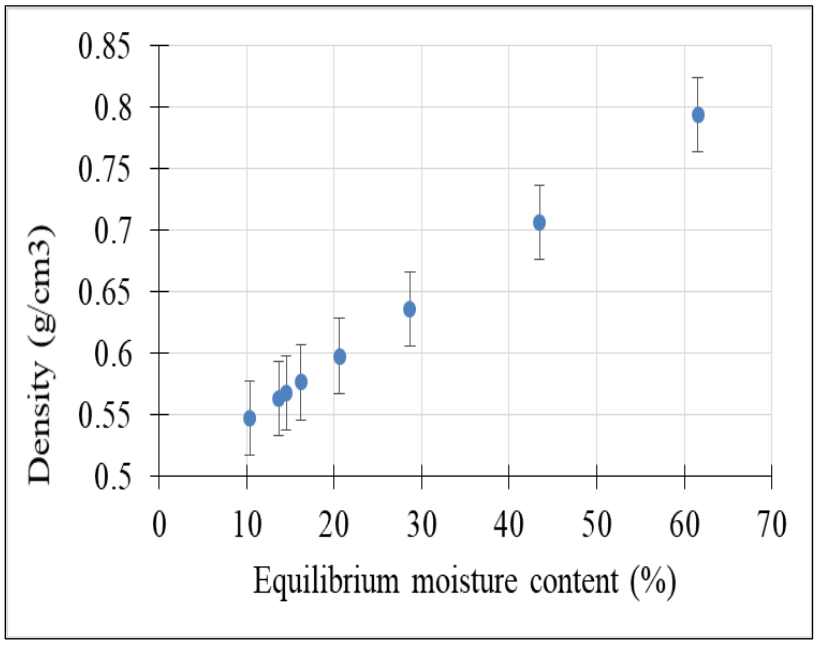

Figure 4.4 Relationship between mean density and EMC

4.4.2 Static and dynamic properties of the green small clear samples

The results of the green static MOR, static, and dynamic MOE are presented in Table 4.1 and Figures 5.5 – 5.8. The mean and coefficient of variation (COV) of the green static MOE and MOR are 7.3GPa and 29%; and 51.6MPa and 25% respectively. The green MOE reported in this study is 25% lower than as stated in FPL (2010), but 87% higher than as reported by Moya et al. (2013) when they studied 15-year-old loblolly pine grown in the subtropical part of Uruguay. Similarly, the MOR of the present study is 70% higher than as reported by Moya et al. (2013).

The differences in the strength and stiffness values are due to several factors such as edaphic, environmental, and the genetic stock of the planting materials.

Moya et al. (2013) stated that the mean diameter at breast height of the trees was 30 cm which is 90% larger than ours of similar age. Generally, the slower growing trees in this study produced a higher proportion of latewood comprising of a thick cell wall, lower MFA, longer fibers, high MOE, and density as compared to the higher proportions of earlywood produced by fast growing trees. Therefore, even though loblolly pine between 11 and 15 - year old is considered juvenile wood (Bendtsen and Senft 1986; Clark et al. 2006), the growth rate and the genetic sources of the planting material can improve the mechanical properties significantly. For this study, the growth rate was slow due to poor site nutrient conditions while the elite families were present. It is likely that the combination of these two factors help to explain the unusually high mechanical properties as such a young age. Others have seen similar strength values for loblolly pine Moya et al. (2013).

There is a strong positive linear relationship between the green static MOE versus $DMOE_{TOFOD}$ and $DMOE_{ROD}$ with adjusted coefficient of determination (R^2_{adj}) of 72% and 68% respectively (Table 4.2). Similarly, the relationship between static MOE vs $DMOE_{TOFGD}$ and $DMOE_{RGD}$ yielded R^2_{adj} values of 71 % and 56% respectively. However, it is worth noting that though the slopes of the regression between the static MOE vs MOE_{TOFOD}, MOE_{ROD}, MOE_{TOFGD}, and MOE_{RGD} were 0.64, 0.86, 0.48, and 0.58 respectively and they were statistically different from zero (Table 4.2). The overlapping nature of the 95% confidence intervals and the similitude of the R^2_{adj} suggested the dynamic MOEs estimated with both oven-dry (OD) density and density at test (GD) provides a reliable relationship with the static MOE. However, when the oven-dry density was used for equations 5 and 6, the dynamic MOE was overestimated by 16% when

compared to the static MOE. The density at test (GD) based dynamic MOE overestimated the static MOE by 72%.

This suggests that though dynamic MOEs estimated with both densities provide similar strength of relationships with the static MOE, density at test (GD) based dynamic MOE significantly overestimate the static MOE. Wang et al. (2004) reported the slopes and the R^2 of the relationships between the green log static MOE and log dynamic MOE estimated by TOF for Red pine, Jack pine, Douglas fir, and Ponderosa pine to be 1.47, 0.79, 0.33, and 0.73, and 75%, 60%, 7%, and 55% respectively. The slopes and the R^2 reported in the present study falls within the range reported by Wang et al. (2004) even though the dimensions of the studied sample differs between the two studies.

It should be noted that all of the measurements in the present study were taken from the same small clear green samples contrary to what is usually reported in the literature where dynamic MOE of trees or logs is regressed against air dried small clear samples (Raymond et al. 2008; Mora et al. 2009; Yin et al. 2011). To the best of the authors' knowledge, there is no reported study on loblolly pine using the green clear samples for both the static and the dynamic MOE determination.

The semblance of the slopes and the R^2 in both studies despite difference in sample dimension suggests that the drivers of the relationship between the static and dynamic MOEs are inherent in the wood independent of the dimensions of the wood material. Essien et al. (2017) attribute the acoustic signal to be sensitive to the same suite of fiber morphology and chemistry as a real stick of wood which is important if acoustics is to be used for determination of stiffness in juvenile or younger wood. This is because Via et al. (2009) found MFA and lignin to be more

relevant to stiffness in younger tissue while density and cellulose are more important for older growth material.

Similarly, there is a positive linear relationship between MOR vs static MOE, $DMOE_{TOFOD}$, $DMOE_{ROD}$, $DMOE_{TOFGD}$, and $DMOE_{RGD}$ with slopes 5.3, 3.3, 4.5, 2.5, and 3.0; and R^2_{adj} of 77%, 51%, 50%, 49%, and 39% respectively (Table 4.2). Butler et al. (2016) found a significant positive relationship between air-dried small clear loblolly pine sample MOR and MOE with slopes between 5.76 to 6.73, and 40 to 56% for R^2. Additionally, Moya et al. (2013) reported strong linear relationship between MOR and MOE of small clear green 25-year-old loblolly pine with R^2 of 77%. Ilic (2001) reported $DMOE_R$ explained 69% variation in the static MOE of air dried small clear alpine ash samples.

This moderate linear relationship between the static MOR and dynamic MOEs reported in the present study support the proposal that the acoustic tools can be used to characterize wood samples into MOR classes. Via et al. (2009) found that lignin and hemicelluloses become very important loading bearing component in the plastic deformation phase of the typical stress to strain curve of wood during bending while cellulose dominates the elastic phase of the curve, hence demonstrating the significant effect of hemicelluloses on MOR.

Essien et al. (2017) demonstrated that the cellulose is the major driver of sound signal at the polymeric level with hemicellulose being the second most important signal conductor. This switch in role of hemicellulose might be the major contributor to the high relationship between the MOR and static MOE as compared to that with the dynamic MOEs. This is a subtle but important point because conventional acoustics are traditionally based on elastic mechanics and MOR has traditionally just been assumed to covary with MOE.

Table 4.1 Descriptive statistics of the green static MOE and MOR, dynamic MOE estimated by resonance log grader ($DMOE_R$), Microsecond Timer ($DMOE_{TOF}$)

	Static MOE (GPa)	Static MOR (MPa)	$DMOE_{ROD}$ (GPa)	$DMOE_{TOFOD}$ (GPa)	$DMOE_{RGD}$ (GPa)	$DMOE_{TOFGD}$ (GPa)
Mean	7.35	51.55	8.55	8.73	12.67	12.85
SD	2.11	12.68	2.06	2.82	2.78	3.75
CoV	28.68	24.60	24.09	32.30	21.96	29.20
Min	3.46	30.6	5.52	2.75	9.11	4.58
Max	10.20	75.0	11.94	12.89	17.66	17.71

$DMOE_{ROD}$ and $DMOE_{RGD}$ are dynamic MOEs estimated by resonance based tool with oven-dry density and density at test respectively.
$DMOE_{TOFOD}$ and $DMOE_{TOFGD}$ are dynamic MOEs estimated by time – of – flight based tool with oven-dry density and density at test respectively.

Table 4.2 Linear models (***y= a + bx***) of the relationships between the green static MOR, MOE (MOE_{st}), and dynamic MOE estimated by resonance log grader ($DMOE_R$), Microsecond Timer ($DMOE_{TOF}$) for 15 small clear samples

y	***x***	95% CL of ***a***	95% CL of ***b***	R^2_{adj}
MOR	MOE_{st}	12.29 (-0.99, 25.59)	5.3 (3.6, 7.1)	77.04
	MOE_{ROD}	12.80 (-10.2, 35.80)	4.5 (1.9, 7.2)	50.37
	MOE_{TOFOD}	22.4 (5.07, 39.72)	3.3 (1.4, 5.2)	51.39
	MOE_{RGD}	13.4 (-14.5, 41.3)	3.0 (0.86, 5.2)	38.86
	MOE_{TOFGD}	20.01 (0.5 , 39.53)	2.5 (1.0 , 3.9)	48.78
MOE_{st}	MOE_{ROD}	25 (-3067, 3117)	0.86 (0.51, 1.21)	67.58
	MOE_{TOFOD}	1745 (-457, 3947)	0.64 (0.40, 0.88)	71.60
	MOE_{RGD}	-37 (-3982, 3908)	0.58 (0.28 , 0.89)	55.80
	MOE_{TOFGD}	1169 (-1268, 3606)	0.48 (0.30, 0.66)	71.10

$DMOE_{ROD}$ and $DMOE_{RGD}$ are dynamic MOEs estimated by resonance based tool with oven-dry density and density at test respectively.
$DMOE_{TOFOD}$ and $DMOE_{TOFGD}$ are dynamic MOEs estimated by time – of – flight based tool with oven-dry density and density at test respectively.

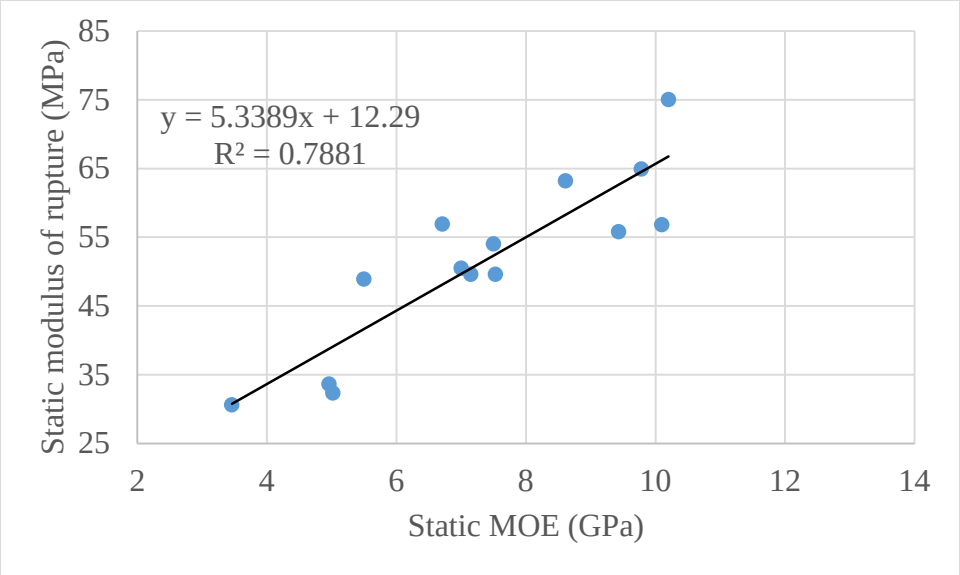

Figure 4.5 Relationship between the green static MOR and static MOE for 15 small clear samples

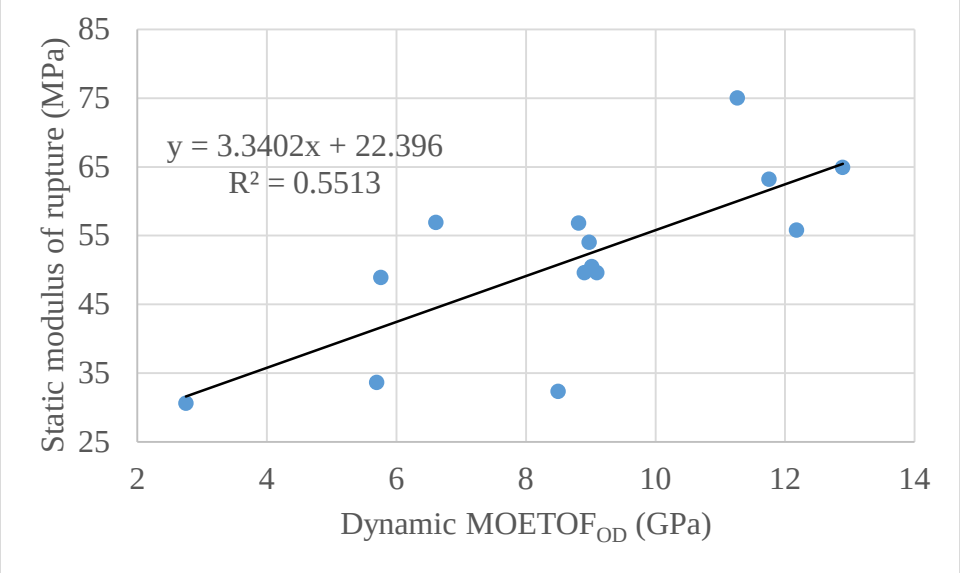

Figure 4.6 Relationship between the green static MOR and dynamic MOE estimated by time – of – flight based tool with oven-dry density ($DMOE_{TOFOD}$)

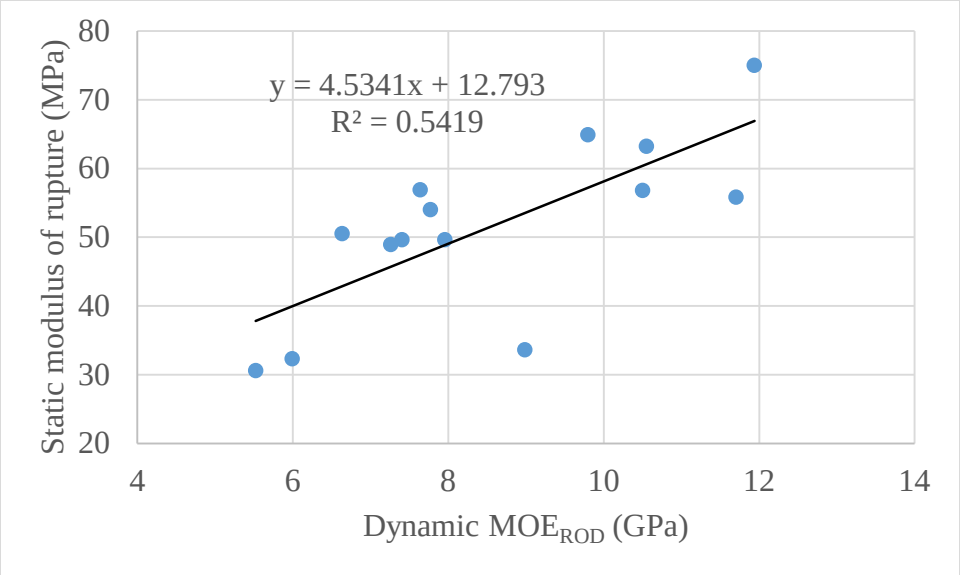

Figure 4.7 Relationship between the green static MOR and dynamic MOE estimated by Resonance based tool with oven-dry density (DMOE$_{ROD}$)

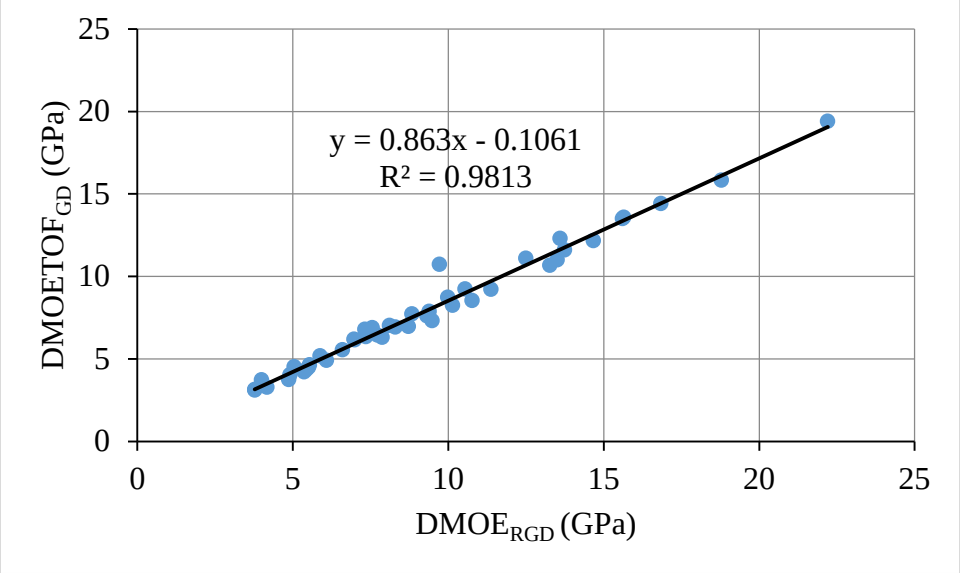

Figure 4.8 Relationship between the dynamic MOE estimated by Microsecond Timer (DMOE$_{TOFGD}$) and Resonance Log Grader (DMOE$_{RGD}$) for the 45 small clear samples

4.4.3 Effect of EMC on velocity and dynamic MOE

From Table 4.3, velocity generally increased with decreasing equilibrium moisture content. This result confirmed several studies conducted in this area (Ilic 2001; Kang and Booker 2002; Goncalves 2008; Hasegawa et al. 2011; Yang et al. 2015). The inverse relationship between velocity and EMC may be due to the impedance which increases with increasing moisture content (Yang et al. 2015). This is because the moisture in the cells (below FSP) interacts with the waves resulting in an absorption, refraction, and reflection of the waves leading to reduction in energy. This process ultimately results in a decreased velocity of wave propagation in wood (Yang et al. 2015). Alternatively, the velocity of sound in free water is approximately 1500m/s which is lower than that of dry wood which is about 4500m/s. As the wood dries, the moisture decreases leaving behind the relatively higher sound conducting wood material as shown in Table 3.

There is a significant difference between the mean rate of change in velocity with EMC below and above the hygroscopic region of the samples (Table 4.4). The mean rate of change in velocity per unit change in EMC is 33.9 m/s and 5.4 m/s for the below and above FSPs respectively for the TOF tool while they are 28.8 m/s and 6.1 m/s respectively for the resonance ones (Table 4.4). Several reports have also shown sharp decrease in acoustic velocity with increasing moisture content below fiber saturation point (Yang et al. 2015; Chan et al. 2011). Chan et al. (2011) found 32 m/s decrease in velocity per unit increase in moisture content below FSP and 6 m/s decrease in velocity for moisture content above FSP when they used resonance – based acoustic tool. From Table 4.4, the change in velocity above the hygroscopic region is not significantly different from zero hence one can deduce that velocity is unaffected by free water present in the cell lumen. This suggests that the cell walls are the major signal conducting avenue

in the wood material instead of the cell lumen hence the presence of free water in the lumen does not significantly affect the velocity. Therefore, for healthy standing (live) trees and fresh logs, one will not expect moisture to drop below the hygroscopic region hence changes in moisture content will not significantly affect velocity. Operationally, this observation is important on two fronts a) one does not need to measure or control for moisture content in the field and perhaps most importantly, b) any change in density due to changes in free water within the tree is just adding random and unnecessary error to the estimate of MOE (Equation 5-6). Instead, only oven dry density can be used in equation 5-6 to capture real trends or differences in mechanical properties between trees.

The effect of EMC on dynamic MOEs estimated with both tools is shown in Figures 4.9 and 4.10. Generally, dynamic MOE increases with decreasing EMC below the fiber saturation point. This is due to confounding and complex relationships between moisture vs velocity, moisture vs density, and density vs velocity. Below the fiber saturation point, velocity becomes the main driver of the dynamic MOE (Equations. 5 and 6) since the bound water content which acts as a signal dispersant, absorbance or reflectance decreases and the density stabilizes (Figure 4.4). The net effect of these factors caused an increase in DMOE for both tools with decreasing EMC (Figure 4.9 and 4.10). On average, $DMOE_R$ decreased by 0.53GPa whereas $DMOE_{TOF}$ decreased by 0.61GPa for EMC from 10% to 29%. Chan et al. (2011) reported 0.71 GPa decrease in $DMOE_R$ for EMC from 17 to 25% when they studied 8 x 5.5 x 105 cm^3 radiata pine sapwood while Ilic (2001) reported 0.81 GPa reduction in $DMOE_R$ for EMC from 16% to 30% when he studied 9.5 x 4.5x 60 cm^3 Eucalyptus heartwood. The difference in $DMOE_R$ reduction values may be due to the moisture range studied as well the type and dimensions of wood species used.

On the other hand, DMOE increased slightly with increasing EMC above the fiber saturation point thus from 43% to 62% (Figure 4.9) (Gerhards 1975; Sobue 1993). $DMOE_R$ increase by 0.18GPa whereas that of $DMOE_{TOF}$ is 0.2GPa. This observation is due to the counterbalancing effect of density and velocity (Figure 4.1, Table 4.3). The percentage increase in squared velocity from 29 to 62% were 11% and 15% for the resonance and TOF based tools respectively while percentage decrease in density for the same EMC range was 33%. This counterbalancing effect in the computation of the DMOE might be responsible for this phenomenon. However, this may be erroneous since one does not expect MOE to increase with moisture above the fiber saturation point FPL (2010). As indicated earlier, change in velocity with moisture above the fiber saturation is 5.8m/s and 6.1 m/s for the TOF and resonance tools respectively which are statistically not significantly different from zero, hence any ambiguity in the dynamic MOE (Figure 4.9) may be due to the density used in the computation.

Consequently, oven-dry density was used to compute the dynamic MOE as shown in Figure 10. It is clear that dynamic MOEs are relatively the same between 43 and 62% EMC but increase with decreasing EMC from 29% to 10%. This trend supports the established fact that above the FSP, mechanical properties do not vary significantly with moisture. Based upon this observation, dynamic MOE deviation was computed for the resonance tool according to Equation 9 and results shown in Figure 4.11.

$$\Delta MOE = 100 * \left(\frac{DMOE_{RGD} - DMOE_{ROD}}{DMOE_{ROD}}\right) \quad \text{Equation 9}$$

From Figure 11, the percentage dynamic MOE deviation is a function of the EMC which decreases with decreasing EMC. It decreased from 27% to 9% below the fiber saturation point (29% to 10% EMC), but it was greater than 40% above the fiber saturation point. This suggests

that using the density at test (GD) to estimate dynamic MOE of the standing tree or fresh log will overestimate it by at least by 40% as compared to using oven-dry density.

Table 4.3 Descriptive statistics of the effect of EMC on velocity estimated by resonance and TOF acoustic tools

	Resonance		**TOF**	
EMC (%)	Mean (km/s)	CoV (%)	Mean (km/s)	CoV (%)
62	3.08	21.81	3.34	21.30
43	3.10	21.30	3.40	21.81
29	3.30	20.21	3.52	20.21
21	3.45	19.19	3.65	19.19
16	3.54	18.55	3.76	18.55
15	3.62	18.80	3.87	18.80
14	3.68	18.65	4.04	12.29
10	3.85	17.95	4.15	11.94

EMC=equilibrium moisture content, CoV= coefficient of variation

Table 4.4 Fit statistics for the simple linear regression E [Y_{ijk}] = a + b*EMC predicting mean velocity for each acoustic tool for EMC below and above fiber saturation points

	Microsecond Timer			Resonance log grader		
Tool	a	b	R2	a	b	R2
EMC below fsp	4.436 (4.201, 4.671)	-0.0339 (-0.047, -0.021)	92.40	4.069 (3.738, 4.400)	-0.0288 (-0.047, -0.010)	89.10
EMC above fsp	3.665 (3.263, 4.067)	-0.0054 (-0.014, 0.003)	84.6	3.437 (2.871, 4.003)	-0.0061 (-0.018, 0.006)	95.78

a = intercept, b =slope, 95% confidence limit in bracket. The range including zero is not statistically different from zero.

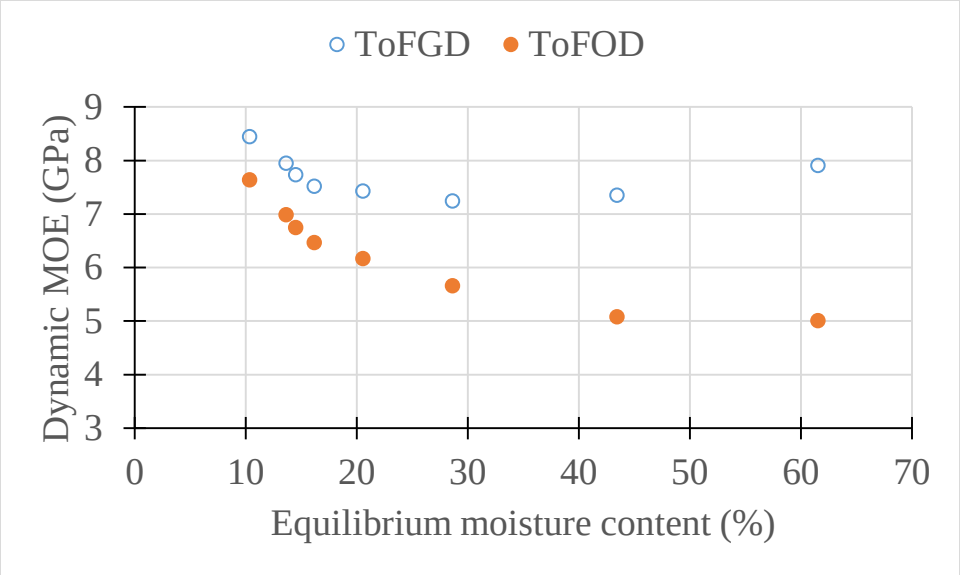

Figure 4.9 Relationship between EMC and mean dynamic MOE estimated by ToF velocity with density at test (GD) (FoFGD) and with oven dry density (ToFOD) (n=45).

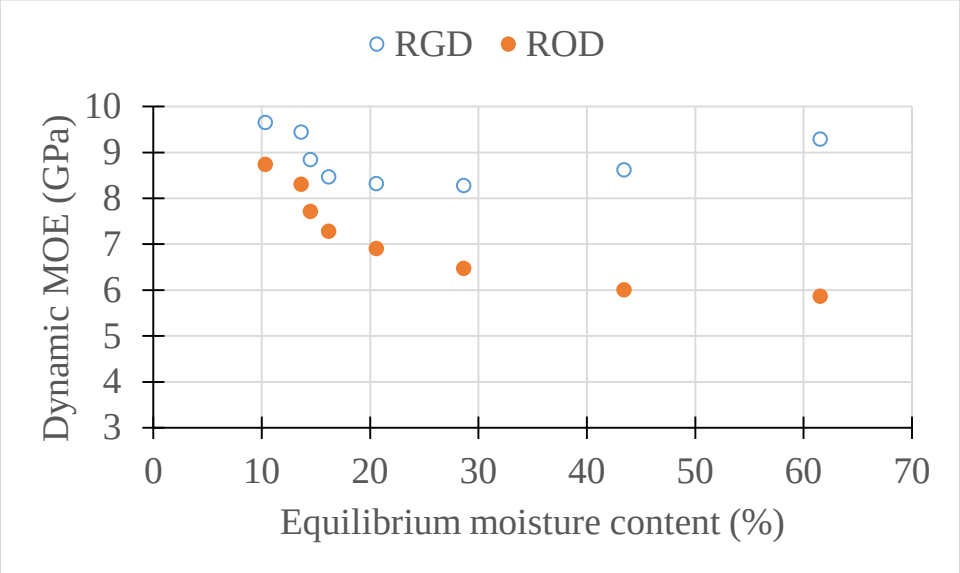

Figure 4.10 Relationship between EMC and mean dynamic MOE estimated by resonance velocity with density at test (GD) (RGD) and with oven dry density (ROD) (n=45)

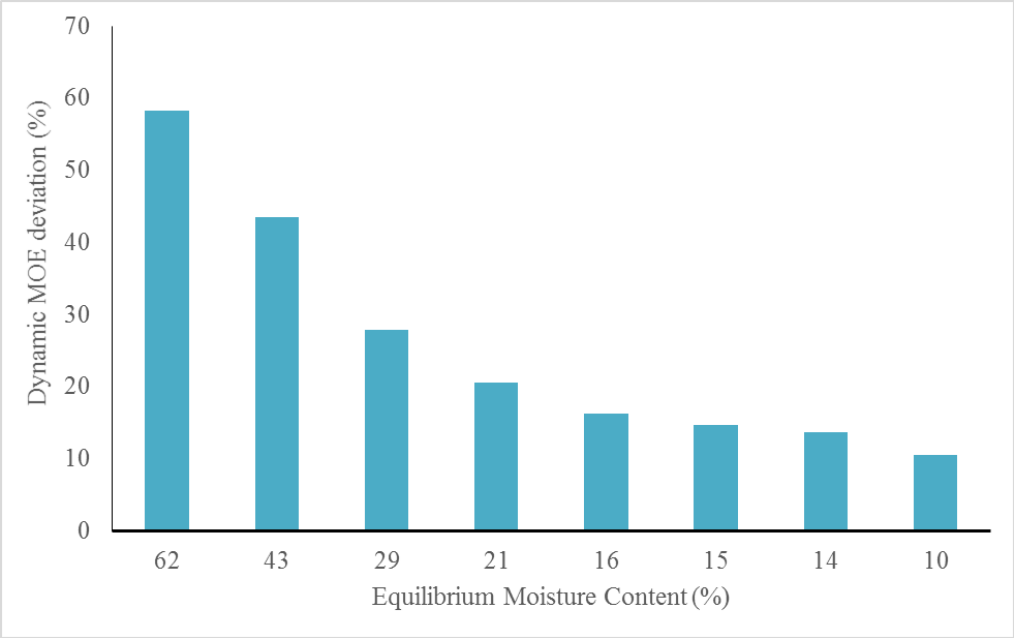

Figure 4.11 Relationship between EMC and dynamic MOE deviation for the Resonance Log grader (RGD) tool (n=45).

4.5 Conclusion

The effect of equilibrium moisture content on acoustic velocity and dynamic MOE estimated by resonance and TOF based acoustic tools were studied. The results indicated a strong positive relationship between the static MOE, MOR and dynamic MOEs estimated by both types of tools with the different densities. Also, the static MOE of the green samples exhibited similar strength of linear relationship with dynamic MOEs estimated with both the oven-dry density and density at test. However, for both acoustic tools, the static MOE was overestimated by about 16% when dynamic MOEs were estimated with oven-dry density (OD), but it was overestimated by about 72% when dynamic MOEs were determined with the density at test (GD). The results suggest that the OD density should be used when computing the dynamic MOE.

From this study, it has been demonstrated that using the density at test (green density) to predict the dynamic MOE of live trees and freshly harvest logs, with the moisture above the FSP, will be at least 40% higher than similar prediction using oven-dry density. Also, the study supports the idea that acoustic tools can be used to characterize wood into strength classes.

Furthermore, equilibrium moisture content of loblolly pine significantly affects velocity measured below and above the hygroscopic region. The results indicated the acoustic velocity decreased by 33.9 m/s and 28.8 m/s for TOF and the resonance tools respectively for unit increase in EMC below fiber saturation point. The change was lower for EMC above FSP - 5.4 m/s for TOF and 6.1 m/s for resonance.

The insignificant slope coupled with better accuracy in MOE supports the hypothesis that the cell wall controls the acoustic velocity while the water in the lumen of the cell wall is insignificant. These results bring into question the standard use of green density to estimate acoustic MOE and oven dry density is instead recommended. On average, $DMOE_R$ decreased by 0.53GPa whereas $DMOE_{TOF}$ decreased by 0.61GPa for EMC from 10% to 29%. These results suggest that the both tools are equally sensitive to variations in EMC below and above FSP.

4.6 References

ASTM Standard D 143-94. (2007) Standard test methods for small clear specimens of timber. ASTM International, West Conshohocken, Pa. Available at www.astm.org [accessed 5 Jan. 2014].

Beall F.C. (2002) Overview of the use of ultrasonic technologies in research on wood properties. Wood Science and Technology 36: 197-212

Bendtsen BA and Senft J. (1986) Mechanical and anatomical properties in individual growth ring of plantation-grown cottonwood and loblolly pine. Wood Fiber Sci 18(1):23 - 38

Bodig J and Jayne BA. (1982). Mechanics of wood and wood composites.

Butler MA, Dahlen J, Antony F, Kane M, Eberhardt TL, Jin H, Myers KL, McTague JP. (2016) The relationship between loblolly pine small clear specimens and dimension lumber test in static bending. Wood and Fiber Sci. 48(2): 81-95.

Chan M J, Walker CJ and Raymond CA. (2011) Effect of moisture content and temperature on acoustic velocity and dynamic MOE of radiata pine sapwood boards. Wood Sci and Technol 45: 609-626 doi: 10.1007/s00226-010-0350-6

Chauhan SS, and Walker JCF (2006) Variations in acoustic velocity and density with age, and their interrelationships in radiate pine. For. Ecol. Manage. **229**(1–3): 388–394. doi:10.1016/j.foreco.2006.04.019.

Clark A, Daniels RF, and Jordan L. (2006) Juvenile/mature wood transition in loblolly pine as defined by annual ring specific gravity, proportion of larewood, and microfibril angle. Wood fiber and Sci. 38(2): 292 – 299

Essien C, Via BK, Acquah G, Gallagher T, McDonald T, Eckhardt LG .(2017). Multivariate Modeling of Acousto-mechanical Response of Fourteen Year Old Suppressed Loblolly Pine (*Pinus taeda*) to Variation in Wood Chemistry, Microfibril Angle, and Density. Wood Sci Technol 51: 475 – 492. doi 10.1007/s00226-017-0894-9

FPL (Forest Products Laboratory) (2010) Wood handbook—Wood as an engineering material. General Technical Report FPL-GTR-190. Madison, WI: U.S. Department of Agriculture, Forest Service, Forest Products Laboratory. 508 p.

Gao S, Wang X, Wang L, and Allison RB. (2012) Effect of temperature on the acoustic evaluation of standing trees and logs: part 1 – laboratory investigation. Wood and Fiber Science 44(3):286-297

Goncalves R, and Leme OA. (2008) The influence of moisture content on longitudinal, radial and tangential ultrasonic velocity for two Brazilian wood species. Wood and Fiber Science 40(4): 580-586

Gerhards CC. (1975) Stress wave speed and MOE of sweetgum ranging from 150 to 15 percent MC. Forest prod J. 25(4): 51 – 57

Harris PD and Andrews MK. (1999). Tools and acoustic techniques for measuring wood stiffness. In: Proceedings of the 3rd wood quality symposium: emerging technologies for evaluating wood quality for processing, Forest Industry Engineering Association, Rotorua, New Zealand

Hasegawa M, Takata M, Matsumura J, Oda K (2011) Effect of wood properties on within-tree variation in ultrasonic wave velocity in softwood. Ultrasonics 52: 296-302

Ilic J (2001) Variation of the dynamic elastic modulus and wave velocity in the fiber direction with other properties during the drying of *Eucalyptus regnans* F Muell. Wood Sci and Technol 35:157-166

Ilic J (2001) Relationship among the dynamic and static elastic properties of air-dry *Eucalyptus delegatensis* R. Baker. Holz als Roh 59:169-175

Kang H and Booker RE (2002) variation of stress wave velocity with MC and temperature. Wood Sci and Technol 36: 41-54

Moya L, Laguarda ML, Cagno M, Cardoso A, Gatto F, O'Neill (2013) Physical and mechanical properties of loblolly and slash pine wood from Uruguayan plantations. For. Pro. J. 63 (3/4): 128 – 137. Doi: 10.13073/FPJ-D-13-00024

Mora, C. R., Schimleck, L. R., Isik, F., Mahon Jr., J. M., Clark III, A., Daniels, R. F. (2009). Relationship between acoustic variable and different measures of stiffness in standing *Pinus taeda* trees, Can. J. For. Res. 39(8), 1421-1429 DOI: 10.1139/X09-062

National Oceanic and Atmospheric Administration (2016) State, regional and national monthly precipitation: area weighted monthly normal, 1981 – 2015. Historical Climatography

Olivito RS. (1996) Ultrasonic measurements in wood. Materials Eval 54:514–517

Raymond CA, Joe B, Anderson DW, and Watt DJ .(2008) Effect of thinning on relationships between three measures of wood stiffness in *Pinus radiata*: Standing trees *vs*. short clear specimens," Can. J. For. Res. 38(11), 2870-2879. DOI: 10.1139/X08-124

Sandoz, J.L.1991. Nondestructive evaluation of building timber by ultrasound. 8th International Symposium on Non-destructive testing of wood. Vancouver.

Sobue N .(1993). Simulation study on stress wave velocity in wood above fiber saturation point. Mokuzai Gakkaishi 39(3): 271 – 276

Via BK, So CL, Shupe TF, Groom LH, Wikaira J (2009) Mechanical response of longleaf pine to variation in microfibril angle, chemistry associated wavelengths, density and radial position. Composites: Part A 40 (1):60-66

Wang X, Ross RJ, Brashaw BK, Punches, Erickson JR, Forsman JW, and Pellerin RE. (2004). Diameter effect on stress-wave evaluation of modulus of elasticity of logs. Wood and Fiber Science 36(3): 368-377.

Wang X, Ross RJ, McClellan M, Barbour RJ, Erickson JR, Forsman JW and McGinnis GD (2001). Nondestructive evaluation of standing trees with a stress wave method. Wood and Fiber Science 33(4): 522-533.

Wang X. (2008). Effects of size and moisture content on stress wave E-rating of structural lumber. 10th World Conference on Timber Engineering. Miyazaki, Japan.

Wang X, Ross EJ, Carter P. (2007). Acoustic evaluation of wood quality in standing tree. Part1; Acoustic wave behavior. Wood and Fiber Science 39(1): 28-38

Yang H, Yu L and Wang L (2015) Effect of moisture content on the ultrasonic properties of wood. Journal For Res 26(3): 753-757

Yin Y, Jiang X, Wang L, Bian M. (2011). Predicting wood quality of green logs by resonance vibration and stress wave in plantation-grown Populus x euramericana. Forest Prod J. 61(2): 136-142

Chapter 5: Elucidating the effect of site and genetic sources on the anatomical, morphological, and mechanical properties of 14-year-old loblolly pine

5.1 Abstract

Tree improvement programs on loblolly pine (*Pinus taeda* L) in the southeastern USA have focused primarily on improving growth, form, disease, and pest tolerance. However, due to the recent reduction of design values for visually graded southern yellow pine lumber (including loblolly pine), attention has been drawn to the material quality of genetically improved loblolly pine. In this study, we assessed the effect of site and genetic families on diameter, slenderness, fiber length, microfibril angle (MFA), velocity and dynamic stiffness (E_{tree} and E_{basic}) of 14- year-old loblolly pine stands.

The results indicated a significant positive linear relationship between dynamic MOEs (E_{tree} and E_{basic}) versus tree diameter, slenderness, and fiber length while dynamic MOE was negatively correlated with MFA. While there was no significant difference in E_{basic} between sites; velocity^2 for site 1 was significantly higher than site 2 but E_{tree} was higher for site 2 than site 1. Again, the mean E_{basic} and E_{tree} reported in the present study presents a snapshot of the expected static MOE for green and 12% moisture conditions respectively.

Random block design analysis found significant differences between families for most of the traits measured and this suggests that forest managers have the potential to select families that exhibit the desired fiber morphology for final product performance.

5.2 Introduction

In the southeastern United States, loblolly pine (*Pinus taeda* L) is the most dominant tree species in the southern yellow pine (SYP) group in terms of cultivation, utilization and genetic improvement (McKeand et al. 2003). One of the most important premium products from this species is still dimension lumber for structural applications. There are several mechanical properties used to categorize the stiffness and strength of wood products. The two most widely measured mechanical properties for stiffness and strength are the modulus of elasticity (MOE) and modulus of rupture (MOR) respectively (FPL 2010). Isik et al. (2011) emphasized that MOE is one of the most important mechanical properties of wood and engineered wood products derived from loblolly pine. Consequently, in 2013, the design values for visually graded southern yellow pine lumber were adjusted in an attempt to reflect the material strength and stiffness of today's market (ALSC 2013). For many product dimensions, these values dropped making United States southern yellow pine (SYP) lumber less competitive on the international market.

Traditionally, small clear wood samples have been used to directly determine the effect of site, genetic source and planting density on the MOE and MOR. For instance, Clark et al. (2008) studied the effect of planting density on MOR and MOE for loblolly pine small clear samples and reported that these properties decreased with decreased planting density. MOE has been found to be highly or moderately heritable (Johnson and Gartner 2006; Lenz et al. 2013) indicating that trees with a superior modulus of elasticity can be bred and deployed for plantation development.

Given that MOE is used to nondestructively classify lumber quality in the manufacturing plant using machine stress grading technology, estimation of MOE in both standing trees and logs would be of considerable use to tree breeders, mill managers, and silviculturists. For this

purpose, several nondestructive instruments have been developed that can directly and/or indirectly measure the intrinsic wood quality of small wood samples, logs or trees (Wang et al. 2001and 2004; Mora et al. 2009). Among these instruments are acoustic–based nondestructive tools which are simple, compact, and easy to operate on small wood samples, logs and standing trees (Dickson et al. 2004). Several researchers have found a strong linear relationship between the predicted MOE of logs and trees against the static MOE small clear samples derived from the same trees or logs for different species (Wang et al. 2002 and 2004; Lachenbruch et al. 2008; Vikram et al. 2008; Raymond et al. 2008; Essien at al. 2016a) although the tree velocity is usually slightly higher than log velocity (Bertoldo and Gonçalves 2015). Currently, the most popular acoustic techniques used are ‘‘time - of - flight’’ and ‘‘resonance’’ for standing tree and logs respectively (Wang et al. 2002; Raymond et al. 2008).

The time–of–flight (TOF) method measures the time it takes for an introduced stress wave to travel from point to point and currently is the only practical acoustic method for estimating MOE in standing trees (Lasserre et al. 2007; Wang 2013; Essien et al. 2016a). Therefore, the TOF tools can be used for pre-harvest, and progeny screening programs. Additionally, they can be used to predict the effect of edaphic, environmental, silvicultural and genetic factors on MOE of standing trees. This presents a unique opportunity for inclusion of stiffness screening in the tree breeding programs.

Lasserre et al. (2007) studied the effect of a genetic source, planting density and site on MOE of 11-year-old radiata pine. They observe MOE increases with increased planting density, but there was a significant interaction between site and genetic source. Roth et al. (2007) observed similar results when they studied the effect of planting density, genotype, and management operations on MOE for 6-year-old loblolly pine. Furthermore, Essien et al. (2016a)

reported thinning operations performed at 13 and 22 years after planting, significantly increased the MOE of standing trees by the 29th year for loblolly pine. Essien et al. (2017) attribute the acoustic signal to be sensitive to the same suite of fiber morphology and chemistry as a real stick of wood which is important if acoustics is to be used for determination of stiffness in juvenile or younger wood. This is because Via et al. (2009) found MFA and lignin to be more relevant to stiffness in younger tissue while density and cellulose is more important for older growth material. With younger material, it is important that acoustics be sensitive to the right factors that truly effect stiffness or the genetics analysis will be misleading.

Different authors have reported different trends for the relationship between velocity and stiffness against diameter at breast height (DBH). Lasserre et al. (2005) and Carson et al. (2014) reported a negative relationship between stiffness and DBH when they studied 11 and 17-year-old radiata pine respectively. Briggs et al. (2007) on the other hand reported a positive relationship for Douglas fir between 32 and 36 years old while the relationship was negative for the 42-year-old trees. The relationship between the velocity and DBH was positive for the thinned stand while it was negative for the unthinned stand (Essien et al. 2016a). The relationship between the velocity and stiffness against DBH seem to be affected by age, tree species and silvicultural management operations of the stands (Wang et al. 2004; Briggs et al. 2007; Essien et al. 2016a).

This divergent relationship between diameter and dynamic MOE estimated by TOF might be due to the fact that the generated sound waves are restricted to the sapwood portion that is penetrated by the probes. Since fast growing trees produce wood with thin and large lumen cells, one would expect a lower velocity and stiffness. Furthermore, the velocity of fast growing trees will be reduced due to a higher percentage of free water in the cell lumen.

Since loblolly pine constitutes the major part of SYP, understanding the main and interactive effects of the available planting stock and site in relation to the MOE is of utmost importance for the growth and sustainability of the forest industry. If statistically, significant relationship exists between the main and interactive effects of site and genetic sources, then a predictive model for loblolly pine must consider the site and genetic sources of the materials.

We hypothesized there will be a significant site and genetic sources effect on the diameter, velocity, and dynamic MOE. Therefore, the main objective of this study was to determine the main and interactive effects of site and genetic sources on diameter, velocity and dynamic MOE on fifteen genetically improved loblolly pine families.

5.3 Materials and Methods

5.3.1 Materials

The materials for this study were selected from a plantation of genetically improved families of loblolly pine (*P. taeda*) established at two sites in the southeastern United State in the year 2000. The study Site 1 was located in Nassau County Florida near Yulee (latitude $30^{o}63'$N and longitude $81^{o}57'$W) and Site 2 at Brantley County Georgia near Nahunta (latitude $31^{o}12'16''$N and longitude $81^{o}58'56''$W. The soil of Site 1 is poorly drained and formed from a thick bed of alkaline loamy and clayey marine sediments terraces with a slope less than 1% and nearly level. The mean long-term temperature and precipitation from 1981 to 2010 are 21^{o}C and 1350mm respectively. The topography of Site 2 is relatively flat with a slope less than 2% and 20m altitude above sea level. The soil is very fine sandy loam, poorly drained and generally poor in nutrients which formed from loamy and silty Coastal Plain sediments. The mean annual

temperature ranged 17 to 19^{o}C and the annual precipitation from 1981 to 2010 averaged 1315mm (NOAA 2016).

A randomized complete block design (RCBD) was used on both sites. The total size of site 1 and 2 was 6744m^2 and 8027m^2 and each site was divided into fifteen blocks measuring 450m^2 and 535m^2 respectively. Eighty (80) seedlings from eighty different genetically improved loblolly pine families were randomly planted on a bed at 1.6m x 3.2m and 1.8m x 3.6m for site 1 and 2 respectively. The same planting design, silvicultural treatments and seed lots of genetically improved loblolly pine families were used on both sites. The stands had not received any commercial thinning since establishment at the time of data collection. The experiments at both sites were established to compare the stability and growth performance of different genetically improved loblolly pine.

Fifteen out of the eighty loblolly pine families were randomly selected and tested on both sites in the spring of 2014, when the trees were 14 years old. It should also be noted that although fifteen seedlings per each genetic family were planted, seedling mortality over time reduced the number of trees in some families. In all 388 trees comprising 184 and 204 for sites 1 and 2 respectively were assessed. The height and diameter of the trees were measured using clinometer and diameter tape respectively.

5.3.2 Acoustic measurements of standing trees

All of the available trees from each of the selected fifteen families on each site were acoustically tested using the FAKOPP Microsecond Timer acoustic tool (Fakopp Enterprise, Agfalva, Hungary) which relied on the TOF principle (Wang et al. 2007; Mora et al. 2009; Essien et al. 2016a). Basically, the accelerometers (the transmitter and the receiver probes) were

positioned on the same side of the tree 120 cm apart with the center of the path occurring at breast height. Both probes were positioned 45^{o} to the tree axis and the stress wave was generated by striking the transmitter probe with a steel hammer at a steady force (Mora et al. 2009). The generated wave was detected by the receiver and the time lapse for the sound wave to travel the distance between the probes was recorded by the data logger. Seven readings each were taken on each tree and tree velocity was estimated as the ratio of the distance to time (Equation 1). The dynamic modulus of elasticity of the trees estimated with green density (E_{tree}) and with basic density (E_{basic}) was computed using Eqns. 2 and 3 (Wang et al. 2007; Essien et al. 2016a)

Bark to bark core samples were taken at the breast height portion of each of the tested trees to determine moisture content, basic and green densities. The dimensions of the cores were measured using a digital caliper to the nearest 0.025 mm and the weight to the nearest 0.001 g. Weight (M_i) and dimensions of the cores were measured while green and were subsequently dried to constant weight in an electronic oven set at 103^{o}C (M_o). The moisture content (MC), basic (ρ_{basic}) and green densities (ρ_{green}) of the cores were determined according to eqns. 4, 5, and 6 respectively.

$$V_T = D / s \qquad \text{Equation 1}$$

$$E_{tree} = V_T^2 * \rho_{green} \qquad \text{Equation 2}$$

$$E_{basic} = V_T^2 * \rho_{basic} \qquad \text{Equation 3}$$

$$MC = ((M_i - M_o)/M_o)*100 \qquad \text{Equation 4}$$

$$\rho_{green} = M_i / V_{green} \qquad \text{Equation 5}$$

$$\rho_{basic} = M_o / V_{green} \qquad \text{Equation 6}$$

where V_T is tree velocity in m/s, D is the distance between the probes in meters, s is time for the stress wave to travel the distance between the probes in seconds, E_{tree} is the dynamic

modulus of elasticity estimated by green density, E_{basic} is the dynamic modulus of elasticity estimated by basic density. MC is green moisture content of the core, M_i is initial green weight, M_o is the oven-dry weight. ρ_{green} is the green density of the disk, V_{green} is the green volume of the core.

5.3.3 MFA and fiber geometry determination

Subsamples of eight families were selected from the fifteen families used for the study. The 15 families were ranked based on the dynamic MOE; 2 families from the mid-rank while 3 families each from the higher and lower stiffness groups were selected for the anatomical study. Thin sections of wood samples measuring 0.09mm were sliced from along the entire length of the cores samples from each family. The thin samples were macerated using equal volumes of hydrogen peroxide (30%) and glacial acetic acid at 80^{o}C for 24 hours for thorough maceration (Peter et al. 2003; Essien 2012). Temporary slides were prepared from the macerated fibers; fiber length, diameter, thickness, and MFA were measured following the procedure described by Peter et al. (2003). The fiber geometry and MFA measurements were performed on forty fibers per family selected from both the earlywood and latewood using Differential Interference Contrast (DIC) Microscope (Olympus BX53) (Essien et al. 2017).

5.3.4 Data analysis

The standing tree t variables were diameter at breast height (Diameter), tree height, slenderness (ratio of total tree height to the diameter at breast height), velocity (V_T) and dynamic modulus of elasticity of tree (E_{tree}). Simple Pearson's correlation coefficients were used to determine the level of linearity among the variables. The standing tree variables were analyzed

using a generalized linear model procedure in SAS 9.4 (SAS 2014) to determine the effect of families, block, site and their interactions on diameter, velocity and dynamic MOEs (E_{tree} and E_{basic}). If site* family interaction was significant at 5%, it indicated slopes of the model were different, thus the two populations were different and therefore were analyzed them separately.

However, if the interaction term was not significant, then the two populations were similar and therefore they can be combined for analysis. In order to account for diameter and ratio of height to the diameter (slenderness) variability effect on velocity, E_{basic}, and E_{tree}, they were introduced as a covariate in the model (2). The covariates were introduced to assess the real effect of site and family on velocity and dynamic modulus of elasticity.

$$Y = \mu + \beta_1 \text{ site} + \beta_2 \text{ family} + \beta_3 \text{ block} + \beta_4 \text{ site*family} + e \quad 1$$

where Y is diameter, slenderness, tree velocity (V_T), microfibril angle, fiber length or tree dynamic modulus of elasticity (E_{tree} and E_{basic}), β_1 is the mean change in Y due to site (site 1 = 1 and site 2 = 0), β_2 is the mean change in Y due to genetic family, β_3, and β_4 is the mean change in Y due to block and site*family interaction term, e is the residue.

$$Y = \mu + \beta_0 \text{ Diameter} + \beta_1 \text{ site} + \beta_2 \text{ family} + \beta_3 \text{ block} + \beta_3 \text{ site*family} + e \quad 2$$

where Y is tree velocity (V_T) or tree dynamic modulus of elasticity (E_{tree} and E_{basic}), β_0 is the mean change in Y due to diameter. If the interaction term was significant at 0.05, then the slopes of the two sites were statistically different from zero. In such cases, least square means are generated for the fixed main parameter and the multiple comparisons performed using Tukey-Kramer adjustment at 0.05.

5.4 Results and Discussions

5.4.1 Relationships between anatomical, morphological, and mechanical properties

There was a significant positive linear relationship between tree diameter and the two quality parameters but tree diameter was negatively related to tree slenderness (Table 5.1). The negative significant linear relationship between diameter and slenderness was expected since slenderness was estimated as the ratio of the total tree height to diameter (Roth et al. 2007). This result confirmed some previous studies where the authors found a significant positive relation between standing tree stiffness and stem slenderness (Roth et al. 2007; Lasserre et al. 2007; Antony et al. 2012).

Wood is an anisotropic material with most of the properties varying with radial, tangential and longitudinal direction. Modulus of elasticity as one of the major mechanical properties of wood varied radially and axially as a result of the interactive effect of density and microfibril angle (MFA) (Megraw et al. 1999; Via et al. 2009). Megraw et al. (1999) and Via et al. (2009) stated that depending on the growth ring age, between 76 to 96% and 66 – 94% of the variation in MOE of loblolly and longleaf pines respectively were explained by density and MFA. Generally, increasing density significantly increased MOE while increasing MFA reduces MOE (Table 5.1). Via et al. (2009) explained that in the mature wood zone, density becomes a very important predictor of MOE since the magnitude of MFA becomes relatively small and stabilizes in this zone; while a high MFA with considerable variation assumes is more influential in the core wood zone. This iteration leads to the formation of stiffer wood material in the outer wood than in the core wood zones. However, this iteration is affected by the edaphic, environmental and silvicultural management practices of the stands.

Consequently, if the plantation is established at a higher planting density, taller and thinner trees are produced due to the high inter-tree competition for light at the juvenile stage. Therefore, the core wood attains stable and small MFA earlier as compared to those established at low planting density leading to increased MOE (stiffness) with slenderness as reported in this study.

The positive relationships between the dynamic MOEs (E_{tree} and E_{basic}) and slenderness confirm the theory that more slender tree requires a higher stiffness to support itself from buckling under its own weight. Fundamentally, a taller tree is subjects to a higher wind loading, and the longer distance to the bottom causes a higher moment. Therefore, the tree requires a stiffer material in order to withstand the wind loading.

The positive relationship between the dynamic MOEs and diameter has been reported by several authors (Wang et al. 2004; Briggs et al. 2007; Essien et al. 2016a). However, other studies such as Lasserre et al. (2005) and Carson et al. (2014) reported a negative relationship between stiffness and diameter when they studied 11 and 15-year-old *Pinus radiata* at different planting densities. Since MOE is moderately or highly heritable (Lenz et al. 2013) but diameter is not genetically correlated with MOE (Li et al. 2007), hence it is possible for a larger diameter tree to produce stiffer wood. An individual family by family analysis for the diameter (Figure 5.1) and MOE (Tables 5.4 and 5.5) show families, for example, T26 and T18 have both higher diameter and dynamic MOEs. Roth et al. (2007) made a similar observation when they studied 6-year-old elite loblolly pine.

Table 5.1 Pearson correlation coefficient among the tree morphological, anatomical and quality parameters

	V_T	E_{tree}	Diameter	Slenderness	E_{basic}	Fiber length	MFA
V_T	1.0	0.773***	0.324***	0.116*	0.869***	0.129*	-0.073ns
E_{tree}		1.00	0.241**	0.214***	0.905***	0.152**	0.072ns
Diameter			1.00	-0.129*	0.260***	0.0927ns	-0.007ns
Slenderness				1.00	0.217***	-0.023ns	0.061ns
E_{basic}					1.00	0.154**	-0.127*
Fiber length						1.00	-0.039ns
MFA							1.00

ns=not significant at 0.05, * = significant at 0.05, ** significant at 0.01, * significant at 0.001, MFA=microfibril angle, E_{basic} = dynamic MOE estimated with V_T^2 *basic density, E_{tree} = dynamic MOE estimated with V_T^2 *green density**

5.4.2 Effect of site and genetic families anatomical, morphological and mechanical properties

The descriptive statistics of the parameters studied are shown in Table 5.2. All the parameters studied with the exception E_{basic} and fiber double wall thickness; varied significantly with the site ($p < 0.05$). Though the mean velocity averaged across the family was significantly higher for site 1; E_{tree}, MFA, slenderness, and fiber diameter were better on site 2 than site 1 (Table 5.2). This is interesting because based on Equations 2 and 3, one would expect the site with higher velocity to exhibit a higher dynamic MOE since the higher order of velocity dominates the variation in the response variable for the equation. However, the density which is a function of fiber diameter and a wall thickness of trees on site 2 was higher than site 1 (Table 5.2). Consequently, both green and basic densities of trees on site 2 will be higher than site 1 due

to the larger fiber lumen (for storage of free water which inflates the weight of the wood) and the thicker wall thickness respectively hence causing the dynamic MOE to lean towards site 2.

Therefore using velocity^2 (Roth et al. 2007), dynamic MOE based on basic density (E_{basic}) and based on green density (E_{tree}) lead to different conclusions. While there is no significant difference in E_{basic} between sites; velocity^2 for site 1 is significantly higher than site 2 but E_{tree} is higher for site 2 than site 1. Therefore practitioners should take care when extrapolation velocity reading of trees from different locations. FPL (2010) reported a mean static MOE for loblolly pine at green and 12% moisture conditions to be 9.7 GPa and 12.7 GPa respectively.

This indicated that the mean E_{basic} and E_{tree} reported in the present study is very similar to static MOE for green and 12% moisture conditions respectively. Generally, the analysis of variance indicated a significant ($p < 0.05$) effect of site and families on the tree size and form, MFA, fiber length, velocity, and dynamic MOEs (E_{tree} and E_{basic}) (Table 5.3). The site x family interaction was significant for the tree size and form; and dynamic MOEs (Table 5.3). This was mainly due to the swapping in ranks of some families between sites. For example, about half the families studied swapped ranks in dynamic MOEs (Tables 5.4 and 5.5) and fiber diameter (Table 5.6).

On the other hand, families 34 and 3 were the main cause of the significant interaction term observed in this study for diameter (Figure 5.1), MFA (Table 5.7) and fiber length (Table 5.8). After adjusting for the slenderness (ratio of height to diameter), neither the main effects nor the interaction significantly ($p>0.05$) affects velocity (Table 5.9). However, when similar adjustments performed on the dynamic MOEs, both the main and the interaction between site x families were significant (Table 5.9).

The stiffness of juvenile pines is significantly influenced by the genetics (Dungey et al. 2006) and edaphic conditions (Lasserre et al. 2007). In this study, the significant main and interactive effect of site and families of dynamic MOEs persist even after adjusting for slenderness. This indicates a strong effect of site and families on MOEs. Site selection is one of the important management decisions in plantation establishment because, besides its effect on the growth, form, and yield of the trees, the site also influences the pest and disease management systems to use. For instance, for a given family planted on different sites, the fertile, well aerated and drained site will produce larger, longer and healthy trees whereas those planted on old cotton, less fertile and compact field will be smaller, thinned crown and eventually dieback.

Generally, most of the families shared similar morphological and internal quality values indicating the stability of the planting stock across sites. Therefore there is a greater potential for farmers to select families with superior wood quality and fast growing performance for plantation establishment. However, for the site sensitive families, resource managers and farmers should allocate appreciate family to the require site if wood quality and growth performance are desired.

Table 5.2 Descriptive statistics of the morphological, anatomical, and quality properties for the 184 and 204 trees for sites 1 and 2 respectively studied.

	Site 1			Site 2		
Parameters	Mean± SD	Min	Max	Mean± SD	Min	Max
V_T(km/s)	4.20±0.46[a]	3.00	5.30	4.07±0.44[b]	2.77	5.17
E_{tree} (GPa)	13.38±3.83[b]	6.64	25.02	14.51±3.70[a]	7.91	24.73
E_{basic} (GPa)	8.93±2.5[a]	3.48	16.18	8.90±2.39[a]	3.70	15.67
MFA (^{o})	26.54±6.26[a]	11.30	43.89	25.45±6.37[b]	5.77	44.73
Height (m)	12.93±1.21[a]	9.86	15.79	12.15±0.85[b]	10.31	14.49
Diameter (cm)	16.73±3.94[a]	6.50	26.10	14.08±2.80[b]	8.00	21.80
Slenderness	72.13±10.75[b]	59.43	101.60	73.79±5.74[a]	53.88	82.06
Fiber length (µm)	3128±904[a]	1409.0	5753.6	2873±667[b]	2873.	5003.4
Fiber diameter (µm)	29.27±3.59[b]	11.05	61.11	31.55±8.8[a]	10.99	56.74
FDWT (µm)	12.30±3.59[a]	2.57	20.27	12.53±5.17[a]	1.65	35.19

***Parameters with the same letters are not statistically significant between sites at 0.05*. SD = standard deviation, FDWT=fiber double wall thickness. MFA= microfibril angle, E_{basic} = dynamic MOE estimated with V_T^2 *basic density, E_{tree} = dynamic MOE estimated with V_T^2 *green density**

Table 5.3 Analysis of variance of the main effect of site, genetic sources and block on anatomical, morphological, and quality properties of 388 trees from both sites studied

		Df	Mean square	F - valve	P - value
Diameter	Site	1	542.79	55.22	**<0.0001**
	Family	14	30.36	3.09	**0.0002**
	Block	14	23.58	2.40	**0.0033**
	Site*family	14	30.56	2.69	**0.0009**
Slenderness	Site	1	345.74	343.65	**<0.0001**
	Family	14	962.85	957.03	**<0.0001**
	Block	14	1.06	1.03	0.4037
	Site*family	14	925.45	919.84	**<0.0001**
MFA	Site	1	300.40	7.78	**0.0057**
	Family	7	83.22	2.15	**0.0098**
	Block	14	23.31	0.60	0.8616
	Site*family	7	38.98	1.01	0.4252
Fiber length	Site	1	4171959	6.86	**0.0093**
	Family	7	2581841	4.24	**<0.0001**
	Block	14	1027576	1.69	0.0578
	Site*family	7	742582	1.22	0.2915
Velocity	Site	1	1.41	6.63	**0.0105**
	Family	14	0.33	1.55	0.0909
	Block	14	0.27	1.27	0.2206
	Site*family	14	0.31	1.48	0.1179
E_{tree}	Site	1	128.39	14.26	**0.0002**
	Family	14	74.89	8.32	**<0.0001**
	Block	14	11.02	1.22	0.2554
	Site*family	14	79.38	8.82	**<0.0001**
E_{basic}	Site	1	0.034	0.01	0.9281
	Family	14	19.38	4.72	**<0.0001**
	Block	14	4.57	1.11	0.3453
	Site*family	14	37.53	9.14	**<0.0001**

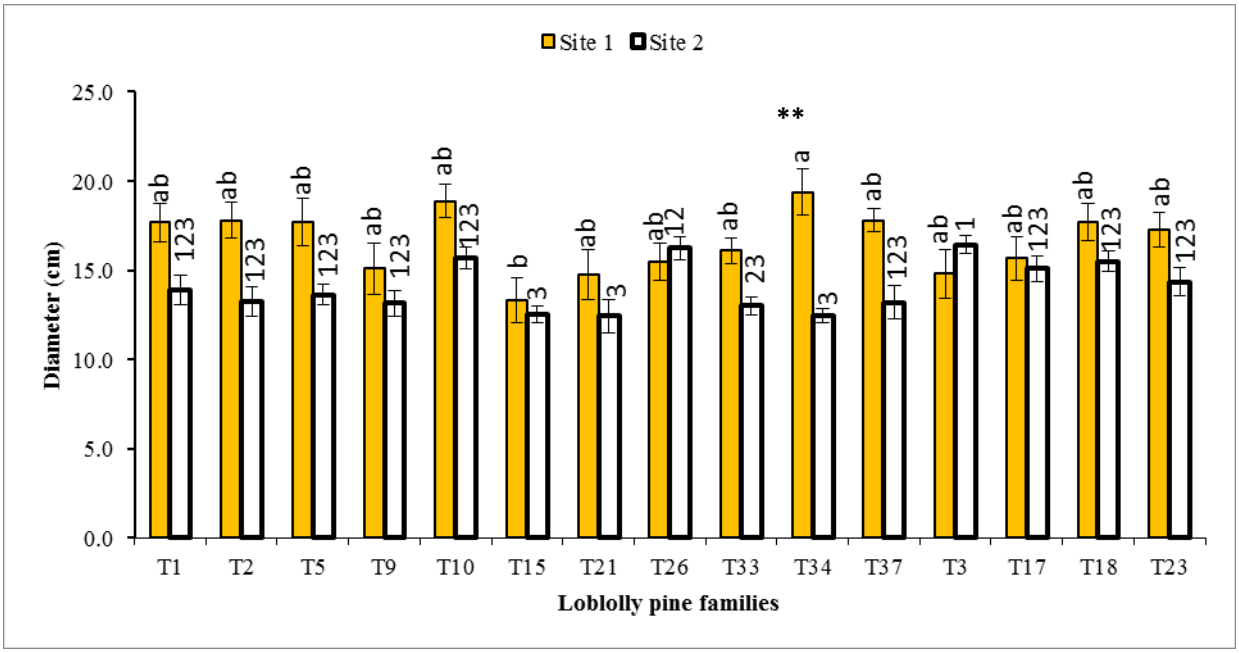

Figure 5.1 Comparison of mean diameter growth of families for each site. ***The error bars are standard deviations of an individual family. Families with the same letter or number are not significantly different at 0.05.** indicates a significant difference between sites.***

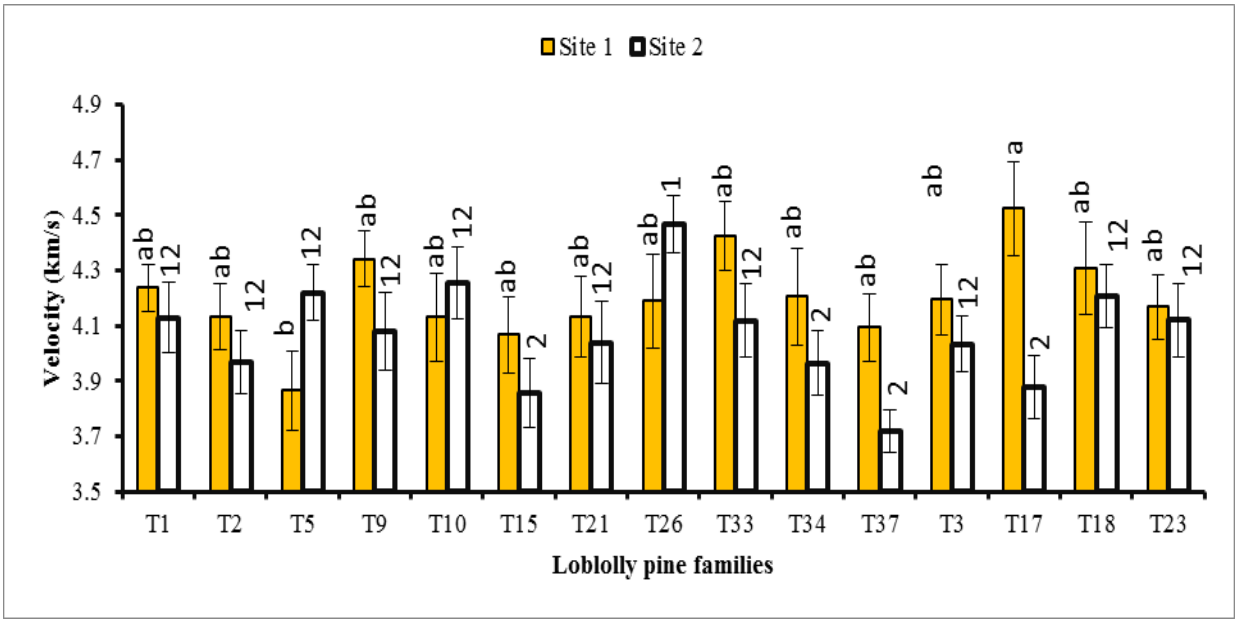

Figure 5.2 Comparison of mean velocity of families for each site. ***The error bars are standard errors of an individual family. Families with the same letter or number are not significantly different at 0.05.***

Table 5.4 Mean (GPa), and standard error (GPa) of dynamic MOE (E_{tree}) for each of the 15 genetic families per site for the whole 400 trees

	Site 1		Site 2			Combined
Families	Mean ± SE	Rank	Mean ± SE	Rank	Between sites	Rank
T1	9.90 ± 0.83^{e}	14	17.68 ± 0.79^{ab}	2	**	6
T2	10.07 ± 0.77^{e}	12	11.25 ± 0.74^{g}	15	ns	15
T5	9.89 ± 0.83^{e}	15	15.81 ± 0.79^{abcdef}	7	**	11
T9	11.97 ± 0.90^{cde}	9	16.17 ± 0.76^{abcdef}	6	ns	7
T10	9.96 ± 0.84^{e}	13	16.82 ± 0.73^{abc}	3	**	5
T15	12.92 ± 0.96^{cde}	8	12.97 ± 0.80^{efg}	11	ns	14
T21	14.58 ± 0.86^{abcde}	5	11.83 ± 0.87^{g}	14	**	13
T26	15.41 ± 0.86^{abcd}	3	18.05 ± 0.79^{a}	1	ns	1
T33	17.59 ± 0.76^{a}	1	15.69 ± 0.77^{adcdef}	8	ns	3
T34	15.12 ± 0.88^{abc}	4	13.53 ± 0.80^{defg}	10	**	4
T37	14.07 ± 0.80^{abcd}	6	12.45 ± 0.76^{fg}	13	**	8
T3	13.21 ± 0.82^{bcde}	7	12.86 ± 0.79^{cdefg}	12	ns	10
T17	11.53 ± 0.86^{de}	10	14.14 ± 0.73^{bcdefg}	9	**	12
T18	16.61 ± 0.80^{ab}	2	16.42 ± 0.76^{abcd}	4	ns	2
T23	10.71 ± 0.79^{e}	11	16.18 ± 0.76^{abcde}	5	**	9

Families within the same site with different letter are significantly different at 0.05 ** indicate means of the families are significantly different between sites at 0.05 while "ns" indicate not significantly different at 0.05

Table 5.5 Mean (GPa), standard error (SE) (GPa), and rank of dynamic MOE (E_{basic}) for each of the 15 genetic families per site

	Site 1		Site 2			Combined
Families	Mean ± SE	Rank	Mean ± SE	Rank	Between sites	Rank
T1	8.13±0.62^{bcd}	10	9.61±0.52^{abcd}	7	ns	7
T2	7.10±0.57^{d}	15	9.20±0.48^{bcde}	9	**	12
T5	7.20±0.62^{d}	14	9.81±0.52^{abcd}	5	**	10
T9	8.72±0.65^{abcd}	7	10.11±0.50^{abc}	3	ns	4
T10	7.84±0.62^{ed}	11	10.62±0.49^{ab}	2	**	5
T15	8.32±0.65^{abcd}	9	6.95±0.53^{ef}	14	ns	15
T21	9.99±0.65^{abcd}	6	7.42±0.57^{def}	13	**	8
T26	10.08±0.65^{abcd}	4	11.13±0.52^{a}	1	ns	1
T33	11.21±0.55^{a}	1	8.32±0.50^{bcde}	10	**	3
T34	10.52±0.66^{abc}	3	7.45±0.52^{def}	12	**	6
T37	10.02±0.57^{abcd}	5	5.65±0.50^{f}	15	**	14
T3	8.38±0.63^{abcd}	8	7.81±0.52^{cdef}	11	ns	13
T17	7.29±0.62^{d}	13	9.42±0.48^{abcd}	8	**	11
T18	11.03±0.60^{ab}	2	9.66±0.50^{abcd}	6	ns	2
T23	7.38±0.60^{d}	12	9.90±0. 50^{abcd}	4	**	9

Families within the same site with different letter are significantly different at 0.05 ** indicate means of the families are significantly different between sites at 0.05 while "ns" indicate not significantly different at 0.05

Table 5.6 Mean (µm), standard error (µm), and rank of fiber diameter for each of the 15 genetic families per site

	Site 1		Site 2			Combine
Families	Mean ± SE	Rank	Mean ± SE	Rank	Between sites	Rank
T15	34.31±2.40[a]	2	36.60±2.17[ab]	3	ns	1
T21	27.24±2.40[a]	7	34.73±2.35[abc]	5	**	7
T26	30.39±2.40[a]	4	39.61±2.15[a]	1	**	2
T33	32.80±2.11[a]	1	33.60±2.07[abc]	6	ns	5
T34	29.02±2.40[a]	6	33.57±2.16[abc]	7	**	6
T37	30.81±2.09[a]	3	33.27±2.07[abc]	8	ns	4
T3	25.04±2.28[a]	8	36.05±2.15[ab]	4	**	8
T18	29.24±2.19[a]	5	38.17±2.07[a]	2	**	3

Families within the same site with different letter are significantly different at 0.05
***** indicate means of the families are significantly different between sites at 0.05 while "ns" indicate not significantly different at 0.05***

Table 5.7 Mean (^{o}), standard error (SE) (^{o}), and rank of microfibril angle (MFA) for each of the 15 genetic families per site

	Site 1		Site 2			Combine
Families	Mean ± SE	Rank	Mean ± SE	Rank	Between sites	Rank
T15	26.92±1.75[ab]	4	22.46±1.75[a]	7	ns	6
T21	28.81±1.76[ab]	3	26.90±1.91[a]	1	ns	2
T26	24.34±1.76[ab]	5	26.38±1.74[a]	2	ns	4
T33	28.85±1.54[ab]	2	24.53±1.67[a]	4	ns	3
T34	27.57±1.76[ab]	6	22.34±1.74[a]	8	**	5
T37	30.50±1.53[a]	1	25.92±1.68[a]	3	ns	1
T3	23.11±1.67[b]	8	22.83±1.74[a]	5	ns	8
T18	23.47±1.60[b]	7	22.60±1.68[a]	6	ns	7

Families within the same site with different letter are significantly different at 0.05 ** indicate means of the families are significantly different between sites at 0.05 while "ns" indicate not significantly different at 0.05

Table 5.8 Mean (µm), standard error (SE) (µm), and rank of fiber length for each of the 15 genetic families per site

	Site 1		Site 2			
Families	Mean ± SE	Rank	Mean ± SE	Rank	Between sites	Rank
T15	2652±247.18[b]	8	2553±213.56[b]	7	ns	8
T21	3061±247.83[ab]	4	2878±232.08[ab]	3	ns	4
T26	3127±247.57[ab]	3	2976±212.4[ab]	2	ns	3
T33	2713±217.67[b]	7	2694±204.08[b]	5	ns	5
T34	2893±247.82[ab]	5	2467±212.46[b]	8	ns	6
T37	2779±215.55[b]	6	2554±204.11[b]	6	ns	7
T3	3865±235.56[a]	2	2743±212.37[ab]	4	**	2
T18	3879±224.57[a]	1	3712±204.12[a]	1	ns	1

Families within the same site with different letter are significantly different at 0.05 ** indicate means of the families are significantly different between sites at 0.05 while "ns" indicate not significantly different at 0.05

Table 5.9 Analysis of variance of the main effect of site, genetic sources and block on anatomical, morphological and quality properties of 388 trees after adjusting for diameter and slenderness

		Df	Ms	F -value	P -value
V_T	Diameter	1	5.96	31.46	**<0.0001**
	Site	1	0.008	0.04	0.837
	Family	14	0.349	1.84	**0.0315**
	Block	14	0.236	1.24	0.241
	Site*family	14	0.313	1.65	0.0641
E_{tree}	Diameter	1	215.01	23.47	**<0.0001**
	Site	1	270.00	38.71	**<0.0001**
	Family	14	73.12	9.22	**<0.0001**
	Block	14	9.090	1.13	0.328
	Family * Site	14	76.35	9.63	**<0.0001**
E_{basic}	Diameter	1	215.01	23.47	**<0.0001**
	Site	1	270.00	38.71	**<0.0001**
	Family	14	73.12	9.22	**<0.0001**
	Block	14	9.090	1.13	0.328
	Site*family	14	76.35	9.63	**<0.0001**
V_T	Slenderness	1	5.69	29.93	**<.0001**
	Site	1	0.15	0.80	0.3718
	Family	14	0.327	1.72	0.0505
	Block	14	0.231	1.22	0.2605
	Site*family	14	0.300	1.58	0.0826
E_{tree}	Slenderness	1	206.17	25.59	**<0.0001**
	Site	1	233.21	28.95	**<0.0001**
	Family	14	70.25	8.72	**<0.0001**
	Block	14	8.89	1.10	0.3524
	Site*family	14	75.27	9.34	**<0.0001**
E_{basic}	Slenderness	1	100.47	27.35	**<0.0001**
	Site	1	8.76	2.39	0.123
	Family	14	18.45	5.02	**<0.0001**
	Block	14	3.69	1.01	0.4468
	Site*family	14	34.63	9.43	**<0.0001**

5.5 Conclusions

The effect of site and genetic families on morphological, anatomical and wood quality properties of fifteen 14-year-old loblolly pines stock was studied. The results indicated significant positive linear relations between dynamic MOEs (E_{tree} and E_{basic}) versus tree diameter, slenderness, and fiber length whiles negatively correlated with MFA.

Furthermore, while there was no significant difference in E_{basic} between sites; velocity^2 for site 1 is significantly higher than site 2 but E_{tree} is higher for site 2 than site 1. Therefore practitioners should take care when extrapolation velocity reading of trees from different locations. Again, the mean E_{basic} and E_{tree} reported in the present study presents a snapshot of the expected static MOE for green and 12% moisture conditions respectively.

Additionally, about half of the selected families had statistically similar morphological and quality properties between sites suggesting the half of the planting stock exhibit stability and homogeneity in the southeastern United States. Therefore, farmers have the opportunity to select some families which are superior in both the morphological and quality traits for plantation development across sites with varying edaphic and environment. Furthermore, farmers have the opportunity to march some elite planting stocks to specific site for greater productivity and quality outturn due to the significant effect of site or family or site by family interaction.

5.6 References

ALSC (2013) American Lumber Standard Committee: Board of Review Board of Review Minutes. American Lumber Standards Committee, Germantown

Antony F, Schimleck LR, Jordan L, Daniels RF, Clark A. (2012) Modeling the effect of initial planting density on within tree variation of stiffness in loblolly pine. Annuals of Forest Science 69:614 – 650 DOI 10.1007/s13595-011-0180-1

Bertoldo C and Gonçalves R. (2015) Influence of measurement position, tree diameter, and bulk wood density on models that predict wave propagation velocity in logs according to the velocity in trees. Forest Products Journal, **65**(3/4):166-172.

Briggs DG, Thienel G, Turnblom EC, Lowell E, Dykstra D, Ross RJ, Wang X, and Carter P. (2007) Influence of thinning on the acoustic velocity of Douglas fir trees in western Washington and Western Oregon. In: Proceedings of the 15th International Symposium on Nondestructive Testing of Wood, September 10-12, 2007, Duluth, Minnesota-USA. Pp113-123

Carson SD, Dave J, Cown D J, Russell B, McKinley RB, and Moore JR (2014) Effects of site, silviculture and seed lot on wood density and estimated wood stiffness in radiate pine at mid-rotation, *New Zealand J. For. Sci.* 44(1), 26-37. **DOI:** 10.1186/s40490-014-0026-3

Clark A, Jordan L, Schimeleck L, Daniels RF (2008) Effect of initial planting spacing on wood properties of unthinned loblolly pine at age 21. Forest Prod J 58(10): 78 – 83

Dickson RL, Joe B, Harris P, Holtorf S, and Wilkinson C (2004) Acoustic segregation of Australian grown *Pinus radiata* logs for structural board production. Aust. For. **67**: 261–266.

Dungey HS, Matheson AC, Kain D, Evans R. (2007) Genetics of wood stiffness and its component traits in Pinus radiate. Can J. For. Res. 36: 1165 – 1178.

Essien C, Cheng Q, Via BK, Loewenstein EF, Wang X (2016a) An Acoustic operations study for loblolly pine standing saw timber with different thinning history BioResources 11(3): 7512 – 7521 DOI: 1 0.15376/biores.11.3.7512-7521

Essien C. (2012) Physical, Anatomical and Treatment characteristics of the wood of *Cola gigantea* and *Ficus sur.* **Master of Philosophy Thesis**, Submitted to Faculty of Renewable Natural Resource - Kwame Nkrumah University of Science and Technology, Kumasi, Ghana. Pp 196

Essien C, Via BK, Cheng Q, Gallagher T, McDonald T, Wang X, Eckhardt LG (2017) Multivariate Modeling of Acousto-mechanical Response of Fourteen Year Old Suppressed Loblolly Pine (*Pinus taeda*) to Variation in Wood Chemistry, Microfibril Angle, and Density. Wood Sci Technol 51: 475 – 492. doi 10.1007/s00226-017-0894-9

FPL (Forest Products Laboratory) (2010) Wood handbook—Wood as an engineering material. General Technical Report FPL-GTR-190. Madison, WI: U.S. Department of Agriculture, Forest Service, Forest Products Laboratory.

Isik F, Mora C R, and Schimleck L R (2011) "Genetic variation in *Pinus taeda* wood properties predicted using non-destructive techniques," Ann. Forest Sci. 68, 283-293. DOI: 10.1007/s13595-011-0035-9

Johnson GR, and Gartner BL (2006) Genetic variation in basic density and modulus of elasticity of coastal Douglas fir. Tree Genetics and Genomes, *3*, 25–33

Raymond CA, Joe B, Anderson DW, and Watt DJ (2008) Effect of thinning on relationships between three measures of wood stiffness in *Pinus radiata*: Standing trees *vs*. short clear specimens, Can. J. For. Res. 38(11), 2870-2879. DOI:10.1139/X08-124

Lachenbruch B, Johnson GR, Downes GM, Evans R (2010) Relationship of density, microfibril angle and sound velocity with stiffness and strength in matured of Douglas fir. Canadian Journal of Forest Research 40:55-65

Lasserre JP, Mason EG, and Watt MS (2007) Assessing corewood acoustic velocity and modulus of elasticity with two impact based instruments in 11-year-old trees from a clonal-spacing experiment of *Pinus radiata* D. Don. For. Ecol. Manage. 239:217–221.

Lasserre JP, Mason EG, and Watt, MS (2005) The effect of genotype and spacing on *Pinus radiata* [D. Don] corewood stiffness in an 11-year-old experiment. For. Ecol. Manage. 205:375–383. doi:10.1016/j.foreco.2004.10.037.

Lenz P, Anty D, Achim A, Beaulieu J, Mackay J (2013) Genetic improvement of White Spruce mechanical wood traits – Early screening by means of acoustic velocity. Forest 4 (3): 575-594. Doi10.3390/f4030575

Li X, Huber DA, Powell GL, White TL, Perter GF (2007) Breeding for improved growth and juvenile corewood stiffness in slash pine. Can. J. For. Res. 37(10): 1886-1893. doi.org/10.1139/X07-043

McKeand S, Mullin T, Byram T and White T (2003) Deployment of genetically improved loblolly and slash pine in the South. J. For. **101**: 32-37.

Mora CR, Schimleck LR, Isik F, Mahon JM, Clark A, and Daniels RF (2009) Relationship between acoustic variable and different measures of stiffness in standing *Pinus taeda* trees," Can. J. For. Res. 39(8), 1421-1429. doi:10.1139/X09-062

National Oceanic and Atmospheric Administration (NOAA 2016) State, regional and national monthly precipitation: area weighted monthly normal, 1981 – 2015. Historical Climatography

Peter GF, Benton DM, Bennett K (2003) A simple direct method for measurement of microfibril angle in single fibers using differential interference contrast microscopy. J. Pulp and Paper Sci. 29: 274 - 280

Statistical Analysis Software (SAS) version 9.4 (2014) Cary, NC, USA

Roth BE, Li X, Huber DA and Peter GF (2007) Effects of management intensity, genetics and planting density on wood stiffness in a plantation of juvenile loblolly pine in the southeastern USA. For. Ecol. Manage 246: 155 – 162 doi 10.1016/j.foreco.2007.03.028

Vikram V, Cherry ML, Briggs D, Cress DW, Evans R, Howe GT (2011) Stiffness of Douglas-fir lumber: effect of wood properties and genetics. Canadian Journal of Forest Research 41(6):1160-1173

Via BK, So CL, Shupe TF, Groom LH, Wikaira J (2009) Mechanical response of longleaf pine to variation in microfibril angle, chemistry associated wavelengths, density and radial position. Composites: Part A 40 (1):60-66

Wang X, Ross R J, McClellan M, Barbour RJ, Erickson JR, Forsman JW, and McGinnis GD (2001) Nondestructive evaluation of standing tree with a stress wave method, Wood Fiber Sci. 33(4), 522-533

Wang X (2013) Acoustic measurement on trees and logs: a review and analysis. Wood Sci and Technol 47:965-975

Wang X, Ross RJ, Brashaw BK, Punches J, Erickson JR, Forsman JW, Pellerin RE (2004) Diameter effect on the stress-wave evaluation of modulus of elasticity of logs. Wood and Fiber Sci. 36(3):368 – 377

Wang X. Ross RJ and Carter P. (2007) Acoustic evaluation of wood quality I standing tree. Part 1: acoustic behavior in standing tree. Wood Fiber Sci. 39(1): 28-38

Chapter 6: Determining the predictive accuracies of whole tree modulus of elasticity (MOE) of 14 – year old loblolly pine using density and dynamic MOEs estimated by three different acoustic tools

6.1 Abstract

Resonance based acoustic tools for evaluating wood properties have been reported to be more accurate in estimating the expected log MOE than time – of – flight (TOF) ones. However, there is no published study on the variations within different brands on these two major classes of acoustic tools. In this study, we developed models to predict the whole tree static MOE ($WMoE_T$) and rupture ($WMoR_T$) using log dynamic MOEs as estimated by two resonance tools (Director HM200 (E_{HM200}) and FAKOPP resonance log grader (E_{RLG})), and a TOF (FAKOPP Microsecond Timer (E_{FMT})) for a 14- year-old loblolly pine stand from two sites.

The TOF overestimated the log velocity by 33% and 30% as compared to the resonance-based tools (Director HM200 and FAKOPP RLG respectively); resulting in the whole log static MOE ($WMOE_L$) been overestimated by 11% and 20% for the resonance (HM200 and RLG respectively), and 90% by the TOF tools. However, the TOF overestimation was reduced to 29% when the air-dry density was used instead of green density. Although the TOF tool overestimated the $WMOE_L$, its $WMoE_T$ predictive performance (R^2=50.68%) lies between the 38.78% and 73.83% for the resonance based tools (HM200 and RGL respectively).

This result supports the theory that TOF tools generate dilatational wave, and hence their velocity will be generally higher than resonance tools. The presence of predictive variation within the resonance suggests the need for within tools calibration.

The linear relationship between the $WMOE_T$ vs E_{tree} was stronger than that of $WMOE_T$ vs E_{HM200} suggest that the TOF acoustic tool measurements are not restricted to the outer wood zone for small diameter logs.

6.2 Introduction

In the southeastern United States, southern yellow pines (SYP) are the most important group of timber species driving the wood industry. However, loblolly pine (*Pinus taeda* L) is the single most dominant tree species in the landscape due to its excellent adaptation and productivity on varying soil types, utilization and genetic improvement (McKeand et al. 2003). The dimension lumber, mainly for structural applications continues to be one of the dominant valuable commodities derived from loblolly pine. For structural applications, SYP is classified based on the MOE either through the visual or the machine stressed grading platform. However, due to the inherent inaccuracies and subjective nature of the visual grading method, and the initial capital intensity associated with the machinery for the machine stress rating method, researcher sort for a cheaper of grading lumber.

For this purpose, several nondestructive instruments have been developed that can directly and/or indirectly measure the intrinsic wood quality of small wood samples, logs or trees (Wang et al. 2001and 2004; Mora et al. 2009). Among these instruments are acoustic – based nondestructive tools which are simple, compact, and easy to operate on small wood samples, logs and standing trees (Dickson et al. 2004). Several researchers have found a strong linear relationship between the estimated MOE of logs and trees against small clear samples derived from same trees or logs for different species (Wang et al. 2001 and 2004; Vikram et al. 2008; Raymond et al. 2008; Lachenbruch et al. 2010; Essien at al. 2016a) although the tree velocity is

usually slightly higher (Bertoldo and Gonçalves 2015). Currently, the most popular acoustic techniques used are ‘‘time - of - flight’’ and ‘‘resonance’’ for standing tree and logs respectively (Wang et al. 2002; Raymond et al. 2008).

The time – of – flight (TOF) method measures the time it takes for an introduced stress wave to travel from point to point and currently is the only practical acoustic method for measuring MOE in standing trees (Lasserre et al. 2007; Wang 2013; Essien et al. 2016a). However, since the standing tree is a continuous system, the signals are introduced to it from sides leading to a formation of dilatational waves (Wang et al. 2007). They explained further that, Poisson’s ratio, MOE and bulk density of the wood materials are required to accurately estimate the velocity of the TOF acoustic tools designed purposely for the standing trees (Equation 1). Poisson’s ratio is the ratio of transverse deformation to axial deformation.

Wood is characterized by six different Poisson’s ratios due to its orthotropic nature. Poisson’s ratio varies within and between species, and also with specific gravity, moisture content, and sources of the material (Bodig and Jayne 1982; FPL 2010). Though Poisson’s ratio varies with moisture content, the variation is not statistically significant hence one value can be used for both green and dry wood materials (Bodig and Jayne 1982) and they went further to propose 0.37 for both hardwood and softwood. Therefore, given the Poisson’s ratio of dried wood is 0.37 (Bodig and Jayne 1982), the TOF velocity will be theoretical 33% higher than that determined using the one-dimensional wave equation used by the resonance based tools (Equation 1).

On the other hand, the resonance – based tool is considered to be a destructive method to the Forester because it requires the transverse section of the log to append the tool and generate the waves. Since the logs have two cut ends, they resemble the long slender material upon which

the one – dimensional wave equation was developed (Mayer 1994), even though, wood is neither isotropic nor homogeneous (Equation 2). However, beside this fundamental difference, the one-dimensional wave equation is still adequate to estimate the velocity of the resonance based acoustic tools (Wang 2001). The resonance – based tools tend to produce repeatable and reliable results of the whole log. This method has been shown to be superior to the TOF method (Wang et al. 2001and 2004; Raymond et al. 2008). However, the TOF tools can be used for pre – harvest, and progeny screening programs where large numbers of trees are involved.

$$V_d = \sqrt{\frac{(1-\emptyset)}{(1+\emptyset)(1-2\emptyset)}\frac{MOE}{\rho}} \qquad \text{Equation 1}$$

where V_d is the dilatational wave velocity, $\emptyset$ is the Poisson's ratio, MOE is the modulus of elasticity of the material, and ρ is the bulk density of the material.

$$V_o = \sqrt{\frac{MOE}{\rho}} \qquad \text{Equation 2}$$

where V_o is the one-dimensional wave velocity, MOE is the modulus of elasticity of the material, and ρ is the bulk density of the material.

Raymond et al. (2008) studied the effect of thinning operations on predicting the whole log stiffness using outer wood density, dynamic MOE estimated by the time – of – flight and resonance tools for 28 to 43-year-old radiata pine. They reported that tree MOE explained 62% of the variation on the static MOE of the small clear samples compared to the 30% by the log MOE and 56% for outer wood density. They concluded that the tree dynamic MOE estimated by the time – of – flight tool was a good predictor of whole log static MOE than outer wood density and log dynamic MOE estimated by resonance tool. This suggests that, though the resonance tools may be accurate in determining the whole log static MOE, their predictive performance in modeling the whole log static MOE is poor compared to that of TOF model performance.

Since loblolly pine constitutes a major part of SYP, understanding the effect of site on MOE is of utmost importance for the growth and sustainability of the forest industry. Furthermore, determining the effect of site on the predictability of whole tree static MOE ($WMOE_T$) using density and/or dynamic MOE (estimated by the two main classes of acoustic tools) will sawmill manager and procurement Forester sort logs and harvest stands to meet expected finished products stiffness respectively. If a strong relationship exists between the whole tree static MOE ($WMOE_T$) and tree dynamic MOE (E_{tree}), it is an indication that the tool can be used to provide information on the expected MOE of the lumber products. Additionally, this study will help validate the theoretical reasoning behind the velocity computation utilize by the TOF based acoustic tools. Finally using two brands of resonance acoustic tools will help us understand the variability within resonance class of acoustic tools for possible calibration if variation exits.

We hypothesize that the tree dynamic MOE will be a better predictor of the expected whole outer wood static MOE ($OMOE_T$) than the whole tree static MOE ($WMOE_T$) and also, the resonance based tools will provide a better whole log static MOE than the TOF ones. This information will help test the reliability of the TOF acoustic tools in predicting the expected MOE of small diameter trees. The available studies compare tools between the TOF and the resonance classes of tools hence generalization of the results becomes problematic. Comparing tools between and within acoustic tools classes will provide deeper insight into the operations of this technology. Therefore, this study has three main objectives:

1. To determine variation of anatomical properties with site

2. To determine the pattern of axial variations in the MOE of tree as determined by four different estimation methods – namely static bending test, two resonance and a time – of – flight (TOF) acoustic tools
3. To predict whole tree MOE ($WMOE_T$), whole tree outer wood MOE ($OMOE_T$), and MOR ($WMOR_T$) using air-dry density (AD), green density (GD), tree dynamic MOE (E_{tree}) estimated TOF (FAKOPP Microsecond Timer), two log dynamic MOEs (Director HM200 (E_{HM200}) and FAKOPP Resonance Log Grader (E_{RLG})).

6.3 Materials and Methods

6.3.1 Materials

The materials for this study were selected from a plantation of elite families of loblolly pine (*P. taeda*) established at two sites in the southeastern United States in the year 2000. The study Site 1 was located in Nassau County Florida near Yulee (latitude $30^o63´$N and longitude $81^o57´$W) and Site 2 at Brantley County Georgia near Nahunta (latitude $31^o12´16´´$N and longitude $81^o58´56´´$W). The soil of Site 1 was poorly drained and formed from a thick bed of alkaline loamy and clayey marine sediments terraces with a slope less than 1% and nearly level. The mean long-term temperature and precipitation from 1981 to 2010 are 21^oC and 1350mm respectively. The topography of Site 2 was relatively flat with a slope less than 2% and 20m altitude above sea level. The soil was very fine sandy loam, poorly drained and generally poor in nutrients which formed from loamy and silty Coastal Plain sediments. The mean annual temperature ranged from 17 to 19^oC and the annual precipitation from 1981 to 2010 averaged 1315mm (NOAA 2016).

Fifteen elite loblolly pine families and one (1) tree per family were randomly selected from each site for this study in spring of 2014 when the trees were 14 years old. Although the trees were selected at random, care was taken to avoid trees with visible defects such as leaning trees, forked stems, chlorotic needles and/or other growth defects. The same set of families was selected for both sites. All the measurements for this study were confined to the 15 trees from the selected family for each site. It should be noted that this was not meant for genetics analysis study as we could only harvest one tree per family per site; however, the purpose of selecting one tree per family was to demonstrate as much variation in the sample logs as possible.

6.3.2 Acoustic measurements of standing trees

Before harvesting the tree, diameter at breast height and a total height of the selected trees were measured. They were acoustically tested using FAKOPP Microsecond Timer (FMT) acoustic tool (FAKOP Enterprise, Agfalva, Hungary) which relied on the TOF principle (Wang et al. 2007; Mora et al. 2009; Essien et al. 2016a). Basically, the accelerometers (the transmitter and the receiver probes) were positioned on the same side of the tree 120 cm apart with the center of the path occurring at breast height. Both probes were positioned 45^{o} to the tree axis and the stress wave was generated by striking the transmitter probe with a steel hammer at a steady force (Mora et al. 2009). The generated wave was detected by the receiver and the time lapse for the wave to travel the distance between the probes was recorded. Seven readings were taken on each tree and tree velocity was estimated as the ratio of the distance to the time (Equation 3). The dynamic modulus of elasticity of the trees (E_{tree}) was estimated using Equation 4 (Wang et al. 2007; Essien et al. 2016a).

6.3.3 Acoustic measurements of logs

The harvested trees were bucked into 200 cm logs and 50 cm long bolts alternately along the entire length, yielding 3 – 5 logs depending on the length of the tree. All the 105 logs obtained from the thirty trees from both sites were used for log acoustic determination using three different acoustic tools - Director HM200 (Fiber-gen, Christchurch, New Zealand), FAKOPP Resonance Log Grader (RLG), and FAKOPP Microsecond Timer (FMT) (FAKOP Enterprise, Agfalva Hungary). The HM200 and the resonance log grader tools are operated based upon the resonance principle. The actual length of the log measured prior to the acoustic testing. For the FAKOPP resonance log grader, a steel hammer is used to generate the stress wave at one end of the log while a microphone placed at the other end of the log to pick up the wave and displayed the velocity in m/s. Seven readings per log were recorded.

For the Director HM200, the log length was entered into the tool after which the tool was held firmly against one end of the log and the steel hammer was used to generate a stress wave. The induced stress waves travel the entire log length and back and forth at a rapid rate of hundreds of passes per second (Wang et al. 2004). The tool collected and processed the wave signal using a Fast Fourier Transformation to display velocity (Wang et al. 2004; Zhou et al. 2013). The resonance based acoustic velocity was determined using the harmonic frequencies according to Equation 5 (Ilic 2001, Auty and Achim 2008). The FAKOPP Microsecond Timer acoustic tool's operation on logs was similar to that described above for the tree. The dynamic MOE of the log was estimated using Eqns. 6, 7, and 8 for Director HM200 (E_{HM200}), FAKOPP resonance log grader (E_{RLG}), and FAKOPP Microsecond Timer (E_{FMT}) respectively.

The ends of the logs and the associated bolts were sealed with wax (Anchorseal Green Wood Sealer, U. C. Coatings Corp. Buffalo, NY, USA) and transported to the Forest Products

Development Center, Auburn University for further processing. At the laboratory, three 2cm thick disks each were obtained from each of the logs to be used to determine the green density and moisture content. The dimensions of the disks were measured using a digital caliper to the nearest 0.025 mm and the weight to the nearest 0.001 g. Weight (M_i) and dimensions of the disks were measured while green and were subsequently dried to constant weight (M_o) in an electronic oven set at 103^{o}C. The moisture content (MC) and green density (ρ_{green}) of the disks were determined according to eqns. 9 and 10 respectively.

$$V_T = D / s \quad \text{Equation 3}$$

$$E_{tree} = V_T^2 * \rho_{green} \quad \text{Equation 4}$$

$$V_L = 2f_nL / n \quad \text{Equation 5}$$

$$E_{HM200} = V_{HM200}^2 * \rho_{green} \quad \text{Equation 6}$$

$$E_{RLG} = V_{RLG}^2 * \rho_{green} \quad \text{Equation 7}$$

$$E_{FMT} = (D / s)^2 * \rho_{green} \quad \text{Equation 8}$$

$$MC = ((M_i - M_o)/M_o)*100 \quad \text{Equation 9}$$

$$\rho_{green} = M_i / V_{green} \quad \text{Equation 10}$$

where V_T is tree velocity in m/s, D is the distance between the probes in m, s is time for the stress wave to travel the distance between the probes in seconds. The V_L is the log velocity in m/s which is V_{HM200} and V_{RLG} for Director HM200 and Resonance Log Grader respectively, f_n is the natural frequency of the n^{th} harmonic of the wave signal in Hz, L is the log length in m. E_{HM200} and E_{RLG} are the dynamic modulus of elasticity of log estimated by Director HM200 and Resonance Log Grader respectively. MC is green moisture content of the disk, M_i is initial green weight, M_o is the oven-dry weight. ρ_{green} is the green density of the disk, V_{green} is the green volume of the disk.

6.3.4 Static modulus of elasticity (MOE) and rupture (MOR) determination

A 3cm thick sample boards were extracted from each log which was further planned to 2.5cm. The boards were ripped into 2.5 cm x 2.5 cm x 41 cm (radial x tangential x longitudinal). Four each straight grained, defect free specimen were selected from the outer wood and core wood zones of all the logs. The outer wood was the first 2.5 cm specimen from the bark and the core wood was the first 2.5 cm specimen closer to and/or including the pith wood material. Eight samples per log were used to determine the static MOE and MOR after the specimens were conditioned to 12% equilibrium moisture content at 55%RH, 22.5^{o}C following the protocols of ASTM D143 (ASTM 2007). The load was applied on the tangential-longitudinal face in a three-point conFigureuration using a Z010 Zwick Roell Testing System (Zwick Roell, Kennesaw, GA, USA) at a constant loading rate of 1.3mm/min to failure. The load was applied in the tangential – longitudinal face because the acoustic velocity of the tree was determined on that surface.

The static modulus of elasticity (MOE_{static}) and modulus of rupture (MOR) was determined following ASTM procedure (ASTM 2007). The moisture content and density at test were determined following the protocols described in ASTM D 142 (ASTM 2007). The density (AD) was determined by measuring the dimensions of the samples with calipers to the nearest 0.025mm and the weight to the nearest 0.001g, all at 12% EMC.

6.3.5 Microfibril angle (MFA) and fiber geometry determination

Thin sections of wood samples measuring 0.09 mm were sliced from along the entire length of the cores samples taken per tree for each family per site. The thin samples were macerated using equal volumes of hydrogen peroxide (30%) and glacial acetic acid at 80^{o}C for 24 hours for thorough maceration (Peter et al. 2003). Temporary slides were prepared from the

macerated fibers and fiber length, fiber diameter, fiber wall thickness and MFA were measured following the procedure described by Peter et al. (2003). The fiber geometry and MFA measurements were performed on forty fibers per tree selected from both the earlywood and latewood using Differential Interference Contrast (DIC) Microscope (Olympus BX53) (Essien et al. 2017).

6.3.6 Data analysis

The static MOE and MOR for all small clear specimens (both core wood and outer wood) derived from the same log were collated and the average used as a whole log static MOE ($WMOE_L$) or modulus of rupture ($WMOR_L$) for the respective position while those of the outer wood specimen alone was represented as $OMOE_L$ and $OMOR_L$ respectively. For example, the average MOE and MOR for the combined core- and outer wood specimen from the butt represent log $WMOE_L$ and $WMOR_L$ of the butt portion respectively.

The descriptive statistics for the log level parameters was performed for each site using MEANS procedure (PROC MEANS) in SAS 9.4 (SAS, 2014). The effect of site on the mean change in log $WMOE_L$ and dynamic MOEs (E_{HM200}, E_{RLG}, and E_{FMT}) with height along the tree was analyzed using generalized linear model procedure (PROC GLM) in SAS 9.4 (SAS, 2014) to fit model 1. The analysis of variance was then conducted to determine how MOE differ along the tree for the three methods as compared to the $WMOE_L$.

$$Y = \mu + \beta_0 \text{ Height} + \beta_1 \text{ site} + \beta_2 \text{ site*height} + e \qquad \text{model 1}$$

where Y is log WMOE or dynamic modulus of elasticity (E_{HM200}, E_{RLG}, and E_{FMT}), μ is the intercept, β_0 is the mean change in Y due to height, β_1 is the mean change in Y due to site (site 1 = 1 and site 2 = 0), β_2 is the mean change in the interaction term, e is the residue. If the

interaction term was significant, then the slopes of the two sites were different and therefore effects of height and/or site on log MOE were assessed using graphical method.

The resonance acoustic tools are considered to be partially nondestructive because they required open end of the log in order to generate the stress waves while the TOF acoustics tools are fully nondestructive because stress waves can be introduced to the standing tree (Dickson et al. 2004; Wang et al. 2004; Essien et al. 2016a).

The resonance acoustic tools are reported to estimate the whole log dynamic MOE while the TOF acoustic tools estimates the outer wood dynamic MOE of the standing tree (Raymond et al. 2008; Zhou et al. 2013). Therefore to justify the reliability and effectiveness of these tools, GLM models were developed to predict the expected tree static MOE (MOE_T) using E_{tree}, E_{HM200}, E_{RLG}, green density (GD), air-dry density (AD), and diameter at breast height (Diam) as predictors. A single linear regression model was developed because neither the site nor its interaction was significant hence all thirty trees were combined for model development.

However, when similar models were developed for the whole tree outer wood static MOE ($OMOE_T$) and ($OMOR_T$), the site and its interaction with some of the predictors were significant and therefore separate models were developed for each site. All of the parameters derived from logs of the same tree was collated and the averaged used to represent the tree.

6.4 Results and Discussions

6.4.1 Relationships among the wood quality parameters at log level

The descriptive statistics of the parameters studied are presented in Tables 6.1 and 6.2. Generally, there was a statistically significant difference in MFA and fiber diameter between sites whereas fiber length and fiber wall thickness were not statistically different between sites

(Table 6.1). The MFA on site 2 was smaller than on site 1. From Table 6.2, the mean mechanical properties were higher on the site 2 than site 1. As this was not a primary focus of the study and only 15 trees per site were selected, the difference in MFA between sites was not expected. The difference in MFA for the same aged trees and families for two different sites were probably attributable to slower growth at the lower MFA site. These trees had much smaller breast height diameters and according to Via et al. (2007), a faster growth rate for *Pinus spp*. tends to coincide with a higher MFA-lignin matrix.

The mean values for most of the properties were not significantly different between sites except for green density, MOR, and log dynamic MOE estimated with Director HM200 (E_{HM200}). The whole log MOE ($WMOE_L$) was overestimated by 11% and 20% for the resonance-based tools (Director HM200 and FAKOPP RLG) respectively. This supports the assertion that the resonance based acoustic tools provide a reliable and accurate prediction of the static MOE. Contrarily, the TOF based acoustic tool (FAKOPP Microsecond Timer) overestimated the $WMOE_L$ by about 90%. However, when the air-dry density was used instead of green density in equation 8, the $WMOE_L$ was overestimated by 29%. From Table 6.2, the log velocity estimated by the TOF (Microsecond Timer (V_{FMT})) was about 33% and 30% more than that estimated by the resonance (HM200 (V_{HM200}) and RLG (V_{RLG}) respectively) tools.

Theoretically, this value is consistent with the 33% potential overestimation value introduced to the TOF acoustic tools due to addition the Poisson's ratio through the multiplier (Equation1) - one of the two elastic properties affecting the velocity of standing tree (Wang et al. 2007). Wang et al. (2007) explained that for the TOF acoustic tools since the signals are introduced to the standing tree from the side, unbounded waves are produced. Hence the velocity of these waves is characterized by both the Poisson's ratio and the MOE of the material as

against the single elastic parameter (MOE) in the bounded waves as determined by the resonance- based acoustic tools (Equation2). Therefore as stated earlier, given the Poisson's ratio of 0.37 as suggested by Bodig and Jayne (1982), the TOF acoustic tools velocity will be 33% higher than resonance based tools.

Consistently, there were stronger correlations between E_{RLG} and other mechanical properties as compared similar correlations with E_{HM200} (Table 6.3). This is unexpected since both tools are resonance based hence one would expect similar strength in correlations with same mechanical properties. It should be noted that, the higher the Poisson' ratio, the wider the difference between the velocity estimated by the TOF (FAKOPP Microsecond Timer) and the resonance (HM200 and RLG) tools. Therefore using Equation 1, the multiplier between TOF and the HM200 is 1.33 and 1.30 for that TOF – RLG. This translated into Poisson's ratios (Ø) of 0.37 and 0.36 as a calibrating factor for TOF (FAKOPP Microsecond Timer) versus Director HM200 and FAKOPP resonance log grader respectively in this study.

Additionally, the use of green density in the computation of the TOF log dynamic MOE (Equation 8) contributes to this exponential overestimation of the $WMOE_L$. It has been established that above the fiber saturation point, velocity decreases by less than 2% per unit increase in moisture content while the density increases exponentially per unit increase in moisture content. This is because the additional free water in the cell lumen increases the weight of the material with little or no alteration to the volume.

As a result of this overestimation, TOF acoustic tools have been recommended for pre-harvesting or screening of trees but not for the estimation of the actual static MOE. However, to reduce the error introduced by the density component of the equation 8, air-dry or basic density

can be used instead of green density. Basic density is proposed because it is used as a yardstick in the computations of structural design values for wood members.

There was weak to high positive linear correlation between the $WMOE_T$ and dynamic MOEs – ranging from 51% with E_{FMT} to 78% with E_{tree} while those for the $WMOR_T$ ranged from 48% for E_{FMT} to 0.84 for E_{RLG} (Table 6.3). The correlation coefficients between the $WMOE_T$ and $WMOR_T$ was 84% which is similar to that of WMOR versus E_{tree} (r = 78%) and E_{RLG} (r=84%). Ilic (2001) and Lachenbruch et al. (2010) reported correlation coefficients of 0.88 and 0.78 respectively for MOR and dynamic MOE when they studied Douglas fir.

It is interesting to note that, the correlation between E_{HM200} and $WMOE_T$ was 53% which is stronger than 42% recorded for EH_{M200} and $OMOE_L$ (Table 6.3). This observation confirms the ability of resonance based acoustic tools to predict whole log MOE as previously stated. However, the same strength of correlation was recorded for the E_{RLG} versus $WMOE_T$ and $OMOE_L$. This confirms that resonance tools used in this study differ in their estimation algorithms as indicated earlier. Contrarily, the same strength of linear correlation was observed for the relations between TOF (FAKOPP Microsecond Timer tool) versus $WMOE_L$ and $OMOE_L$ (Table 6.3). This suggests that the TOF acoustic tools estimation of the dynamic MOE might not be limited to the outer wood zone (Wang et al. 2007; Raymond et al. 2008) but it can predict whole log dynamic MOE.

However, the size (diameter) of the logs plays a vital role in the predictive ability of TOF tools. The diameter of logs used in the study ranged from 12 to 20 cm which falls within the typical class of small diameter as proposed by Wolfe (2000). The size of our logs might account for this observation.

Table 6.1 Summary statistics of fiber geometric properties and microfibril angle (MFA) of the ninety logs used for the study.

	Site 1			Site 2		
Variables	Mean	Min	Max	Mean	Min	Max
Fiber length (μm)	3096.7±578[a]	2197.3	4420.2	2850.6±514.8[a]	1946.5	4690.2
Fiber diameter (μm)	29.16 ± 4.2[a]	21.19	37.77	32.45±5.90 [b]	21.89	43.07
Fiber wall thickness (μm)	12.34 ±1.78[a]	9.75	16.25	12.78±1.88[a]	8.87	17.03
MFA (^{o})	26.69 ± 3.4 [b]	20.13	32.96	25.01±2.94[a]	19.35	32.48

The variable with the different superscript indicated significantly different at 0.05 between sites.

Table 6.2 Summary statistics of density, dynamic and static MOEs, MOR, and resonance-based acoustic velocity of the ninety logs used for the study.

	Site 1			Site 2		
Variables	Mean	Min	Max	Mean	Min	Max
Moisture content (%)	88.97±27.47[a]	32.88	138.15	82.92±22.22[a]	48.59	140.60
Green density(g/cm^3)	0.77±0.15 [b]	0.51	1.05	0.86±0.10 [a]	0.63	1.04
Air dry density (g/cm^3)	0.53±0.10 [a]	0.35	0.73	0.58±0.07 [a]	0.44	0.74
$OMOE_L$(GPa)	10.31±1.45 [a]	7.32	13.90	9.97±2.52 [a]	3.09	15.05
$WMOE_L$ (GPa)	8.07±1.51[a]	5.10	11.19	8.17±2.02[a]	2.84	12.22
E_{HM200} (GPa)	7.81±2.86 [b]	3.47	13.71	11.03±2.73 [a]	5.00	18.35
E_{RLG} (GPa)	9.82±1.52 [a]	6.64	13.06	10.55±51 [a]	8.01	14.25
E_{FMT} (GPa)	16.02±3.77[a]	9.62	22.48	16.7±3.78[a]	9.84	24.99
$OMOR_L$ (MPa)	82.37±23.75 [b]	39.40	130.50	93.28±20.09[a]	47.60	130.00
$WMOR_L$ (MPa)	65.71±21.19 [b]	28.57	98.03	78.04±16.06[a]	40.70	110.50
V_{HM200} (km/s)	3.12±0.43 [a]	2.09	3.88	3.55±0.34 [a]	2.82	4.33
V_{RLG} (km/s)	3.40±0.11 [a]	3.13	3.64	3.45±0.17 [a]	3.29	3.96
V_{FMT} (km/s)	4.51±0.36[a]	3.78	5.1	4.39±0.44[a]	3.35	5.18

The variable with the different superscript indicated significantly different at 0.05 between sites. $WMOR_L$ and $WMOE_L$ are the combined means of all the small clear core- and outerwood samples per each log, $OWMOR_L$ and $OWMOE_L$ are the means for the outer wood portion of the logs. V_{HM200} = velocity estimation by Director HM200, V_{RLG} = velocity estimation by resonance log grader V_{FMT} = velocity estimation by Fakkopp Microsecond Timer

Table 6.3 Pearson correlation coefficient of the mean values of the thirty trees used for the study.

	GD	AD	$OMOE_T$	$WMOE_T$	$OMOR_T$	$WMOR_T$	E_{tree}	E_{RLG}	E_{HM200}	MFA	F. length	E_{FMT}
GD	1.00	0.81**	0.54**	0.71**	0.81**	0.84**	0.86**	0.88**	0.83**	0.19ns	004ns	0.60**
AD		1.00	0.58**	0.76**	0.92**	0.92**	0.78**	0.74**	0.74**	0.26*	0.05ns	0.62**
$OMOE_T$			1.00	0.93**	0.70**	0.64**	0.68**	0.78**	0.42*	0.18ns	0.26*	0.51**
$WMOE_T$				1.00	0.85**	0.84**	0.77**	0.78**	0.53**	-0.21ns*	0.30*	0.51**
$OMOR_T$					1.00	0.98**	0.79**	0.75**	0.70**	-0.25ns*	0.19ns	0.55**
$WMOR_T$						1.00	0.79**	0.84**	0.71**	0.16ns	0.27*	0.48**
E_{tree}							1.000	0.75**	0.70**	0.18ns	0.06ns	0.37**
E_{RLG}								1.00	0.71**	0.20ns	-0.06ns	0.68*
E_{HM200}									1.00	-0.06ns	0.11ns	0.52*
MFA										100	-0.24ns*	0.12ns
F. length											1.00	0.23ns*
E_{FMT}												1.00

ns indicates nonsignificant at 10%; ns* indicates significant at 10%; * indicates significantly at 5% ** significant 1%. GD= green density, AD = air-dry density, $OMOE_T$= outerwood static MOE for the tree, $WMOE_T$= whole static MOE for the tree, $OMOR_T$= outerwood static MOR for the tree, $WMOR_T$= whole static MOR for the tree, E_{tree}= dynamic MOE of the tree estimated with TOF, E_{RLG}= dynamic MOE of logs estimated with fakopp resonance log grader, E_{HM200}= dynamic MOE of logs estimated with director HM200, MFA=microfibril angle, F. length = fiber length E_{FMT}= dynamic MOE of logs estimated with Fakkopp Microsecond Timer,

6.4.2 Changes in stiffness along tree height

The mean stiffness estimated by Director HM200 (E_{HM200}), FAKOPP Resonance Log Grader (E_{RLG}) and FAKOPP Microsecond Timer (E_{FMT}) was greater than that of $WMOE_L$ (Table 6.2). Generally, both $WMOE_L$ and dynamic MOEs ($E_{HM200,}$ E_{RLG}, and E_{FMT}) increased from the butt to the second log and then decreased afterward (Figure 6.1). The results from the GLM analysis in which the effect of height and site on stiffness are presented in Table 6.4. Generally, there was a significant height effect on the stiffness estimated by the resonance based acoustic tools (Director HM200 and FAKOPP resonance log grader); indicating the axial MOE variation of the tree.

As anticipated, the E_{HM200} was affected by site while E_{RLG} is not sensitive to site. This is expected since similar deviations have been mentioned earlier. Contrarily, the dynamic MOE estimated by the TOF based acoustic tool (FAKOPP Microsecond Timer (FMT)) was significantly affected by site but insensitive to height (Table 6.4). The whole log stiffness ($WMOE_L$), as estimated by the static method, was not affected by either site or height. The sensitivity of the resonance tools to height may be due to their functionality since they are built purposely for logs as against the TOF which are built to function on standing trees. Therefore for optimum log sorting results, the resonance tools should be sensitive enough to be able to detect slight difference in log MOE.

However, since the site by height interaction term for all techniques was not significant, implying that the slopes of the regression line were parallel therefore both factors exert an additive effect on stiffness. This result confirmed several previous studies (Antony et al. 2012; Via et al. 2009; Raymond et al. 2008). Antony et al. (2012) reported a general decrease in stiffness with height when they studied the effect of mid-rotation fertilization on mechanical

properties of 33-year-old loblolly pine. Via et al. (2009) found a general decrease in stiffness from butt to the top of longleaf pine. While similar results were reported by Raymond et al. (2008) when they studied thinned and unthinned matured radiata pine stands. This trend was probably due to the interactive effect of density and MFA which vary with growth ring along the height of the tree (Antony et al. 2012; Via et al. 2009). There was a general increase from butt log to the second log then a decrease afterward for all the methods used. Roper et al. (2004*a*), found similar findings and explained that this trend is possibly due to the high proportion of low stiffness corewood in the butt logs leading to the overall reduction in the mean value of first butt logs.

Table 6.4 Analysis of variance of the effect of site and height along the tree on dynamic and static log MOE of the ninety logs used for the study

		Df	**Mean square**	**P-value**
E_{HM200}	Height	4	16.591	**0.049**
	Site	1	55.040	**0.005**
	Site*height	3	23.594	0.18
E_{RLG}	Height	4	8.664	**0.002**
	Site	1	1.020	0.442
	Site*height	3	0.724	0.736
E_{FMT}	Height	4	0.923	0.788
	Site	1	44.997	**0.011**
	Site*height	3	16.494	0.282
WMOE	Height	4	3.561	0.386
	Site	1	0.033	0.921
	Site*height	3	2.129	0.598

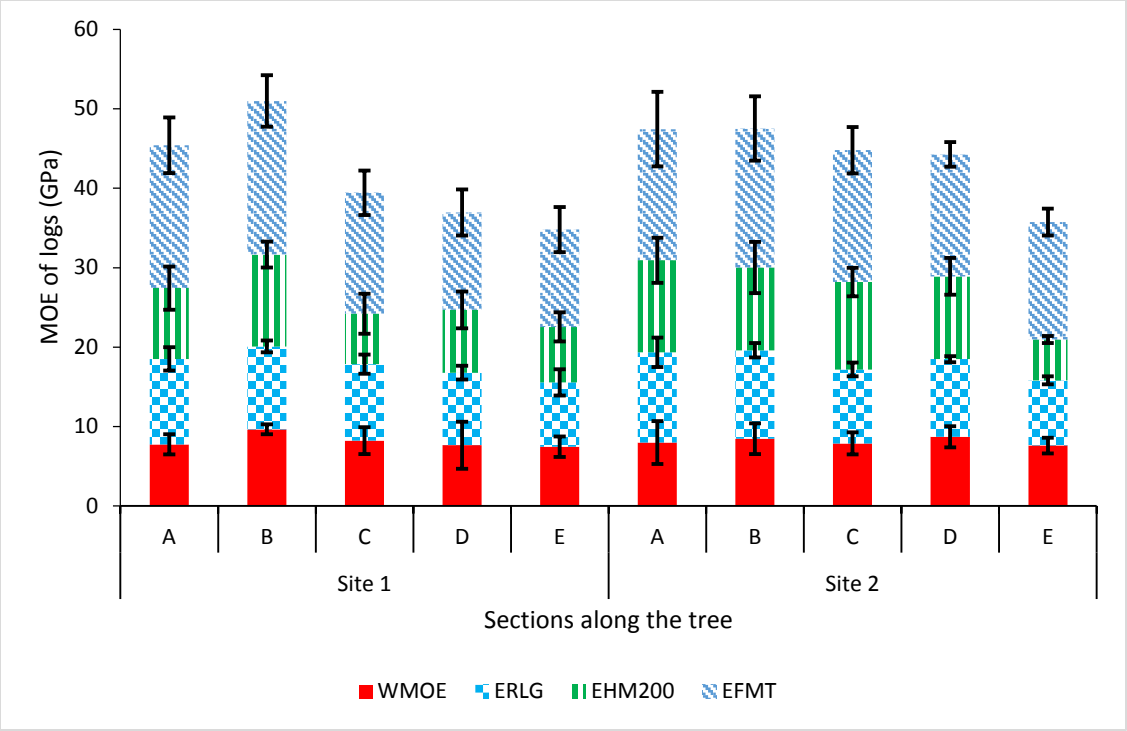

Figure 3 The mean change in dynamic MOE estimated by Director HM200 (E_{HM200}), FAKOPP Resonance Log Grader (E_{RLG}), FAKOPP Microsecond Timer (E_{FMT}) and whole log static MOE ($WMOE_L$) with height along the bole of the tree for sites 1 and 2. **The bars are the standard deviation.**

6.4.3 Relationships between different MOEs, MOR, and density for the thirty trees

One of the major objectives of this study was to access the predictive accuracies of three nondestructive evaluation methods in comparison with the static bending modulus of elasticity and rupture of small clear samples obtained from the same trees. The dynamic MOE of the thirty standing trees (E_{tree}) estimated using TOF (FAKOPP Microsecond Timer), the average dynamic MOE values of the logs obtained from the thirty trees using resonance (Director HM200 (E_{HM200}) and FAKOPP Resonance Log Grader (E_{RLG})), and TOF (FAKOPP Microsecond Timer(E_{FMT})); and the mean values of whole tree static MOE ($WMOE_T$), whole tree outerwood MOE ($OMOE_T$), whole tree modulus of rupture ($WMOR_T$), whole tree outerwood MOR ($OMOR_T$) determined using the static bending test of small clear samples, green (GD) and air-dry densities (AD) for each tree were used for analysis at this level.

Generalized linear regression models (GLM) were developed to predict whole tree static MOE ($WMOE_T$), $WMOR_T$, E_{HM200}, E_{RLG}, and E_{FMT} for each site using E_{tree}, E_{HM200}, E_{RLG}, E_{FMT} green density (GD), air – dry density (AD) and diameter (Diam). The results indicated the models for the $WMOE_T$ with the other variables were unaffected by site, indicating that the slopes of the regression between the sites are similar. Therefore, the combined fitted regressions are presented in Table 6.5. The results indicated that E_{tree}, E_{HM200}, E_{RLG}, $E_{FMT,}$ green density (GD), and air – dry density (AD) were significant predictors of tree $WMOE_T$. These variables explained 62%, 34%, 74%, 51%, 58%, and 72% variations in $WMOE_T$ respectively while diameter was not a significant predictor explaining only 17% variation in the WMOE. The coefficient of determination of the regression model between the $WMOE_T$ and E_{tree} was similar to that reported by Mora et al. (2009), Raymond et al. (2008), and Wang et al. (2004) while that for $WMOE_T$ versus E_{HM200} was similar to those reported by Yin et al. (2010) and Raymond et al. (2008). Contrarily, a similar relationship between the $OMOE_T$ versus dynamic MOEs and densities were sensitive to site effect indicating that the slopes of the regression models between OMOE and the dynamic MOEs differ with the site. As a result, different regression models were fitted for each and the combined sites (Table 6.6). This suggested that $OMOE_T$ cannot be used as a reliable basis for tree screening purposes since it is site dependent. Several authors have reported that the major setback of the time – of – flight (TOF) acoustic tool is that the signal is limited to the outerwood zone of the tree, therefore, it cannot provide accurate stiffness data of the $WMOE_L$ (Dickson et al. 2004; Lassere et al. 2007; Raymond et al. 2008) .

However, the present results contradicted this opinion. This is because once the E_{tree} was estimated close the outerwood zone, one would expect a stronger linear relationship between $OMOE_T$ vs E_{tree} than that of $WMOE_T$ vs E_{tree}. Furthermore, the strength of the relationship

between E_{tree} with $WMOE_T$ and $OMOE_T$ consistently laid within the range of values of $WMOE_T$ and $OMOE_T$ variables versus dynamic MOEs estimated by the other two resonance tools (Tables 6.3, 6.5 and 6.6). The resonance – based acoustic tools have been reported to provide accurate, reproducible and weighted quality information of the whole log (Yin et al. 2010; Dickson et al. 2004; Raymond et al. 2008). Therefore since the linear relationship between the $WMOE_T$ vs E_{tree} was stronger than that of $WMOE_T$ vs E_{HM200} suggest that the time- of -flight acoustic tool measurements are not restricted to the outer wood zone. This supports the previous results reported by Wang (2013) and Essien et al. (2017). As stated earlier, Wang et al. (2007) reported that the signal generated by TOF is dilatational in nature with different wave characteristics as compared to the one-dimensional wave generated by the resonance based tools. Essien et al. (2017) used multivariate statistical technique coupled with density, cellulose, hemicellulose, lignin, and MFA reported that it is plausible that the acoustic signal generated by the TOF acoustic tools collect some quality information in the inner wood zone of the standing tree with small diameter. The present and the previous studies provide strong evidence that both the TOF (for standing tree) and resonance acoustic (for logs and boards) tools can provide aggregate cross sectional quality information for small diameter materials. The relationship between $WMOR_T$ vs dynamic MOEs and densities were sensitive to site except for the E_{RLG} and air-dry density indicating the slopes of the regression models were not parallel across sites (Table 6.6). Significant models with R^2 values of 0.75 and 0.49 were observed for the relationship between $WMOR_T$ and E_{tree} for sites 1 and 2 respectively. However, the relationship between $WMOR_T$ vs E_{HM200} was significant on site1 but not on site 2 with *p-values* of 0.004 and 0.0711 respectively (Table 6.6). On the contrary, the relationship between $WMOR_T$ vs E_{RLG} was not affected by site while $WMOR_T$ vs E_{tree} was significant on both sites. Though the relationship between the

WMOR and E_{tree} was affected by site, it was statistically significant explaining 75% and 49% variations in the $WMOR_T$ for sites 1 and 2 respectively. This suggests that the TOF acoustics tools can be used to screen trees for strength.

Table 6.5 ANOVA of fitted regression predicting whole tree static MOE (WMOE), MOE by HM200 (E_{HM200}), MOE by resonance log grader (E_{RLG}) using MoE of standing tree (E_{tree}), MoE by HM200 (E_{HM200}), MOE by resonance log grader (E_{RLG}), air-dry density (AD), green density (GD) and diameter (Diam) of the thirty tree used for the study

	Intercept	Coefficient	R^2	P -values
$WMOE_T$	-0.2185	0.58 * E_{tree}	61.58	<.0001
$WMOE_T$	3.345	0.44 * E_{HM200}	38.78	0.0073`
$WMOE_T$	-6.41	1.45 *E_{RLG}	73.85	0.0016
$WMOE_T$	2.27	0.35*E_{FMT}	50.68	<.0001
$WMOE_T$	-8.342	0.03 * AD	71.50	<.0001**
$WMOE_T$	-2.7477	0.013 * GD	58.22	<.0001
$WMOE_T$	-0.532	0.619 * Diam	17.14	0.203
E_{RLG}	5.451	0.337 * E_{tree}	72.86	0.0019
E_{RLG}	-1.278	0.02 * AD	53.92	0.031
E_{RLG}	3.753	0.008 * GD	87.49	<.0001
E_{RLG}	6.77	0.267 * Diam	39.18	0.127
E_{HM200}	1.687	0.646 * E_{tree}	73.74	<.0001
E_{HM200}	-1.74	0.022 * AD	66.21	0.0002
E_{HM200}	-5.754	0.02*GD	76.75	<.0001
E_{HM200}	2.39	0.615 * Diam	40.43	0.005**
E_{FMT}	2.88	0.96 * E_{tree}	41.75	0.0006
E_{FMT}	-13.28	0.052 * AD	55.45	<.0001
E_{FMT}	3.72	0.015 * GD	30.6	0.005
E_{FMT}	-3.75	1.46 * Diam	29.72	0.0077

** indicates significant site effect at 0.05

Table 6.6 ANOVA of fitted regression predicting tree OMOE and tree WMOR using E_{tree}, E_{HM200}, E_{RLG}, air-dry density (AD), green density (GD) and diameter (Diam) of the 15 trees per site used for the study. The slope, intercept and R^2 values of equation for sites 1 and 2 as well as combined

Variable1	Variable 2	Site 1	Site 2	Combined
$OMOE_T$	E_{RLG}	3.215 + 0.752* E_{RLG} R^2=51.95*	-.338+1.62* E_{RLG} R^2=87.27*	-6.339+1.62* E_{RLG} R^2=77.12*
	E_{HM200}	8.569 + 0.223*E_{HM200} R^2=29.70^{ns}	3.423+ 0.593* E_{HM200} R^2=45.69*	3.424+0.59* E_{HM200} R^2=43.77*
	AD	5.316+0.0094* AD R^2=50.92*	-9.853*0.034* AD R^2=67.69*	-9.853+0.034*AD R^2=65.43*
	GD	5.911+ 0.0057 *GD R^2=49.62*	-3.582+0.0157* GD R^2=50.32*	-3.582+0.0157*GD R^2=50.71*
	E_{tree}	7.637 + 0.194 E_{tree} R^2=27.25^{ns}	0.226 + 0.674 E_{tree} R^2=61.57*	0.226+ 0.67 E_{tree} R^2=56.66*
WMOR	E_{RLG}	-12.74 + 9.276* E_{RLG} R^2=56.46*	-3.20 + 8.537* E_{RLG} R^2=85.63*	-3.203 + 8.55* E_{RLG} R^2=71.77^{ns}
	E_{HM200}	10.04+7.138 * E_{HM200} R^2=69.35*	48.01 + 2.72* E_{HM200} R^2=22.91^{ns}	48.01 + 2.72*E_{HM200} R^2=59.83*
	AD	-72.11 + 0.261* AD R^2=88.31*	-55.35 + 0.232* AD R^2=72.95	-55.35 + 0.232* AD R^2=85.38^{ns}
	GD	-59.84 + 0.162* GD R^2=92.08*	4.856 + 0.085* GD R^2=34.94*	4.856+ 0.085* GD R^2=76.30*
	E_{tree}	-26.821 + 6.744* E_{tree} R^2=74.62*	21.807 + 3.891 E_{tree} R^2=48.82*	21.81+3.891* E_{tree} R^2=70.47*

In sites 1 and 2** indicate the model is significant at 5% while ns indicates the model is not significant
In combined model ** indicate slopes between the sites are significantly different at 5% while ns indicates the slopes are not significant between sites.

6.5 Conclusions

Generally, the log velocity estimated by the TOF based acoustic tool (FAKOPP Microsecond Timer) was 33% and 30% more than that estimated by the resonance-based tools (Director HM200 and FAKOPP RLG) respectively. This supports the theory that TOF tools generate waves governed by dilatational waves hence inherently their estimated velocity will be higher than resonance based tools. Additionally, the whole log static MOE ($WMOE_L$) was overestimated by 11% and 20% for Director HM200 and FAKOPP RLG respectively whereas FAKOPP Microsecond Timer overestimated the $WMOE_L$ by about 90%. However, when the air-dry density was used instead of green density, the $WMOE_L$ was overestimated by 29%. Therefore air – dried or basic density can be used to minimize the overestimation error.

The strength of the linear relationship between E_{HM200} and $WMOE_T$ was 53% which is stronger than 42% recorded for EH_{M200} and $OMOE_L$. This observation confirmed the ability of resonance based acoustic tools to predict whole log MOE. However, the correlation coefficients for the other resonance tool, E_{RLG} versus $WMOE_L$ and $OMOE_L$ were similar suggesting that its predictive performance is same for both the whole tree and outer wood MOEs. Similarly, same strength of linear correlation existed between TOF (FAKOPP Microsecond Timer) E_{FMT} versus $WMOE_L$ and $OMOE_L$. This suggests that the TOF acoustic tools can predict the dynamic MOE of a small round timber as the resonance tools do.

The $WMOE_T$ was a good site quality indicator compared to the outer wood static MOE ($OMOE_T$) because the latter is site dependent. Also, E_{tree}, E_{RLG}, and AD were strong predictors; GD, E_{HM200}, and E_{FMT} were moderate predictors while diameter was a poor predictor of $WMOE_T$; although E_{FMT} outperformed the E_{HM200}. This buttress the fact that for small diameter timber, both the resonance and TOF based acoustic tools can predict the log dynamic MOE.

There was a strong statistically significant linear relationship between the $WMOR_T$ and the E_{tree} for both sites suggesting that the TOF acoustics tools can be used to screen trees for strength.

The significant effect of site on dynamic MOEs estimated by different acoustic tools as well as the outer wood static MOE ($OMOE_T$) suggest that users of these tools should be careful when interpreting data obtained from various parts along and across the tree over different edaphic and environmental conditions.

The cause of the consistent variations within the resonance tools with the respect to other mechanical properties is not known hence further study needs to be conducted to understand the underlying factors. Also, this consistent variation provides evidence for tools calibrations within the same class (resonance) of acoustic tools.

6.6 References

ASTM Standard D 143-94. (2007). Standard test methods for small clear specimens of timber. ASTM International, West Conshohocken, Pa. Available at www.astm.org [accessed 5 Jan. 2014].

Antony F, Schimleck LR, Jordan L, Daniels RF, Clark A. (2012). Modeling the effect of initial planting density on within tree variation of stiffness in loblolly pine. Annals of Forest Science 69:614 – 650 DOI 10.1007/s13595-011-0180-1

Auty D and Achim A. (2008).The relationship between standing tree acoustic assessment and timber quality in Scots pine and the practical implications for assessing timber quality from naturally regenerated stands. Forestry, 81(4): 475–487. doi:10.1093/forestry/cpn015.

Bertoldo and Gonçalves. (2015). Influence of measurement position, tree diameter, and bulk wood density on models that predict wave propagation velocity in logs according to the velocity in trees. Forest Products Journal, **65**(3/4):166-172.

Bodig J and Jayne BA. (1982). Mechanics of wood and wood composites.

Dickson RL, Joe B, Harris P, Holtorf S, and Wilkinson C. (2004). Acoustic segregation of Australian grown *Pinus radiata* logs for structural board production. Aust. For. 67: 261–266.

Essien C, Cheng Q, Via BK, Loewenstein EF, Wang X. (2016). An Acoustic operations study for loblolly pine standing saw timber with different thinning history BioResources 11(3): 7512 – 7521 DOI: 1 0.15376/biores.11.3.7512-7521

Essien C, Via BK, Acquah G, Gallagher T, McDonald T, Wang X, Eckhardt LG (2017) Multivariate Modeling of Acousto-Mechanical Response of Fourteen Year Old Suppressed Loblolly Pine (*Pinus taeda*) to Variation in Wood Chemistry, Microfibril Angle, and Density Wood Sci Technol 51: 475 – 492. doi 10.1007/s00226-017-0894-9

Forest Products Laboratory (FPL). (2010). Wood handbook—Wood as an engineering material. General Technical Report FPL-GTR-190. Madison, WI: U.S. Department of Agriculture, Forest Service, Forest Products Laboratory.

Ilic J (2001) Relationship among the dynamic and static elastic properties of air-dry Eucalyptus delegatensis R. Baker. Holz als Roh-und WerksTOFf 59: 169-175

Lachenbruch B, Johnson GR, Downes GM, Evans R (2010) Relationship of density, microfibril angle and sound velocity with stiffness and strength in matured of Douglas fir. Canadian Journal of Forest Research 40:55-65

Lasserre JP, Mason EG, and Watt MS (2007) Assessing corewood acoustic velocity and modulus of elasticity with two impact based instruments in 11-year-old trees from a clonal-spacing experiment of *Pinus radiata* D. Don. For. Ecol. Manage. 239:217–221.

McKeand S, Mullin T, Byram T and White T (2003) Deployment of genetically improved loblolly andslash pine in the South. J. For. 101: 32-37.

Meyer MA (1994) Dynamic behavior of materials. John Wiley and Sons, Inc. NY, USA.

Mora CR, Schimleck LR, Isik F, Mahon JM, Clark A, and Daniels RF (2009) Relationship between acoustic variable and different measures of stiffness in standing *Pinus taeda* trees. Can. J. For. Res. 39(8), 1421-1429. doi:10.1139/X09-062

National Oceanic and Atmospheric Administration (2016) State, regional and national monthly precipitation: area weighted monthly normal, 1981 – 2015. Historical Climatography

Peter GF, Benton DM, Bennett K (2003) A simple direct method for measurement of microfibril angle in single fibers using differential interference contrast microscopy. J. Pulp and Paper Sci. 29: 274 – 280

Raymond CA, Joe B, Anderson DW, and Watt DJ .(2008).Effect of thinning on relationships between three measures of wood stiffness in *Pinus radiata*: Standing trees *vs*. short clear specimens," Can. J. For. Res. 38(11), 2870-2879. DOI:10.1139/X08-124

Roper J, Ball R, Davy B, Downes G, Fife D, Gaunt D, Gritton D, Ilic J, Koehler A, McKindley R, Morrow A, Northway R, Penellum B, Rombouts J, and Pongracic S (2004a) Resource evaluation for future profit: Part A – wood property survey of the Green Triangle Region. Forest and Wood Products Research and Development Corporation. Project PN03.3906, Resources Characterization and Improvement Program. www.fwprdc.org.au

Statistical Analysis Software (SAS) version 9.4 (2014) Cary, NC, USA

Vikram V, Cherry ML, Briggs D, Cress DW, Evans R, Howe GT (2011) Stiffness of Douglas-fir lumber: effect of wood properties and genetics. Canadian Journal of Forest Research 41(6):1160-1173

Via BK, So CL, Shupe TF, Groom LH, Wikaira J (2009) Mechanical response of longleaf pine to variation in microfibril angle, chemistry associated wavelengths, density and radial position. Composites: Part A 40 (1):60-66

Via BK, So CL, Groom LH, Shupe TF, Stine M, Wikaira J (2007) within tree variation of lignin, extractives, and microfibril angle coupled with the theoretical and near infrared modeling of MFA. IAWA: 28 (2):189 - 209

Wang X, Ross R J, McClellan M, Barbour RJ, Erickson JR, Forsman JW, and McGinnis GD (2001) "Nondestructive evaluation of standing tree with a stress wave method," Wood Fiber Sci. 33(4), 522-533

Wang X, Ross RJ, Brashaw BK, Punches J, Erickson JR, Forsman JW, Pellerin RE (2004) Diameter effect on the stress-wave evaluation of modulus of elasticity of logs. Wood and Fiber Sci. 36(3):368 – 377

Wang X. Ross RJ and Carter P. (2007) Acoustic evaluation of wood quality I standing tree. Part 1: acoustic behavior in standing tree. Wood Fiber Sci. 39(1): 28-38

Wolfe R (2000) Research challenges for structural use of small –diameter round timbers. Forest Prod J. 50(2): 21.-29

Yin Y, Nagao H, Liu X and Nakai T. (2010) Mechanical properties assessment of *Cunninghamia lanceolata*plantation wood with three acoustic-based nondestructive methods. J. Wood Sci. 56:33-40

Zhou Z. R, Zhao MC, Wang Z, Wang B J, and Guan X (2013) Acoustic testing and sorting of Chinese poplar logs for structural LVL products, BioResources 8(3), 4101-4116. DOI: 10.15376/biores.8.3.4101-4116

Chapter 7: An Acoustics Operations Study for Loblolly Pine (*Pinus taeda*) Standing Saw Timber with Different Thinning History

7.1 Abstract

There is currently a request from landowners in the southeastern United States to provide a nondestructive tool that can differentiate the quality between stands of 25 and 30 years of age subjected to different thinning treatments. A typical site with various thinning regimes was used to vary the wood quality and to determine whether acoustics had the ability to separate for stiffness differences at a given age and local geography. A stand at age 29 with three different spacing (prior thinning) levels was chosen. Three hundred trees (100 per treatment) were randomly selected and acoustically tested for sound velocity using the Time-of-Flight (TOF) method for unthinned, thinned, and twice-thinned stands, respectively. The key finding of the study was that the estimated stiffness of the previously thinned treatments was actually greater than that of the unthinned group, despite having diameters as much as 28% larger. During a forest cruise, knowing that a higher-diameter stand is similar or higher in stiffness could raise the dollar value and harvest priority.

7.2 Introduction

In 2013, the design values for visually graded southern pine were adjusted in an attempt to reflect the material strength and stiffness of today's market (ALSC 2013). On average, these values dropped, making United States southern yellow pine (SYP) lumber less competitive on the international market. The reasons for these lower values were likely the acceleration of growth, coupled with earlier harvest, and perhaps, changes in supply patterns under a cyclic economy (Butler et al. 2016). SYP is now harvested 10 to 15 years earlier than in decades past, resulting in a higher juvenile wood core and perhaps lower mean outerwood stiffness properties (Butler et al. 2016). As a consequence, the market appears to be in disequilibrium, with sawmills demanding better-quality material while forestry suppliers demand a higher dollar value for the additional growth necessary to reach previous stiffness values. In response, some manufacturing facilities in the state of Alabama have gone as far as placing a specific age limit to ensure a higher-quality log. However, such a technique is inefficient because there may be some stands at a lower age that can meet Southern Pine Inspection Bureau SPIB stiffness values (Butler et al. 2016). As such, a measurement system that could partition higher performing stands, regardless of age, could be helpful in the fight to transition the southern United States from a quantity-based market to a quantity- and quality-based market.

Improved genetics is part of the solution for lower rotation ages and a higher stiffness. However, most improvements have already been made in other traits and making improvements for stiffness will invariably lower gains in other traits (Via et al. 2004). Additionally, in the event of significant genetic gains, the landowner may just lower the rotation age to improve profits, as has been done in the past (Butler et al. 2016). The rotation age needed to meet design values can also vary by up to ± 10 years, depending on various genetic and environmental factors

Reprinted from bioresources doi: 10.15376/biores.11.3.7512-7521

(Biblis et al. 1993 and 1995). Finally, unless grown outside the United States (Moya et al. 2013), any genetic gains will take approximately 25 years to be realized in the field from seedling to saw timber harvest. As such, being able to quantify and inventory the potential stiffness of a southern pine stand through some rapid techniques would perhaps be more efficient and allow for stands to be harvested at the right stiffness, as opposed to some specified age.

Thinning is also sometimes assumed by manufacturers to lower the quality of the wood. This perception is not necessarily true for saw timber, as the ratio of latewood to earlywood changes drastically from the time of thinning to the time of harvest. After thinning, for the next few years, less latewood is produced, and the stiffness is also reduced because of the lower density and higher microfibril angle of earlywood. Then, the density trend with age typically returns to the regular trajectory (Giroud et al. 2015). For example, after thinning, an increase in microfibril angle is only persistent for a few years for Douglas fir, but it then continues to decrease with time (Erickson and Arima 1974). For southern pine, reductions in latewood production are also only prevalent for less than three years after thinning, resulting in only a temporary loss of stiffness (Larson et al. 2001).

Acoustics is a well-established method that has been utilized in manufacturing, and more recently, to determine the quality of standing trees and logs (Zhou et al. 2013; Gonçalves et al. 2013). The use of acoustics for trees is particularly interesting because management decisions about which trees or stands to harvest could be made, resulting in a more efficient use of raw material. Gonçalves et al. (2013) demonstrated that a time-of-flight method could be highly correlated to the deflection of a tree stem tested under a cantilever test scheme. As such, the differentiation of stands should be possible with a good sample size per stand. To date, the instrumentation has been commercialized by acoustics manufacturers, but industrial use has not

caught on in the United States. Historically, a lack of use of acoustics in the southeastern U.S. may be attributable to the high stiffness associated with southern pine grades (Butler et al. 2016). However, with the recent change in U.S. southern pine design values, manufacturers are paying closer attention to the source of the raw material, in hopes of regaining product value through machine stress rated (MSR) grading. Unfortunately, MSR grading is not as useful if the surrounding wood basket is low in stiffness because of a high concentration of young plantation wood. For example, Dahlen et al. (2013) found three mills that could not meet stiffness requirements because of high variation in raw materials between mills.

The objective of this study was to investigate whether there was a difference in time-of-flight signals/acoustic stiffness for three stands of similar geography and age but vastly different spacing regimes. Furthermore, the hypothesis (common assumption on the part of manufacturers) was tested that thinning results in lower quality/stiffness later in the growth cycle.

7.3 Materials and Methods

The study was conducted on a permanent loblolly pine research plot established to investigate the long-term effects of silvicultural operations on growth, tree health, and site productivity. The site is located in Auburn, AL (Figure 7.1) with the site index of 23 – 30m for 50-year base age. The 20-ha stand was established in 1986 at a density of 1875 seedlings per ha using a mechanized planter. Part of the stand was row-thinned to approximately 1139 seedlings per ha in 1999, and part of the thinned plot was subsequently thinned to 854 seedlings per ha in 2008. The acoustic measurements were performed in 2014.

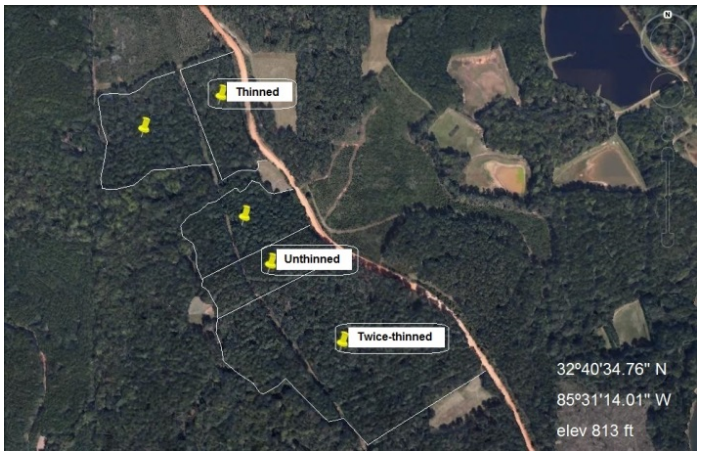

Figure 7.1 Location of the plots within the study area

One hundred trees were randomly selected from each of the thinning regimes—unthinned, thinned, and twice-thinned. The three plots were located on the same topography and site conditions. The trees were selected to reflect the true stocking density of each thinning regime, and the trees were clustered. Diameter at breast height (DBH) was measured at 1.3 m from the ground. The selected trees were acoustically tested using the Director ST 300 instrument (Fibre-gen, Christchurch, New Zealand), which relies on the TOF principle. The accelerometers (the transmitter and the receiver) were positioned 120 cm apart (60 cm above and below the diameter at breast height) and inserted at a 45° angle to the tree trunk, parallel to each other, on the same side of the tree, and about 2 cm deep into the wood (Wang et al. 2001; Mora et al. 2009; Isik et al. 2011).

Acoustic measurements were taken from both the northern and southern sides of the trees to test aspect effects. Three readings were taken on the same position of each side, for a total of six readings per tree. Data were checked for consistency and normality. The three readings each from the northern and the southern parts of each tree were averaged. The data were then grouped into diameter frequency classes of 5-cm DBH intervals, except for the 20- to 25-cm class, which had a 6-cm DBH interval. A standard mixed model procedure with restricted maximum

likelihood method in SAS was used to estimate the means of diameter and velocity of each thinning regimes. The velocities (V) were converted into dynamic modulus of elasticity (MOE) using the equation MoE = $V^2\rho$ and a constant green density (ρ) of 847 kg/m^3 (FPL, 2010). Constant green density was used because according to Raymond et al. (2008) it introduces a non-significant marginal error as compared to using green densities of each thinning regimes. Data analyses were performed using SAS (version 9.4; Cary, NC) and Excel Analysis ToolPak (2010; Microsoft, Redmond, WA) at an alpha (α) level of 5%.

7.4 Results and Discussions

7.4.1 Diameter Distribution

The diameter distribution of the selected trees for each thinning regime is presented in Figure 7. 2. The DBH frequency classes follow the typical probability density function of the Weibull distribution (Lorimer and Krug, 1983). The diameter modal classes for the unthinned, thinned, and twice-thinned plots were 31 to 35 cm, 31 to 35 cm, and 36 to 40 cm, respectively. The mean diameters were 30.3, 34.2, and 38.7 cm for unthinned, thinned, and twice-thinned stands, respectively (Figure 7.3). The diameter of the twice-thinned stand was approximately 28% and 13% higher than those of the unthinned and thinned stands, respectively, and the diameter of the thinned stand was approximately 13% higher than that of the unthinned stand. The diameter growth of the twice-thinned stand was significantly higher than those of the thinned and unthinned stands, and the thinned stand was also significantly higher than that of the unthinned stand (Table 7.1; Figure 7.3). This result is in agreement with several previous studies

on the effect of thinning treatment on the diameter growth of trees (Tappeiner et al. 1982; Wang et al. 2000; Carson et al. 2014).

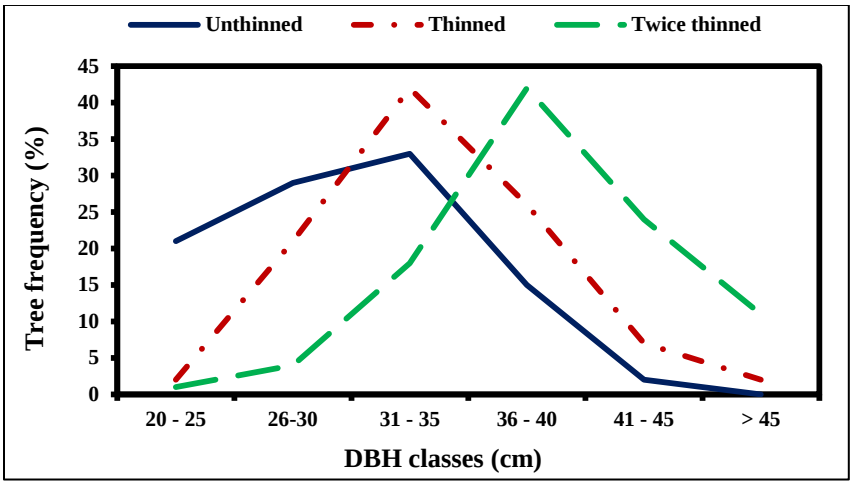

Figure 7. 2 DBH frequency distribution curves for the various thinning regimes

Generally, tree plantations are established at a higher planting density than required for the final crops and are typically subsequently thinned once or twice during the rotation (Tappeiner et al. 1982). The higher level of initial planting density limits excessive branching and allows for full occupancy of the site as soon as possible to maximize productivity and minimize weed competition. Thinning operations provide early income to the landowner to offset the cost of stand establishment, along with promoting diameter growth of the remaining trees. High initial planting density is used to ensure that the crops attain their maximum height growth as early as possible, yet thinning operations are used to optimize the radial growth of the trees. It is clear from the results of this study that thinning operations successfully promote larger diameter growth of trees (Edmond et al. 2000).

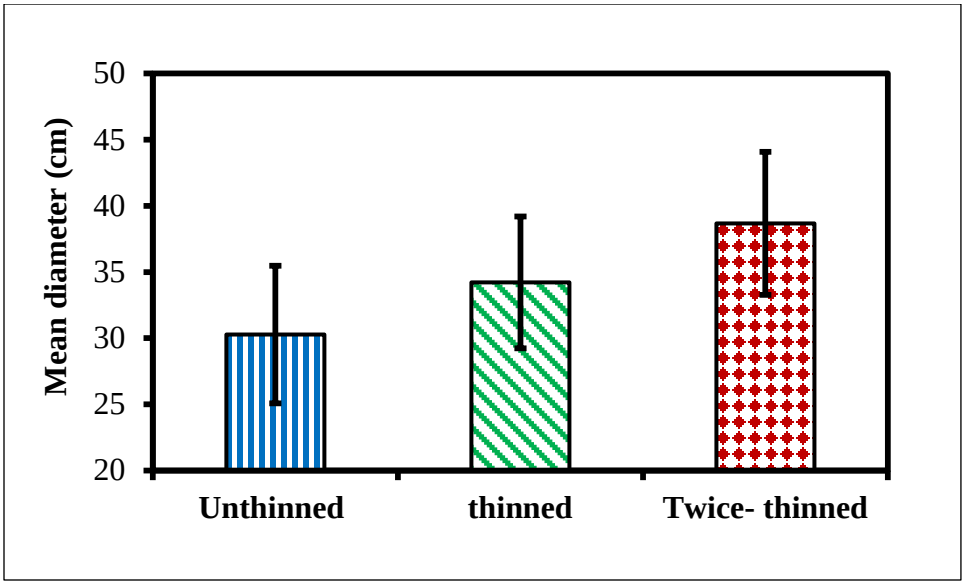

Figure 7.3 Mean DBH of the stands of various thinning regimes.
Error bars are the standard deviation.

Table 7.1 Analysis of Variance of Diameter the Fixed Effect of the Mixed Model

Treatment	Estimate	Standard error	t-value	Pr> l t l
Unthinned	30.28	0.3667	82.58	<.0001
Thinned	34.22	0.508	7.76	<.0001
Twice thinned	38.67	0.529	101.49	<.0001

7.4.2 Effects of Thinning Treatments

The velocity frequency distribution patterns were different from the diameter frequency distribution (Figure 7.4). The thinned stand had a bimodal distribution curve, with 26 to 30 and 41 to 45 cm as the modal classes. The twice-thinned stand had a modal class of 31 to 35 cm. On the other hand, the unthinned portion had a nearly linear velocity increase with a diameter (Figure 7.4). This indicates that the trees with a smaller diameter in each thinning category have a lower velocity.

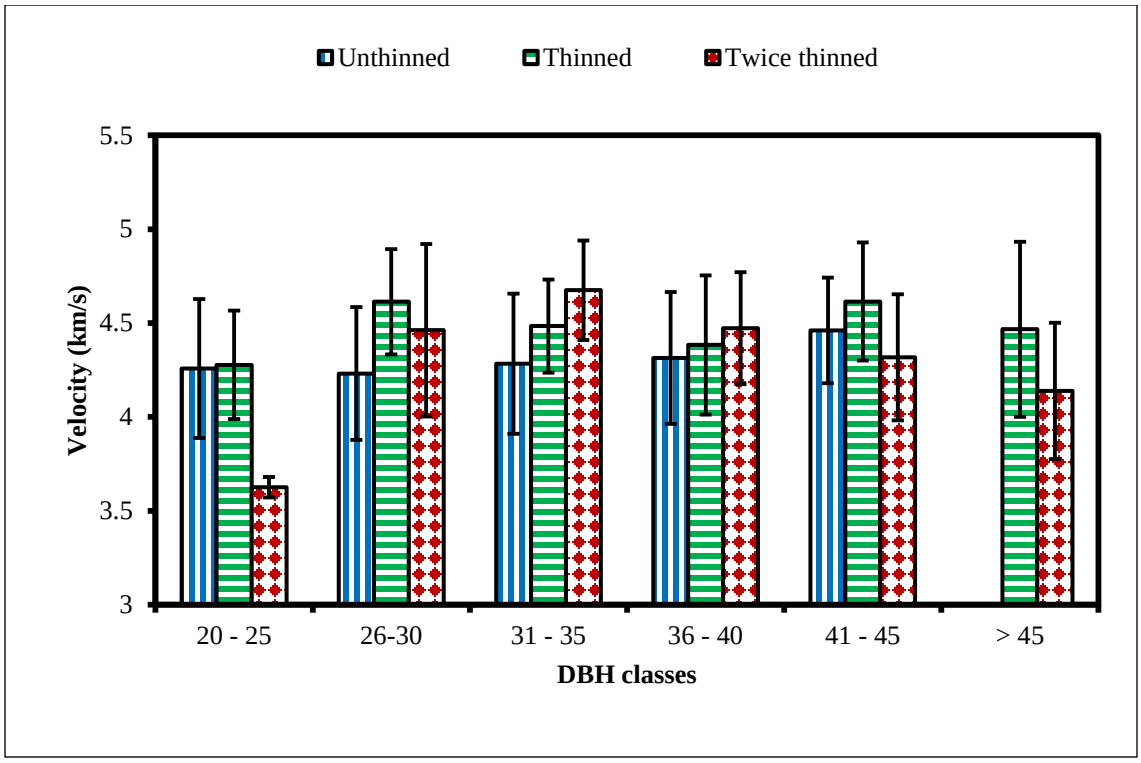

Figure 7.4 Mean acoustic velocity of the stands for the various thinning regimes against the diameter classes. **The error bars are the standard deviation**.

The mean acoustic velocity of the thinned stand was 5.6% and 2.3% higher than the unthinned and twice-thinned stands, respectively, while that of the twice-thinned stand was 3.4% higher than that of the unthinned stand (Table 7.2; Figure 7.5). The acoustic velocities of the thinned and twice-thinned stands were significantly higher than of the unthinned stand (Table 7.2). There was a significant difference between the thinned and twice-thinned stands ($p=0.019$) (Table 7.2). Generally, trees from the thinned stands had higher acoustic velocity than those from the unthinned stand (Table 7.2; Figure 7.5). This result confirms previous studies that thinning increased the acoustic velocity of stands in the long term (Carter et al. 2005). However, in the short term (between 2 and 3 years), thinning is likely to cause a decrease in velocity because of the reduction in the intra-tree competition for water, light, and nutrients, which subsequently causes increased growth, hence the production of thin-walled fibers and low-density and high-

microfibril angle (MFA) wood (Briggs and Smith 1986). Thinning promotes growth and if performed at a later age may lead to the production of a higher volume of mature wood, which generally has higher density and acoustic velocity than an unthinned stand (Carter et al. 2005). Bendtsen (1978) asserted that the effect of rapid growth alone on wood properties was minor in comparison with the difference between the properties of juvenile wood and mature wood. Carter et al. (2005) explained further that the lower velocity observed in unthinned stands might be due to earlier caesura of the production of latewood resulting from high inter-tree competition. The reduced production of latewood would lead to a lower proportion of latewood in the outerwood of the tree detected by the acoustic tool, hence recording lower acoustic velocity values for the unthinned stand (Figure 7.5).

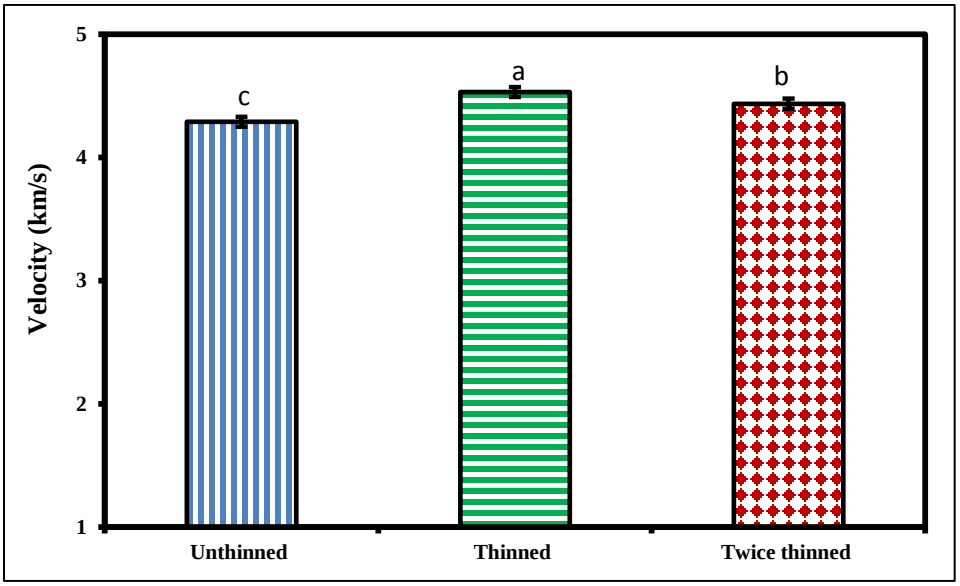

Figure 7.5 Mean acoustic velocity of unthinned, thinned and twice thinned stands. **Different letters indicate significant at α = 0.05. The error bars are standard deviation**

The acoustic velocity of the thinned stand was statistically different from that of the twice-thinned stand (Figure 7.5). These results confirm some reports that a heavily-thinned stand had significantly lower acoustic velocity than a moderately thinned one (Wang et al. 2000; Raymond et al. 2008; Carson et al. 2014). This difference may be due to the high proportion of the mature latewood laying the path of flight of the acoustic tool in the thinned stands compared to the twice-thinned. The TOF acoustic tool is sensitive to the outerwood, primarily mature and dense wood, therefore it is probable that the twice-thinned stand might not have enough mature wood within the 2 cm range detected by the acoustic tool as compared to the thinned stand. This result implies that it plausible for larger diameter trees emanated from stands subjected to the same thinning treatment to exhibit higher acoustic velocity than small diameter trees from the same stand.

Table 7.2 Analysis of Variance of the Fixed Effect of the Mixed Model

Treatment	Estimate	Standard error	t-value	Pr> l t l
Unthinned	4.29	0.0412	-3.52	0.0005
Thinned	4.53	0.0409	2.35	0.019
Twice thinned	4.43	0.0298	148.98	<.0001

The thinning treatment significantly affected the stiffness of the trees (Table 7.3). The thinned and twice-thinned stands had significantly higher stiffness than the unthinned stands ($p<0.0001$ and $p=0.007$, respectively). The thinned stand was approximately 11% and 4% higher in stiffness than the unthinned and the twice-thinned stands, respectively, while the twice-thinned stand was approximately 6% higher in stiffness than the unthinned stand. The mean stiffness of the thinned stand was higher than that of the twice-thinned stand. These results conform to those of a study by Wang et al. (2001). They found that thinning operations increased dynamic MOE

in thinned stands as compared with the non-thinned stands on the same sites. However, as stated earlier, thinning of southern pine in the short term (between 2 and 3 years) has been found to negatively affect the stiffness because of the production of low-density and high-MFA wood (Larson et al. 2001). This effect diminished with time because of the production of mature and dense wood years after the thinning operations. Therefore, it is possible that as the tree grows beyond 10 years after the second thinning, the stiffness of the thinned and the twice-thinned stands may converge, thereby rendering the diameter growth gained with the twice-thinned stand advantageous.

Table 7.3 Descriptive Statistics of Modulus of Elasticity Variation among Tree Stands

	Unthinned	Twice-Thinned	Thinned
Mean	15.86[a]	16.85[b]	17.56[b]
Standard Error	0.21	0.25	0.242
Coefficient of Variation	13.0	14.71	13.76
Sample Variance	4.27	6.14	5.844
Range	9.21	13.20	9.599
Minimum	11.20	9.09	12.38
Maximum	20.41	22.29	21.98
95% Confidence Interval	15.40–16.31	16.39–17.30	17.11 – 18.02
Count	100	100	100

Different letters indicate significance at α=0.05.

7.5 Conclusions

Thinning effects diameter at breast height (DBH) and acoustic velocity. Thinning operations increased the acoustic velocity, stiffness, and DBH of a plot of 29-year old loblolly pine. The study should be replicated in other parts of southern USA to authenticate this result.

Each of the thinning categories exhibited different velocity frequency trajectory with diameter growth. Hence, models developed for predicting wood properties using acoustic velocity could indicate the thinning history of the stand. This information will be very useful in timber bidding and cruising decision-making processing.

The invention of this acoustic tool provides forest managers an opportunity to plan timber harvesting activities when the trees had fully recovered their velocity trajectory after the thinning operations. This will help landowners to harvest the trees to meet the expected stiffness class of the product manufacturers which will subsequently improve the value of the trees.

7.6 References

ALSC (2013). American Lumber Standard Committee: Board of Review Board of Review Minutes. American Lumber Standards Committee, Germantown

Bendtsen AB. (1978) Properties of wood from improved and intensively managed trees. For. Prod. J. 28(10), 61-72.

Biblis EJ, Brinker R. Carino HF, and McKee CW. (1993) Effect of stand age on flexural properties and grade compliance of lumber from loblolly pine plantation timber For. Prod. J. 43(2), 23-28.

Biblis EJ, Carino H, Brinker R, and McKee CW. (1995) Effect of stand density on flexural properties of lumber from two 35-year-old loblolly pine plantations, Wood Fiber Sci. 27(1), 25-33

Briggs DG, and Smith WR. (1986) Effects of silvicultural practices on wood properties - A review, in *Douglas-fir: Stand Management for the Future*, C. D. Oliver, D. P. Hanley, and J. A. Johnson (eds.), College of Forest Resources, University of Washington, Seattle, WA, pp. 108-117.

Butler MA, Dahlen J, Daniels RF, Eberhardt TL, and Antony F. (2016) Bending strength and stiffness of loblolly pine lumber from intensively managed stands located on the Georgia lower coastal plain, Eur. J. Wood Wood Prod. 74(1), 91-100. DOI: 10.1007/s00107-015-0956-3

Carson SD, Dave J, Cown DJ, Russell B, McKinley RB, and Moore JR. (2014) Effects of site, silviculture, and seed lot on wood density and estimated wood stiffness in radiate pine at mid-rotation, New Zealand J. For. Sci. 44(1), 26-37.

Carter P, Briggs D, Ross RJ, and Wang X. (2005) Acoustic testing to enhance western forest values and meet customer wood quality needs, in: *Productivity of Western Forests: A Forest Products Focus*, C. A. Harrington and S. H. Schoenholtz (eds.), Gen. Tech. Rep. PNW-GTR-642, U.S. Department of Agriculture, Forest Service, Pacific Northwest Research Station, Portland, OR, pp. 121-129

Dahlen J, Jones PD, Seale RD, and Shmulsky R. (2013) Mill variation in bending strength and stiffness of in-grade southern pine No. 2 2× 4 lumber, Wood Sci. Tech. 47(6), 1153-1165. DOI : 10.1007/s00226-013-0564-5

Erickson HD, and Arima T. (1974) Douglas fir wood quality studies. Part II. Effects of age and stimulated growth on fibril angle and chemical constituents, Wood Sci. Tech. 8, 255-65.

Edmonds RL, Agee JK, and Gara RI.(2000). Forest Health and Protection. McGraw-Hill, New York, NY.

FPL (Forest Products Laboratory) (2010) Wood Handbook-Wood as an Engineering Material, General Technical Report FPL-GTR-190, U.S. Department of Agriculture, Forest Service, Forest Products Laboratory, Madison, WI.

Giroud G, Defo M, Bégin J, and Ung CH. (2015) Application of near-infrared spectroscopy to determine the juvenile-mature wood transition in black spruce, Forest Prod. J. 65(3), 129-138. DOI: 10.13073/FPJ-D-14-00045

Gonçalves R, Pedroso CB, and Massak, MV. (2013) Acoustic and bending properties in Pinus elliottii beams obtained from trees of different ages, J. Wood Sci. 59(2), 127-132. DOI :10.1007/s10086-012-1311-5

Isik F, Mora CR, and Schimlec LR. (2011) Genetic variation in Pinus taeda wood properties predicted using nondestructive techniques, Ann. Forest Sci. 68, 283-293. DOI: 10.1007/s13595-011-0035-9

Larson PR, Kretschmann DE, Clark AI, and Isebrands JG. (2001) Formation and Properties of Juvenile Wood in Southern Pines: A Synopsis, General Technical Report FPL-GTR-129, USDA, Forest Service, Forest Products Laboratory, Madison, WI.

Lorimer GC, and Krug AG. (1983) Diameter distribution in even – aged stands of shade-tolerant and mid-tolerant tree species, American Midland Naturalist 109(2), 331-345

Mora CR, Schimleck LR, Isik F, Mahon Jr JM, Clark III A, and Daniels RF. (2009) Relationship between acoustic variable and different measures of stiffness in standing *Pinus taeda* trees, Can. J. For. Res. 39(8), 1421-1429. DOI:10.1139/X09-062

Moya L, Laguarda MF, Cagno M, Cardoso A, Gatto F, and O'Neill H. (2013) Physical and mechanical properties of loblolly and slash pine wood from Uruguayan plantations, Forest Prod. J. 63(3), 128-137.

Raymond CA, Joe B, Anderson DW, and Watt DJ. (2008).Effect of thinning on relationships between three measures of wood stiffness in Pinus radiata: Standing trees vs. short clear specimens, Can. J. For. Res. 38(11), 2870-2879. DOI: 10.1139/X08-124

Tappeiner JC, Bell JF, and Brodie JD. (1982) Response of young Douglas fir to 16 years of intensive thinning, Research Bulletin 38: Forest Research Laboratory, Oregon State University, Corvallis, OR.

Via BK, Stine M, Shupe TF, So CL, and Groom L. (2004) Genetic improvement of fiber length and coarseness based on paper product performance and material variability– A review, IAWA J. 25(4), 401-414. DOI:10.1163/22941932-90000373

Wang SY, Lin FC, Jane MC, Lin CJ, and Hun, CP. (2000) Effect of thinning and pruning on DBH and ultrasonic wave velocity in Taiwania cryptomerioide, World Conference on Timber Engineering, Whistler, BC, Canada. July 31- August 3, 2000.

Wang X, Ross RJ, McClellan M, Barbour RJ, Erickson JR, Forsman JW, and McGinnis GD. (2001) Nondestructive evaluation of standing tree with a stress wave method, Wood Fiber Sci. 33(4), 522-533

Zhou ZR, Zhao MC, Wang Z., Wang BJ, and Guan X. (2013) Acoustic testing and sorting of Chinese poplar logs for structural LVL products, BioResources 8(3), 4101-4116. DOI: 10.15376/biores.8.3.4101-4116

Chapter 8: Is there a statistically significant difference within tree acoustic tools? A case of loblolly pine and sweetgum

8.1 Abstract

The use of time-of-flight (TOF) acoustic method for tree quality assessment is particularly interesting because management decisions about which trees or stands to harvest could be made, resulting in a more efficient use and allocation of raw materials. The static stiffness of small clear samples, structural members, and logs have been found to be highly correlated with the dynamic stiffness of trees estimated with the TOF method. This indicates that the acoustic tools can be used to correctly differentiate trees or stands into dynamic stiffness classes. However, a slight variation between the velocities determined by each type of acoustic tools can introduce substantial error in the prediction of dynamic MOE of the trees which can seriously affect management decisions. In this study, we explored the potential variability within the tree acoustic tools commercially available on the market using loblolly pine and sweetgum. Forty loblolly pine trees were used to develop calibration models to correct the "off calibrated tools" and the models used to predict the velocity of sweetgum as determined by four different tree acoustic tools. The results indicated statistically significant difference exists within the four tools. Surprisingly, there is a statistically significant difference between tools from the same manufacturer. As a result of this within and between tool variations, the dynamic MOE of the trees can be overestimated close to 200% for one of the tools as compared to the reference tool.

However, after the calibration, all the tools had statistically similar velocity. The same set of calibration models used for the loblolly pine trees were used for sweetgum. This suggests that with enough data, calibration models can be developed to calibrate acoustic tools used on both hardwood and softwood with similar properties. The results from this study imply the need for the independent body to regulate the accuracies of the tree acoustic tools used for the forest operations in the United States.

8.2 Introduction

The timberland in the United States increased by about 1% from 2007 to 2012, and the proportion of the timberland area occupied by saw-timber size tree increase consistently in the northern and southern parts of United States. In the southern United States, the proportion saw-timber increase from 30% in 1953 to 53% in 2012. Conversely, the pole-timber size trees decreased from 40% to 26% within the same period. The southern United States is responsible for supplying 60% of the industrial round timber used within the country and responsible for over 15% of the global timber supply. In 2012, it was estimated that southern yellow pine (SYP) constitutes about 84% of the 3 billion cubic meters (trees with dbh 12.5cm or greater) of the total growing stocks of softwood available in the timberland of southern United States. Therefore, SYP constitutes the most important group of species in the southern United States (USDA 2016). Oswalt et al. (2014) reported that the productivity on the private timberland in the southern United States is about 17% higher compared to public timberland due to genetics improvement and intensive management practices. This enhanced productivity leads to an increment in the juvenile wood core proportion which has lower quality properties (Faust et al. 1999).

Consequently, the design values for visually graded southern yellow pine were adjusted in an attempt to reflect the material strength and stiffness of today's market (ALSC 2013). On average, these values dropped, making U.S. southern yellow pine (SYP) lumber less competitive on the international market. The reasons for these lower values were likely the acceleration of growth, coupled with earlier harvest, and perhaps, changes in supply patterns under a cyclic economy (Butler et al. 2016). SYP is now harvested 10 to 15 years earlier than in decades past, resulting in a higher juvenile wood core and perhaps lower mean outerwood stiffness properties (Butler et al. 2016). As a consequence, the market appears to be in disequilibrium, with sawmills demanding better-quality material while forestry suppliers demand a higher dollar value for the additional growth necessary to reach previous stiffness values. In response, some manufacturing facilities in the state of Alabama have gone as far as placing a specific age limit to ensure a higher-quality log. However, such a technique is inefficient because there may be some stands at a lower age that can meet Southern Pine Inspection Bureau SPIB stiffness values (Butler et al. 2016). As such, a measurement system that could partition higher performing stands, regardless of age, could be helpful in the fight to transition the southern United States from a quantity-based market to a quantity- and quality-based market.

Improved genetics is part of the solution for lower rotation ages and a higher stiffness. However, most improvements have already been made in other traits and making improvements for stiffness will invariably lower gains in other traits (Via et al. 2004). Additionally, in the event of significant genetic gains, the landowner may just lower the rotation age to improve profits, as has been done in the past (Butler et al. 2016). The rotation age needed to meet design values can also vary by up to ± 10 years, depending on various genetic and environmental factors (Biblis et al. 1993, 1995). Finally, unless grown outside the United States (Moya et al. 2013), any

genetic gains will take approximately 25 years to be realized in the field from seedling to saw timber harvest. As such, being able to quantify and inventory the potential stiffness of a southern pine stand through some rapid techniques would perhaps be more efficient and allow for stands to be harvested at the right stiffness, as opposed to some specified age.

In 2012, the growing stocks of all hardwood in the southern United States was estimated to be about 6 billion cubic meters (trees with dbh 12.5cm or greater) which constitute 61% of all total growing stocks. Sweetgum is the fourth most available hardwood timber species in the southern United States, accounting for 11% of the total hardwood growing stocks (Oswalt et al. 2014). According to FPL (2010), the specific gravity, density, mechanical properties, gluability, and physical properties of sweetgum are comparable to those of loblolly pine. Biblis and Lee (1982) concluded that the plywood produced from sweetgum veneer and that from loblolly pine veneer had comparable physical, mechanical, and shrinkage characteristics. However, besides the general anatomical and morphological difference between pines and sweetgum; low-density hardwoods including sweetgum have persistent large branches, large sized knots, interlocked and spiral grains which are different from the pines (Faust et al. 1990). Faust et al. (1990) concluded that the sweetgum structural lumber is as strong and stiff as that of yellow-popular hence sweetgum can be used for structural applications. As indicated earlier, stiffness is one of the major characteristic properties required for the tree to be used as a structural lumber material.

Acoustics is a well-established method that has been utilized in manufacturing, and more recently, to determine the quality of trees and logs (Wang et al. 2001; Zhou et al. 2013; Gonçalves et al. 2013; Essien et al. 2017). The use of acoustics for trees is particularly interesting because management decisions about which trees or stands to harvest could be made, resulting in a more efficient use of raw material. Gonçalves et al. (2013) demonstrated that a

time-of-flight method could be highly correlated to the deflection of a tree stem tested under a cantilever test scheme. As such, the differentiation of stands should be possible with a good acoustic velocity determination. To date, the instrumentation has been commercialized by acoustics manufacturers, but industrial use has not caught on in the United States. Historically, a lack of use of acoustics in the southeastern United States may be attributable to the high stiffness associated with southern pine grades (Butler et al. 2016). However, with the recent change in United States southern pine design values, manufacturers are paying closer attention to the source of the raw material, in hopes of regaining product value through machine stress rated (MSR) grading. Unfortunately, MSR grading is not as useful if the surrounding wood basket is low in stiffness because of a high concentration of young plantation wood.

Therefore, to improve the industrial confidence in the use of the acoustic tools for tree assessment prior to harvesting, there should be uniformity in the velocity values determined for the same tract of the plantation. There are several types of acoustic tools conFigured to determine the velocity of trees and seedling (Wang et al. 2001; Roth et al. 2007; Gonçalves et al. 2013; Essien et al. 2016a) but there is no published work assessing the variations within these tools. Generally, once the acoustics tools have been calibrated by the manufacturer, one does not expect a statistically significant difference between the mean velocities determined for the same tree using the different acoustic tool. Therefore, the existence of significant differences between the mean velocities determined by the common types of the tree acoustic tools can lead to a significant loss of revenue to the timber mills or/and the landowners as well as prolonging industrial adoption of the technology. In the southeastern United States, loblolly pine (*Pinus taeda*) is the most dominant tree species in the southern yellow pine (SYP) group in terms of cultivation, utilization and genetic improvement (McKeand et al. 2003). Hence most the tree

acoustic studies in the southern United States use southern yellow pine including loblolly pine. As stated earlier, sweetgum is the fourth most dominant hardwood in the southern United States that has comparable properties with the southern yellow pine. Hence in this study, we selected four acoustic tools to test wood quality properties of both loblolly pine and sweetgum trees.

We hypothesized that there will be no statistically significant difference between the mean velocities determined by the four selected acoustic tools. This is because all the selected acoustic tools have been duly calibrated by their respective manufacturers hence they are expected to predict accurate velocity which is comparable statistically. Therefore, in this study, we used four acoustic tools from two manufacturers (two from each manufacturer) to determine the potential variation within and between tools from the same manufacturer using loblolly pine and sweetgum. Also, we explored the possibility of developing calibration strategies to correct any anomaly that might be present between the tools.

8.3 Materials and Methods

8.3.1 Materials

The study composed of two sections. The first section entails using loblolly pine to develop calibration models to make all the acoustic tools produce similar readings. In the first of the study, the materials were obtained from a thirty-year old pine stand located beside the Forest Products Development Center, within Auburn University main campus, Auburn AL. Forty trees were randomly sampled for assessment. However, care was taken to avoid trees with a visible defect such as leaning, forked stems, chlorotic needles, as well as other less significant growth defects. The diameter at breast height (DBH) and a total height of the trees were measured.

The second phase of the study entails using the developed calibration models to adjust the acoustic velocity determined for sweetgum – a diffuse porous hardwood species. The trees used for this part of the study were selected from naturally regenerated sweetgum trees in the Mary Oliver Thomas Demonstration Forest located five miles outside of the Auburn University main campus. Forty trees were randomly selected within the stand and the diameter at breast height and total height measured.

8.3.2 Acoustic measurements of standing trees

All of the selected trees were acoustically tested using a pair each of FAKOPP Microsecond Timer acoustic tool (AU and WT) (Fakopp Enterprise, Agfalva, Hungary) and Director ST300 (AU300 and WT300) (Fiber-gen, Christchurch, New Zealand). These type of acoustic tools relied on the time-of-flight (TOF) principle (Wang et al. 2007; Mora et al. 2009; Essien et al. 2016a). Basically, the accelerometers (the transmitter and the receiver probes) were positioned on the same side of the tree 120 cm apart with the center of the path occurring at breast height. Both probes were positioned 45^{o} to the tree axis and the stress wave was generated by striking the transmitter probe with a steel hammer at a steady force (Mora et al. 2009). The generated wave was detected by the receiver and the time lapse for the sound wave to travel the distance between the probes was recorded by the data logger. Seven readings each were taken on each tree and tree velocity was estimated as the ratio of the distance to time (Equation 1). The dynamic modulus of elasticity of the trees estimated with oven-dry density ($E_{oven\text{-}dry}$) was computed using Eqns. 2 (Wang et al. 2007; Essien et al. 2016a)

Bark – to – bark 5 mm core samples were taken at the breast height portion of each of the tested trees to determine moisture content, oven-dry, and green densities. ASTM D2395 (ASTM

D2395 – 07) procedure was followed in determining the density of the core samples. The core samples were subdivided into four sections with the length varying according to the diameter of the tree. The dimensions of the cores were measured using a digital caliper to the nearest 0.0025 mm and the weight to the nearest 0.0001 g. Weight (M_i) and dimensions of the cores were measured while green and were subsequently dried to constant weight in an electronic oven set at 103^{o}C (M_o). The moisture content (MC), basic ($\rho_{oven\text{-}dry}$) and green densities (ρ_{green}) of the cores were determined according to eqns. 4, 5, and 6 respectively. The averages of the four subdivided core samples from the same cores were used for further analysis.

$$V_T = D / s \qquad \text{Equation 1}$$

$$E_x = V_T^2 * \rho_{oven\text{-}dry} \qquad \text{Equation 2}$$

$$MC = ((M_i - M_o)/M_o)*100 \qquad \text{Equation 4}$$

$$\rho_{green} = M_i / V_{green} \qquad \text{Equation 5}$$

$$\rho_{oven\text{-}dry} = M_o / V_o \qquad \text{Equation 6}$$

where V_T is tree velocity in m/s, D is the distance between the probes in meters, s is time for the stress wave to travel the distance between the probes in seconds, E_x is the dynamic modulus of elasticity estimated by X tool velocity and oven-dry density, MC is green moisture content of the core, M_i is initial green weight, M_o is the oven-dry weight. ρ_{green} is the green density of the core, $\rho_{oven\text{-}dry}$ is the oven-dry density, and V_o is the oven-dry volume of the core.

In the estimation of the dynamic MOE of the trees, we decided to use the oven-dry density because according to FPL (2010), oven-dry density is used to determine the design values of wood. Furthermore, it has been reported that velocity increases significantly with decreasing moisture content below the hygroscopic region (fiber saturation point), above this region, however, the change in velocity with moisture content is statistically not significant

(Olivito 1996; Chan et al. 2011; Gao et al. 2012). This shows that the actual water affecting the velocity is the bound water within the cell wall but not the free water in the cell lumen. Since the moisture content of most healthy trees is above the fiber saturation point, one does not expect velocity to vary significantly. Therefore, using oven-dry density with the tree velocity can provide useful basic information about tree wood quality.

8.3.3 Data analysis

The seven readings taken on an individual tree were collated and the mean used for the analysis. Simple descriptive analysis and charts were performed using SAS to ascertain whether some of the tools require calibration. Since the same set trees were tested using the four tools, we used both two-sampled t-test and paired t-test to determine whether the mean velocity determined by the tools were statistically different from the reference tool (Fakopp Microsecond Timer acoustic tools (AU)) (Johnson and Wichern 2007). This is essential because if the tools are going to be certified for operation in a particular jurisdiction, there should be a standardized tool against which the remaining tools will be compared with.

Calibration models were developed for the tools whose mean velocity was statistically different from the reference tool (AU) using the 40 loblolly pine trees. Several models in the nonlinear and linear families were developed and standard error of calibrated (SEC) evaluated. The smaller the SEC, the better the model fits the dataset (Esbensen 2002). Two parameters exponential model had similar SEC as the linear model but for simplicity, the linear models were adapted. The two-sample t-test and paired t- test were conducted on the fitted dataset. The developed models were then used to predict the velocity of naturally regenerated sweetgum.

8.4 Results and Discussion

8.4.1 Variation within and between species

The results of the physical properties of the forty loblolly pine and sweetgum trees used in this study are presented in Tables 8.1 and 8.2 respectively. The coefficient of variations (CV) of the oven-dry (8.94%) and green (10.28%) densities of the loblolly pine is close to the CV value of 10% reported for specific gravity by FPL (2010). However, the CV values of 7.72% and 6.53% for the oven-dry and green densities respectively for sweetgum were lower than the reported by FPL, (2010). This suggests that the variation within density values of the sweetgum is less dispersed as compared to the loblolly pine.

It is interesting to note that though the oven-dry of the two species are statistically different, the green density is not statistically significant ($p>0.05$). This observation is due to the variation of moisture content between the species. The mean moisture content of sweetgum is 108% which is significantly higher than 71% recorded for loblolly pine. The weight of the moisture in the sweetgum compensated for the weight of the real wood material in the loblolly pine hence balancing out the difference between the real wood weights of the studied species. The variation in moisture content between the species may be due to the difference in age of the study materials. Whiles the loblolly pine was about 30 years old, the mean age of the sweetgum was 15 years old with a range from 8 to 17 years old. This indicates that the sweetgum wood is mainly juvenile.

Table 8.1 Descriptive statistics of the forty loblolly pine tree used for calibration

Variables	Mean	SD	CV	Min	Max	95% CL
Green density (g/cm^3)	1.10	0.11	10.28	0.86	1.34	1.06,1.13
Oven-dry density (g/cm^3)	0.65	0.06	8.94	0.55	0.74	0.63, 0.66
Moisture content (%)	70.64	14.5	20.52	44.28	97.07	66.13,75.15
DBH(cm)	30.57	4.95	16.19	18.80	39.80	29.02,32.11

SD =standard deviation; CV = coefficient of variation; CI= confidence interval of the mean
DBH= diameter at breast height

Table 8.2 Descriptive statistics of the forty sweetgum trees

Variables	Mean	SD	CV	Min	Max	95% CI
Green density (g/cm^3)	1.09	0.07	6.53	0.91	1.33	1.07, 1.11
Oven-dry density (g/cm^3)	0.60	0.05	7.72	0.52	0.71	0.59, 0.61
Moisture content (%)	108.52	11.03	10.17	87.06	139.17	105.30,111.75
DBH (cm)	14.83	3.76	25.34	9.5.	25.00	13.72, 15.93

SD =standard deviation; CV = coefficient of variation; CI= confidence interval of the mean
DBH= diameter at breast height

8.4.2 With Acoustic tools velocity variation for calibration species - loblolly pine tree

The mean velocity determined by the four acoustic tools for the two species are presented in Tables 3 and 4, and Figures 8.1 and 8.2 respectively. Generally, the velocity dataset for loblolly pine from the AU, WT, and AU300 are equally dispersed around the mean with the coefficient of variation (CV) of 10.8, 10.5 and 10.4% respectively (Table 8.3). The mean velocity of WT, WT300, and AU300 are 110 m/s, 520 m/s, and 3690 m/s respectively more than the reference tool (AU) (Table 8.3); translating into 3%, 14%, and 103%. From Table 8.3 and Figure 8.1, the mean velocity of WT300 and AU300 are significantly higher than those of the reference (AU) and WT. There is, however, no significant difference between AU and WT while significant

difference exists between AU300 and WT300 (Table 8.3). A similar trend was observed for the sweetgum (Table 8.5 and Figure 8.2). In the case of sweetgum, however, the velocity of the reference tool (AU) was 1% more than the WT while it was 7% and 89% less than those determined by AU300 and WT300 tools respectively.

However, when paired t-test was conducted on the loblolly pine dataset, the results indicated all the tools are significantly different from one another (Table 8.4). While the results in Tables 8.3 and 8.5 tested the equality of the means under the two sample t – test algorithm with the assumption that the mean velocity of each tool is independent of each other (Johnson and Wichern 2007) Hence based on the assumption of independence, the velocity values determined with the reference tool (AU) is independent on those determined with the other tools. Hence population means of velocity determined by AU and WT are statistically not different.

However, the paired t – test assumed dependence of the tools since the same set of trees from the same population are used for the study (Johnson and Wichern 2007). Hence under dependence assumption for the paired t – test, the dataset is treated as repeated measurements on the same trees. As a result, a tree with high velocity will exhibit the same trend for all the tools (Figure 3). Therefore depending on the statistical assumption taken, slightly different results can be obtained. As stated earlier, all the tools are statistically different from one another under the paired t – test assumption.

Notwithstanding, however, both results detected significant difference exists between the tools. This implied sampled tools from different types of acoustic tools can be off calibration hence introduce error into the dynamic modulus of elasticity (MOE) estimated for the tract. For instance, the same tract of plantation will produce significantly different dynamic MOE when assessed by different loggers within the same locality but using different acoustic tools. This

could lead to a serious problem for the mill managers who require wood with specific stiffness to meet the end products specifications.

This result confirms the need for periodic calibration and recalibration to acoustic tools to ensure consistent accuracy.

The velocities determined by the four tools for both loblolly pine and sweetgum were converted into dynamic MOEs using Equation 2 and results presented in Tables 8.6 and 8.7 respectively. While AU, WT, and WT300 predicted mean dynamic MOE of less than 10GPa, AU300 estimated over 31.08GPa (Table 8.6). It is clear from Figure 8.3 that, the anomaly is likely due to the calibration of the tools since stiffer trees exhibit higher velocity for all the tools. As indicated earlier, the velocity of the reference tool (AU) for loblolly pine is 3%, 14%, and 103% lower than WT, AU300, and ST300 respectively (Table 8.3). However, the dynamic MOE of the reference (AU) tool for loblolly pine is 6, 31, and 320% lower than WT, WT300, and AU300 respectively (Table 8.6). Similarly, for sweetgum, the reference tool's dynamic MOE is 14 and 261% lower than WT300 and AU300 tools respectively (Table 8.7). This observation emphasizes the point that a slight variation in velocity can lead to a significant change in the predicted dynamic MOE. Essien et al. (2016b) reported green static MOE of plantation grown loblolly pine to be 7.35 GPa. Based on this, the dynamic MOE estimated for the AU and WT are not statistically different from the green static MOE (Table 8.6)

Table 8.3 Descriptive statistics of the velocity determined by four tools for loblolly pine

Variables	Mean	SD	CV	Min	Max	95 % CI	Ratio x/ AU
AU (km/s)	3.59	0.39	10.77	2.66	4.41	3.47, 3.71	1
WT (km/s)	3.70	0.39	10.54	2.65	4.50	3.57, 3.82	1.03
WT300 (km/s)	4.11	0.43	10.39	2.80	4.84	3.97, 4.24	1.14
AU300 (km/s)	7.28	1.30	17.85	3.84	9.61	6.88, 7.69	2.03

AU = "fakopp microsecond timer (reference)"; WT = "fakopp microsecond timer", WT300= "WT director ST300; AU300= "AU director ST300. where X= WT, WT300, or AU300

Table 8.4 Paired t- test 95% confidence interval for mean velocity of loblolly pine comparison of test tools against reference (AU)

Variables	Mean	SD	95% confidence interval of mean between AU and other tools
AU (km/s)	3.59	0.39	
WT (km/s)	3.70	0.39	-0.162, -0.052
WT300 (km/s)	4.11	0.43	-0.592, -0.4434
AU300 (km/s)	7.28	1.30	-4.010, -3.375

AU = "fakopp microsecond timer (reference)"; WT = "fakopp microsecond timer", WT300= "WT director ST300; AU300= "AU director ST300. SD= standard deviation Tools with confidence interval including zero are not significantly different at 5% alpha level.

Table 8.5 Descriptive statistics of the velocity determined by four tools for sweetgum

Variables	Mean	SD	CV	Min	Max	95% CI	Ratio x/ AU
AU (km/s)	3.54	0.21	5.94	2.97	3.96	3.48, 3.61	1.00
WT (km/s)	3.50	0.23	6.61	2.95	4.05	3.43, 3.57	0.99
WT300 (km/s)	3.79	0.25	6.47	3.20	4.28	3.72, 3.86	1.07
AU300 (km/s)	6.70	0.79	11.80	4.90	8.24	6.46, 6.94	1.89

AU = "fakopp microsecond timer (reference)"; WT = "fakopp microsecond timer", WT300= "WT director ST300; AU300= "AU director ST300. SD =standard deviation; CV = coefficient of variation; CI= confidence interval of the mean; x = WT, WT300, and AU300.

Table 8.6 Descriptive statistics of the estimated dynamic MOE for the forty loblolly pine tree used for calibration

Variables	Mean	SD	CV	Min	Max	95% CI	Ratio x/ AU
EAU (GPa)	7.40	1.59	21.52	4.02	11.04	6.91, 7.90	1.00
EWT (GPa)	7.85	1.62	20.58	4.00	11.49	7.35, 8.35	1.06
EWT300 (GPa)	9.69	1.94	20.04	4.45	13.30	9.08, 10.29	1.31
EAU300 (GPa)	31.08	10.61	34.14	8.38	52.54	27.77, 34.39	4.20

EAU = dynamic modulus of elasticity estimated by AU microsecond timer
EWT = dynamic modulus of elasticity estimated by WT microsecond timer
EWT300 = dynamic modulus of elasticity estimated by WT director 300
EAU300 = dynamic modulus of elasticity estimated by AU director 300; SD = standard deviation; CV = coefficient of variation; CI = 95% confident interval of the mean

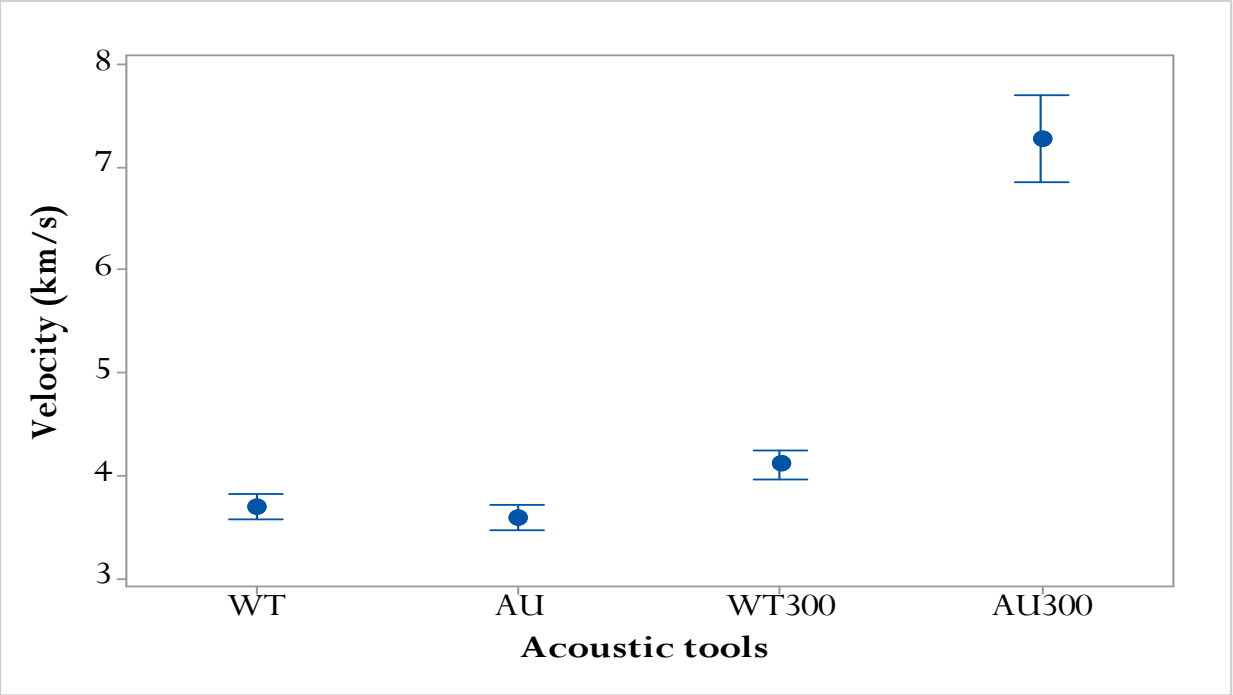

Figure 8.1 Interval plot of the mean velocity determined by the four time – of – flight acoustic tools for loblolly pine. AU = "fakopp microsecond timer (reference)"; WT= "fakopp microsecond timer", WT00 = "WT director ST300; AU300 = "AU director ST300. The bars are 95% confidence interval of the mean. Tools with overlapping intervals are not significantly different at 5% alpha level.

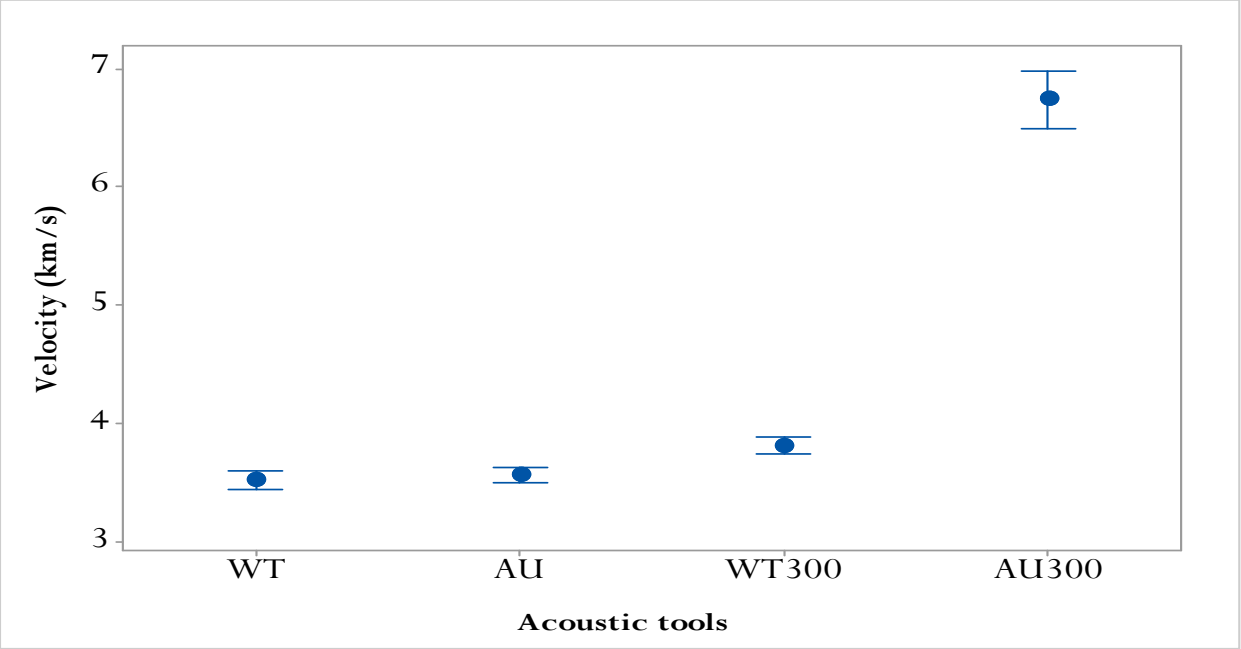

Figure 8.2 Interval plot of the mean velocity determined by the four time – of – flight acoustic tools for sweetgum trees. AU and WT are fakopp microsecond timer; WT300 and AU300 are the director ST300. (bars are 95% confidence interval for the mean)

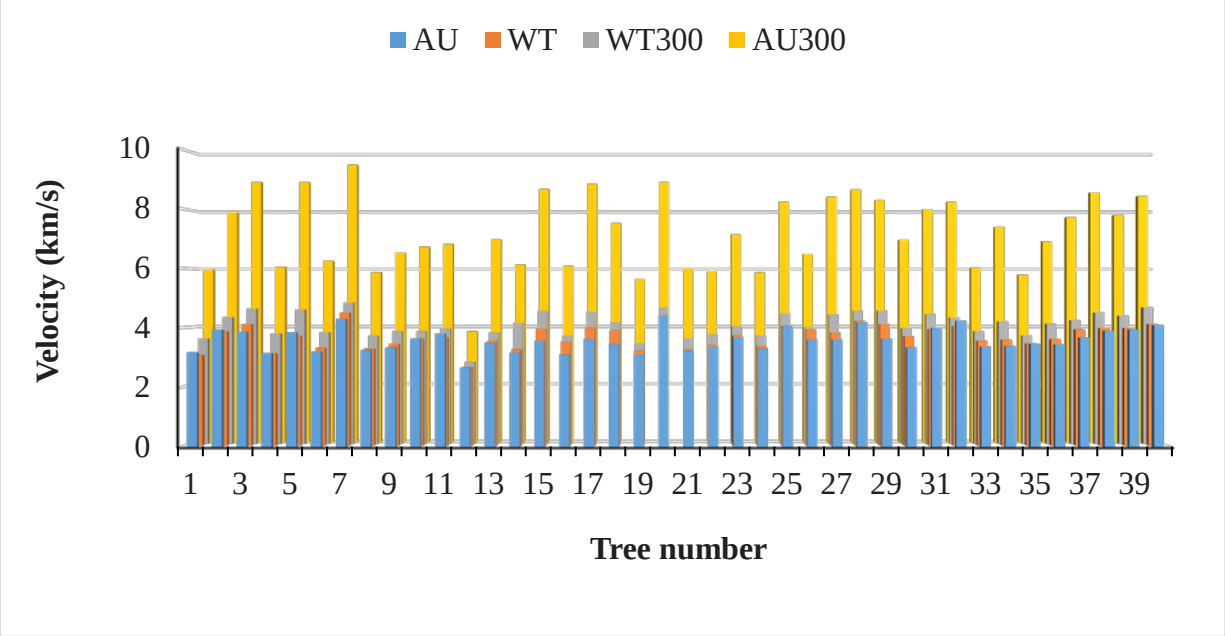

Figure 8.3 Bar chart of the number of trees of loblolly pine against mean velocity estimated by the four time – of – flight acoustic tools.

Table 8.7 Descriptive statistics of the estimated dynamic MOE for the forty sweetgum tree used for the prediction

Variables	Mean	SD	CV	Min	Max	95% CI	Ratio x/ AU
EAU (GPa)	7.64	1.08	14.13	3.67	9.99	7.32, 7.96	1.00
EWT (GPa)	7.46	1.36	18.20	5.64	12.75	7.06, 7.86	0.98
EWt300 (GPa)	8.75	1.33	15.22	6.42	12.43	8.36, 9.14	1.14
EAu300 (GPa)	27.58	6.40	23.20	14.82	40.38	25.70, 29.46	3.61

EAU = dynamic modulus of elasticity estimated by AU microsecond timer
EWT = dynamic modulus of elasticity estimated by WT microsecond timer
EWT300 = dynamic modulus of elasticity estimated by WT director 300
EAU300 = dynamic modulus of elasticity estimated by AU director 300; SD = standard deviation; CV = coefficient of variation; CI = 95% confident interval of the mean

8.4.3 Development of Calibration models

Due to the presence of the significant difference in the mean velocity determined by each tool, calibration models were developed to correct this anomaly. The reference tool (AU) is considered as the response variable and the other three tools as predictors. The results of the models are shown in Table 8.8. The adjusted R^2 for the models ranged from 70% for the WT300 to 81% for WT with corresponding SEC ranging 211m/s to 169 m/s. The descriptive statistics and the 95% confidence interval of the fitted values are shown in Table 8.9. From Tables 8.9 and 8.10, the mean velocity estimated by all the acoustic tools is not statistically different from one another.

The developed models which were based on the loblolly pine trees were used to predict the velocity for sweetgum. The diagnostic statistics and coefficients of the fitted models for the sweetgum are presented in Table 8.11. The standard error of prediction (SEP) ranged from 88.4 m/s for the AU300 to 99.2 m/s for the WT acoustic tools (Table 8.11). This suggests that errors

associated with the models are minimal. The two-sampled t – test revealed that there is no significant difference between the reference tools (AU) and the remaining tools (Table 8.12)

Table 8.8 Diagnostic of the fitted calibration models predicting the reference tool (AU) velocity using the other three tools.

Response	Predictors	Intercepts	Coefficient	Adj R^2	SEC
AU	WT	0.280	0.895	80.92	0.169
	WT300	0.454	0.7633	70.23	0.211
	AU300	1.745	0.2532	72.48	0.205

AU = "fakopp microsecond timer (reference)"; WT = "fakopp microsecond timer", WT300= "WT director ST300; AU300= "AU director ST300.SEC= standard error of calibration

Table 8.9 Descriptive statistics and 95 % confidence interval of the fitted values.

Variables	Mean	SD	CV	Min	Max	95 % CI
AU (km/s)	3.589	0.387	10.78	2.66	4.41	3.469, 3.709
WT (km/s)	3.696	0.349	10.56	2.65	4.50	3.589, 3.805
Wt300 (km/s)	3.589	0.326	9.08	2.59	4.15	3.488, 3.690
Au300 (km/s)	3.589	0.330	9.19	2.716	4.18	3.485, 3.691

AU = "fakopp microsecond timer (reference)"; WT = "fakopp microsecond timer", WT300= "WT director ST300; AU300= "AU director ST300.Tools with overlapping confidence interval are not significantly different at 5% alpha level.

Table 8.10 Paired t-test 95% confidence interval for mean velocity comparison of test tools against control (AUtreesonic) - paired t-test

Variables	Mean	Std Deviation	95% confidence interval of mean between AUtreesonic and other tools
AU (km/s)	3.589	0.387	
WT (km/s)	3.589	0.349	-0.0532, 0.0532
Wt300 (km/s)	3.589	0.326	-0.0667, 0.0667
Au300 (km/s)	3.589	0.330	-0.0648, 0.0648

AU = "fakopp microsecond timer (reference)"; WT = "fakopp microsecond timer", WT300= "WT director ST300; AU300= "AU director ST300.Tools with confidence interval including zero are not significantly different at 5% alpha level.

Table 8.11 Coefficients, intercepts, R-squared prediction, and Standard error of

prediction of the sweetgum velocity predicted by tools.

Response	Predictors	Intercepts	Coefficient	R^2 pre	SEP
AU	WT	0.477ns	0.899	75.81	0.0992
	Wt300	0.207ns	0.997	76.39	0.0980
	Au300	0.260ns	0.954	79.97	0.0884

AU = “fakopp microsecond timer (reference)”; WT = “fakopp microsecond timer”, WT300= “WT director ST300; AU300= “AU director ST300.

Table 8.12 Descriptive statistics of model predicted the velocity of the four tools for sweetgum trees.

Variables	Mean	SD	CV	Min	Max	95% CI	Ratio x/ AU
AU (km/s)	3.54	0.210	5.94	2.97	3.96	3.50, 3.607	1.00
WT (km/s)	3.41	0.207	6.07	2.93	3.91	3.35, 3.50	0.96
WT300 (km/s)	3.34	0.187	5.60	2.89	3.72	3.34, 3.50	0.94
AU300 (km/s)	3.44	0.201	5.83	2.98	3.83	3.38, 3.50	0.97

AU = “fakopp microsecond timer (reference)”; WT = “fakopp microsecond timer”, WT300= “WT director ST300; AU300= “AU director ST300.

8.5 Conclusion

In this study, we explored the potential variability within the tree acoustic tools commercially available on the market using loblolly pine and sweetgum. Forty loblolly pine trees were used to develop a calibration model and the model used to predict the velocity of sweetgum as determined by four different tree acoustic tools. The results indicated statistically significant difference exists within the four tools. As a result of this within tool variations, the dynamic MOE of the trees can be overestimated close to 200% for one of the tools as compared to the reference tool. However, after the calibration, all the tools had statistically similar velocity. This result implies the need for an independent body to regular the accuracies of the tree acoustic tools used for the forest operations in the United States.

8.6 Acknowledgement

We appreciated the technical and logistical support from students and staff of Forest Health Dynamics Laboratory and Forest Products Development Center of Auburn University. The financial support for this work is provided by Robert Lewis Adams Graduate Fellow

8.7 References

ALSC (2013). American Lumber Standard Committee: Board of Review Board of Review Minutes. American Lumber Standards Committee, Germantown

Biblis EJ, Brinker R, Carino HF, and McKee CW. (1993). Effect of stand age on flexural properties and grade compliance of lumber from loblolly pine plantation timber, Forest Prod. J. 43(2), 23-28.

Biblis EJ, Carino H, Brinker R, and McKee CW. (1995). "Effect of stand density on flexural properties of lumber from two 35-year-old loblolly pine plantations," Wood Fiber Sci. 27(1), 25-33.

Butler MA, Dahlen J, Daniels RF, Eberhardt TL, and Antony F. (2016). Bending strength and stiffness of loblolly pine lumber from intensively managed stands located on the Georgia lower coastal plain, Eur. J. Wood Wood Prod. 74(1), 91-100. DOI: 10.1007/s00107-015-0956-3

Chan M J, Walker CJ, Raymond CA (2011) Effect of moisture content and temperature on acoustic velocity and dynamic MOE of radiata pine sapwood boards. Wood Sci and Technol 45: 609-626 doi: 10.1007/s00226-010-0350-6

Esbensen KH. (2002). Multivariate data analysis in practice: An introduction to multivariate data analysis and experimental design, fifth ed. CAMO Process AS, Oslo, Norway, 598 p.

Essien C, Cheng Q, Via BK, Loewenstein EF, Wang X (2016a) An Acoustic operations study for loblolly pine standing saw timber with different thinning history BioResources 11(3): 7512 – 7521 DOI: 1 0.15376/biores.11.3.7512-7521

Essien C, Via BK, Cheng Q, Gallagher T, McDonald T, Wang X, Eckhardt LG (2017). Multivariate Modeling of Acousto-mechanical Response of Fourteen Year Old Suppressed Loblolly Pine (*Pinus taeda*) to Variation in Wood Chemistry, Microfibril Angle, and Density. Wood Sci Technol 51: 475 – 492 doi 10.1007/s00226-017-0894-9

Essien C, Via BK, Cheng Q, Gallagher T, McDonald T, Eckhardt LG (2016b) Sensitivity of acoustic tools to variations in equilibrium moisture content of loblolly pine. Proceedings of the 70th Forest Products Society International Convention. Portland, OR. USA

Forest Products Laboratory. (FPL 2010). Wood Handbook-Wood as an Engineering Material, General Technical Report FPL-GTR-190, U.S. Department of Agriculture, Forest Service, Forest Products Laboratory, Madison, WI.

Faust TD, McAlister RH, and Zarnoch SJ (1990). Strength and stiffness properties of sweetgum and yellow – popular structural lumber. J. For. Pro. 40(10): 58 - 64

Gonçalves R, Pedroso CB, and Massak MV. (2013). Acoustic and bending properties in Pinus elliottii beams obtained from trees of different ages, J. Wood Sci. 59(2), 127-132. DOI :10.1007/s10086-012-1311-5

Gao S, Wang X, Wang L, Allison RB (2012) Effect of temperature on the acoustic evaluation of standing trees and logs: part 1 – laboratory investigation. Wood and Fiber Sci 44(3):286-297

Johnson, R.A. and Wichern, D.W. (2007). Applied multivariate statistical analysis. Pearson Education Inc. Upper Saddle River, NJ. USA.

McKeand S, Mullin T, Byram T and White T (2003) Deployment of genetically improved loblolly and slash pine in the South. J. For. **101**: 32-37.

Mora, C. R., Schimleck, L. R., Isik, F., Mahon Jr., J. M., Clark III, A., and Daniels, R. F. (2009). The relationship between acoustic variable and different measures of stiffness in standing Pinus taeda trees," Can. J. For. Res. 39(8), 1421-1429. DOI:10.1139/X09-062

Moya, L., Laguarda, M. F., Cagno, M., Cardoso, A., Gatto, F., and O'Neill, H. (2013). "Physical and mechanical properties of loblolly and slash pine wood from Uruguayan plantations," Forest Prod. J. 63(3), 128-137.

Olivito RS (1996) Ultrasonic measurements in wood. Materials Eval 54:514–517

Oswalt, S.N., Smith, W.B., Miles, P.D., Pugh, S.A. (2014). Forest resources of the United States, 2012: a technical document supporting the Forest Service Update of the 2010 RPA Assessment. Gen. Tech. Rep. WO-91. Washington, DC: U.S. Department of Agriculture, Forest Service, Washington Office. 218 p.

Statistical Analysis Software (SAS) version 9.4 (2014) Cary, NC, USA

Roth BE, Li X, Huber DA and Peter GF (2007) Effects of management intensity, genetics and planting density on wood stiffness in a plantation of juvenile loblolly pine in the southeastern USA. For. Ecol. Manage 246: 155 – 162 doi 10.1016/j.foreco.2007.03.028

USDA Forest Service. (2016). Update of the future of America's forest and rangelands: Forest Service 2010 Resources Planning Act Assessment. Gen. Tech. Rep. WO-94. Washington, DC: U.S. Department of Agriculture, Forest Service, Washington Office. 250p.

Via BK, Stine M, Shupe TF, So CL, and Groom L. (2004). Genetic improvement of fiber length and coarseness based on paper product performance and material variability– A review, IAWA J. 25(4), 401-414. DOI:10.1163/22941932-90000373

Wang X, Ross, RJ, McClellan M., Barbour RJ, Erickson JR, Forsman, J. W., and McGinnis, G. D. (2001). "Nondestructive evaluation of standing tree with a stress wave method," Wood Fiber Sci. 33(4), 522-533

Wang X., Ross RJ and Carter P. (2007) Acoustic evaluation of wood quality I standing tree. Part 1: acoustic behavior in standing tree. Wood Fiber Sci. 39(1): 28-38

Zhou, Z. R., Zhao, M. C., Wang, Z., Wang, B. J., and Guan, X. (2013). Acoustic testing and sorting of Chinese poplar logs for structural LVL products, BioResources 8(3), 4101-4116. DOI: 10.15376/biores.8.3.4101

9.0 Summary and Conclusions

9.1 Fundamental considerations of acoustics as a nondestructive evaluation technique in wood and trees

The wood chemistry (cellulose, hemicellulose, and lignin), density, and microfibril angle (MFA) coupled with multiple linear regression and path analysis were used to predict velocity and static properties of elite loblolly pine. The chemistry, density, and MFA have been found to significantly influence the static properties of wood. Therefore, understanding the influence of these properties on acoustic velocity, which is used as a surrogate for stiffness, is very important for wood characterization.

Both multiple linear regression and path analysis indicates that cellulose, hemicellulose, and density were significant variables responsible for predicting the stiffness and velocity of loblolly pine with an R^2 of 0.73 and 0.59 respectively. This provides molecular level evidence to confirm the capability of time – of – flight (TOF) acoustic tools to estimate stiffness.

Furthermore, at the molecular level, cellulose was the most important conductor of stress waves; followed by the hemicelluloses; while lignin acts as a dispersant or sink, thereby reducing sound transmittance. The importance of cellulose and hemicellulose in stress wave conductance at the molecular level implied the significant effect of the cell wall material (S2 layer) on stiffness and the acoustic velocity of wood.

In order to provide a consistent and credible velocity database for efficient and effective forest management decisions, the optimum range of distances between the probes of the tree

acoustic tool has to be determined. The distance between the probes together with other morphological, anatomical, and crown properties of loblolly pine were investigated.

Acoustic velocity of loblolly pine is dependent on the between probe distance used for its determination. The velocity determined at distances below 60 cm is significantly different from that determined at 120 cm. Furthermore, at distances below 60 cm, the waveform of the stress wave is dominated by the fundamental frequency of the transmitter probe, which explains the statistically nonsignificant difference between velocities determined within this region. Using 120 cm as a standard distance, the velocity is overestimated by 3.3, 7.3, 10.4, and 13.9% for 100, 80, 60, and 40 cm respectively. This translates into dynamic MOE values of 13, 50, 102, and 197 MPa for 100, 80, 60, and 40 cm respectively. Consequently, distances from 80 to 120 cm constitute the optimum range for velocity determination for this TOF acoustic tool. This implies that the acoustic tool is configured to operate effectively at distances from 80 cm and above.

There are significant positive relationships between velocity and foliage transparency, taper, tracheid wall thickness and tracheid length. However, velocity had significant negative relations with the crown ratio, microfibril angle, and lumen diameter. Finally, microfibril angle and the fiber wall thickness are the main anatomical properties driving the signal at the micro-level. This observation further emphasizes the significance of the cell wall material on stress wave propagation in the wood at the micro-level.

The two major kinds of the acoustic tools used in the wood industry are the resonance and TOF, a classification based on the algorithms used to determine the velocity as well as the applicable products. While the resonance tools are used on products with cut ends such as logs,

lumber, and small clear samples, the TOF tools work effectively on trees as well as all the aforementioned products. Therefore, the effect of equilibrium moisture content on acoustic velocity and dynamic MOE estimated by resonance and TOF based acoustic tools might differ. Small clear samples measuring 2.5 x 2.5 x 41 cm in green condition were dried progressively to 5% moisture content in a conditioning chamber set at 55% relative humidity and 22.7^{o}C temperature. The dynamic MOE for both resonance and TOF acoustic tools were estimated using both the oven-dry and green densities.

The equilibrium moisture content (EMC) of loblolly pine significantly affects velocity measured below and above the hygroscopic region. The acoustic velocity decreased by 33.9 m/s and 28.8 m/s for TOF and the resonance tools respectively for a unit increase in EMC below fiber saturation point. The change was lower for EMC above FSP - 5.4 m/s for TOF and 6.1 m/s for resonance.

The statistically nonsignificant slope in velocity above the FSP coupled with better accuracy in predicting green static MOE using velocity with oven-dry density supports the hypothesis that the cell wall material controls the acoustic velocity while the water in the cell lumen plays a nonsignificant role in stress wave propagation.

The static MOE of the green samples exhibited similar strength of the linear relationship with dynamic MOE estimated with both the oven-dry density and density at test. However, for both acoustic tools, the static MOE was overestimated by about 16% when dynamic MOEs were estimated with oven-dry density (OD), but it was overestimated by about 72% when dynamic MOE were determined with the density at test (GD). It was demonstrated that using the density at test (green density) to predict the dynamic MOE of trees and freshly harvested logs where the

moisture content is above the FSP, will lead to at least 40% higher than similar prediction using oven-dry density.

Based on this observation, oven – dry or basic density is recommended for dynamic MOE computation for tree or products with moisture content above FSP.

Since there are small variations within small clear samples, further studies using structural size lumber or logs will help provide additional evidence to support the use of oven-dry or basic density in predicting dynamic MOE of green wood or tree.

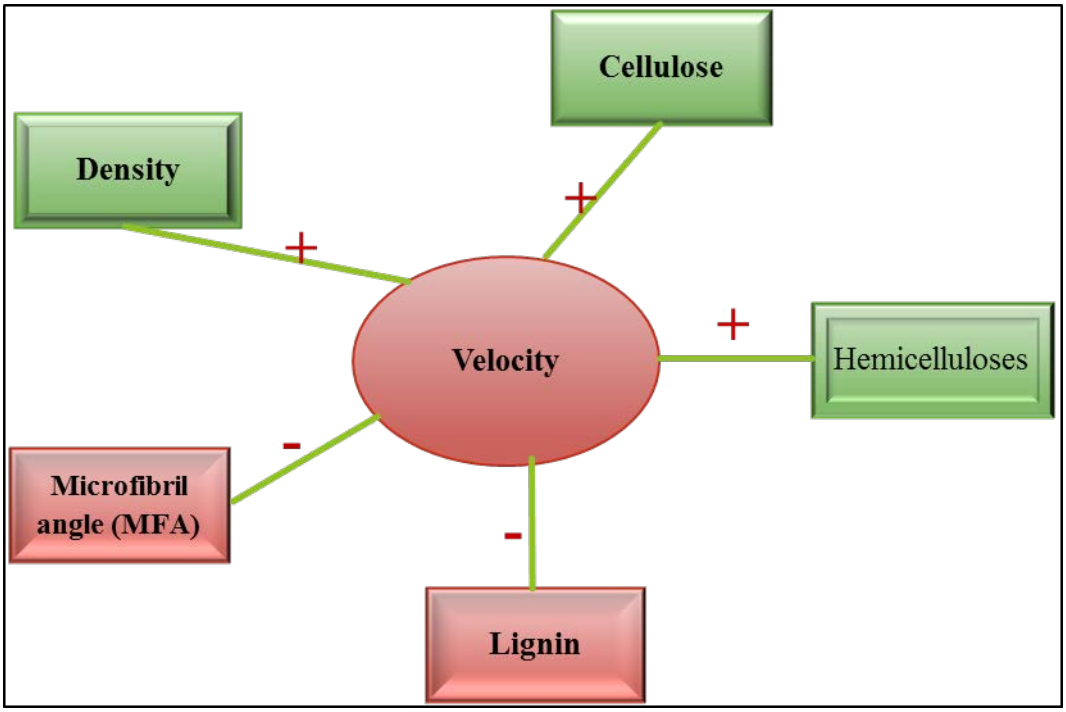

Figure 9.1 Proposed model for the relationships between velocity and wood density, MFA, and polymeric constituents

9.2 Application of acoustic techniques on elite loblolly pine families and sweetgum

The effect of site and genetic families on morphological, anatomical and wood quality properties of fifteen 14-year-old loblolly pine families was studied. The dynamic MOE of the

trees were determined using the velocity with either basic density ($DMOE_B$) or green density ($DMOE_G$).

There were significant site and genetic family effect on diameter, microfibril angle, fiber length, and dynamic MOEs. While there was nonsignificant difference in $DMOE_B$ between sites; $velocity^2$ for site 1 was significantly higher than site 2, but $DMOE_G$ was higher for site 2 than site 1. This suggests that depending on the type of density used in computing the dynamic MOEs, difference decision can be made. Therefore, practitioners should take care when extrapolation velocity reading of trees from different locations. Again, the mean $DMOE_B$ and $DMOE_G$ reported in the present study presents a snapshot of the expected static MOE for green and 12% moisture conditions respectively.

Additionally, about half of the selected genetic families had statistically similar morphological and wood quality properties between sites. Therefore, farmers have the opportunity to select genetic families (T26 and T 18) which are superior in both the morphological and wood quality traits for plantation development across sites with varying edaphic and environment. Furthermore, farmers have the opportunity to match some elite planting stocks to specific site for greater productivity and quality outturn due to the significant effect of site or family or site by family interaction. Further studies with genetic families sampled from more sites need to be conducted in order to fully understand the effect of site by genetic family interaction as reported for most of the properties studied.

Generally, the log velocity estimated by the time – of – flight (TOF) based acoustic tool (fakopp microsecond timer) was 33% and 30% more than that estimated by the resonance-based tools (director hm200 and fakopp resonance log grader (rlg)) respectively. This supports the

theory that TOF tools generate waves governed by dilatational waves hence inherently their estimated velocity will be higher than resonance based tools.

Additionally, the whole log static MOE ($WMOE_L$) was overestimated by 11% and 20% for director hm200 and fakopp rlg respectively whereas fakopp microsecond timer overestimated the $WMOE_L$ by about 90%. However, when the air-dried density was used instead of green density, the $WMOE_L$ was overestimated by 29%. Therefore air – dried or basic density can be used to minimize the overestimation error.

The whole tree static MOE ($WMOE_T$) was a good site quality indicator compared to the outer wood static MOE ($OMOE_T$) because the latter is site dependent. Also, TOF estimated dynamic MOE for tree (E_{tree}), fakopp rlg estimated dynamic MOE of log (E_{RLG}), and AD (air-dry density) were strong predictors; GD (green density), director hm200 estimated dynamic MOE of log (E_{HM200}), and TOF estimated dynamic MOE of log (E_{FMT}) were moderate predictors while diameter was a poor predictor of $WMOE_T$; although E_{FMT} outperformed E_{HM200}. This buttress the fact that for small diameter timber, both the resonance and TOF based acoustic tools can predict the log dynamic MOE.

There was a strong statistically significant linear relationship between the $WMOR_T$ and the E_{tree} for both sites suggesting that the TOF acoustics tools can be used to screen trees for strength. The cause of the consistent variations within the two resonance tools (director hm200 and fakopp resonance log grader) with the respect to other mechanical properties is not known hence further study needs to be conducted to understand the underlying factors

The mean velocity of WT, WT300, and AU300 were 110 m/s, 520 m/s, and 3690 m/s respectively more than the reference tool (AU); translating into 3%, 14%, and 103% for loblolly pine. The mean velocity of WT300 and AU300 were significantly higher than those of the

reference (AU) and WT. There is, however, no significant difference between AU and WT while significant difference exists between AU300 and WT300. In the case of sweetgum, however, the velocity of the reference tool (AU) was 1% more than the WT while it was 7% and 89% less than those determined by AU300 and WT300 tools respectively. This result implies the need for an independent body to regular the accuracies of the tree acoustic tools used for the forest operations in the U.S.